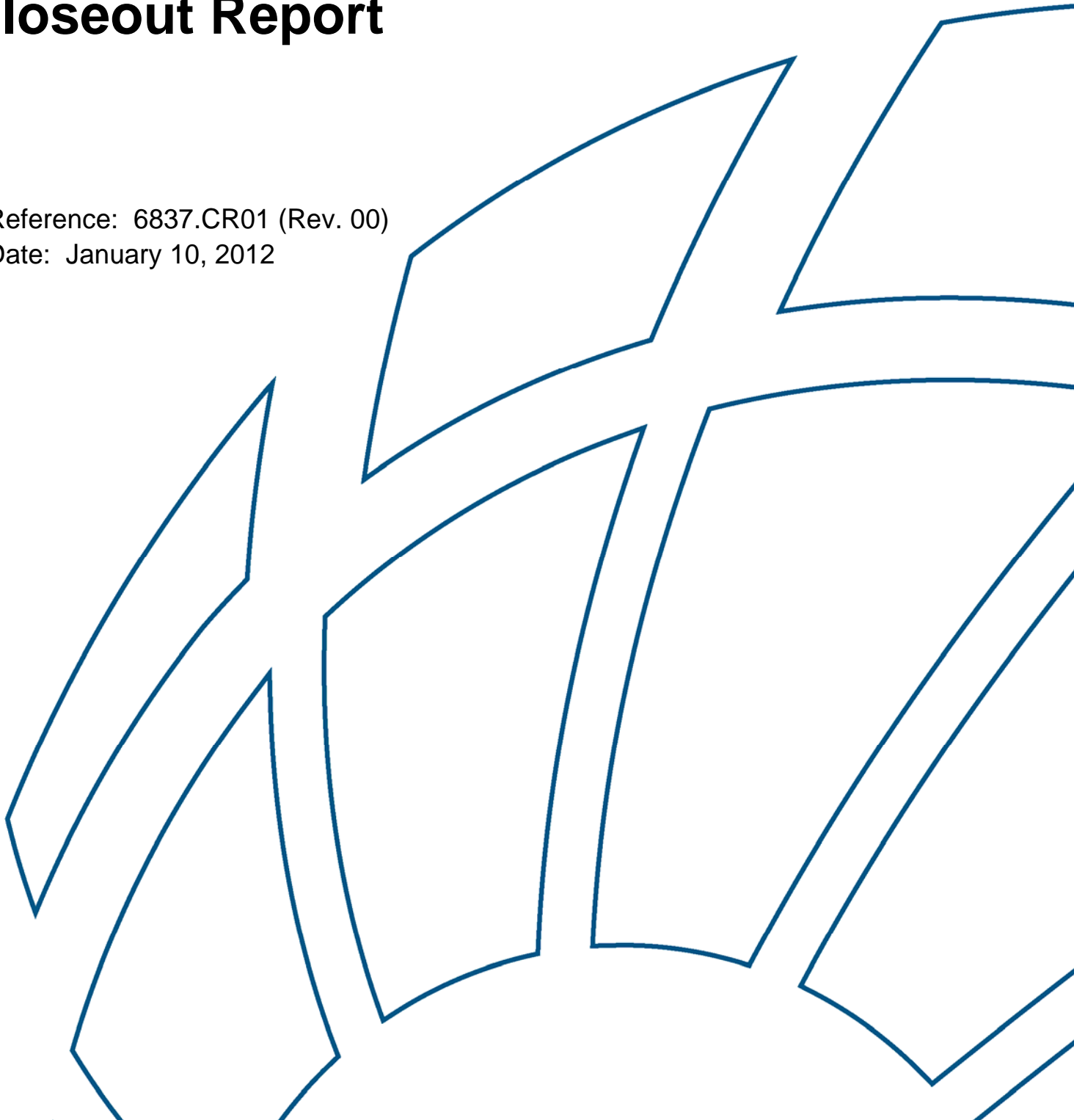


Dent Fatigue Life Assessment DOT #432 Closeout Report

Reference: 6837.CR01 (Rev. 00)
Date: January 10, 2012



DENT FATIGUE LIFE ASSESSMENT

DOT #432 (DTPH56-10-T-000013)

CLOSEOUT REPORT

January 10, 2012

Submitted to:

U.S. DEPARTMENT OF TRANSPORTATION
Pipeline and Hazardous Materials Safety Administration
Office of Pipeline Safety
1200 New Jersey Avenue, SE
Washington, D.C. 20590

Submitted by:

BMT FLEET TECHNOLOGY LIMITED
311 Legget Drive
Kanata, ON
K2K 1Z8

BMT Contact: Vlad Semiga
Tel: 613-592-2830, Ext. 255
Fax: 613-592-4950
Email: vsemiga@fleetech.com

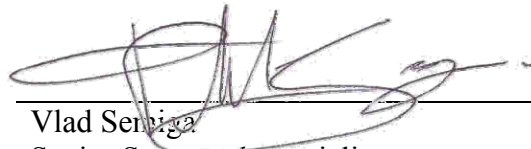
BMT Fleet Technology Limited accepts no liability for any errors or omissions or for any loss, damage, claim or other demand in connection with the usage of this report, insofar as those errors and omissions, claims or other demands are due to any incomplete or inaccurate information supplied to BMT Fleet Technology Limited for the purpose of preparing this report.

BMT DOCUMENT QUALITY CONTROL DATA SHEET

REPORT: Dent Fatigue Life Assessment
DOT #432 (DTPH56-10-T-000013)
Closeout Report

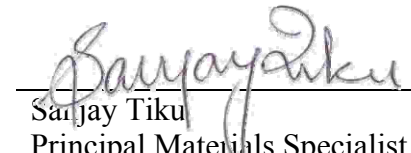
DATE: January 10, 2012

PREPARED BY:



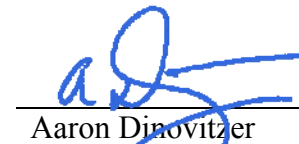
Vlad Semiga
Senior Structural Specialist

REVIEWED BY:



Sanjay Tiku
Principal Materials Specialist

APPROVED BY:



Aaron Dinovitzer
Vice President, E&T

PROJECT TEAM:

Brock Bolton
Vlad Semiga
Sanjay Tiku
Aaron Dinovitzer

REVISION HISTORY RECORD

Revision No.	Date of Issue	Description of Change
00	4 January 2012	Submission in response to Contract Amendment 001 provided November 28, 2011.

TABLE OF CONTENTS

ACRONYMS AND ABBREVIATIONS iv

1 INTRODUCTION 1

 1.1 Project Objective..... 1

 1.2 Project Scope 1

2 PROJECT STATUS..... 3

 2.1 Task 1: Kick-off Meeting..... 3

 2.2 Task 2: State of Knowledge Review and Documentation 3

 2.3 Task 3: Documentation and Further Validation of Dent Modeling 3

 2.4 Task 4: Development and Validation of Fatigue Life Estimation Approach 3

 2.5 Task 5: Development and Calibration of Generalized Severity Ranking..... 4

 2.6 Task 6: Development of Critical Operational Stress/Strain Concept 4

 2.7 Task 7: Industry Workshop..... 4

 2.8 Task 8: Project Management and Reporting..... 4

 2.8.1 Pipeline Safety Research Peer Review 4

3 SUMMARY AND RECOMMENDATIONS..... 5

- ANNEX A TASK 2: STATE OF KNOWLEDGE REVIEW AND DOCUMENTATION
- ANNEX B TASK 3- DOCUMENTATION AND FURTHER VALIDATION OF DENT MODELLING
- ANNEX C TASK 4- DEVELOPMENT AND VALIDATION OF FATIGUE LIFE ESTIMATION APPROACH
- ANNEX D TASK 5- DEVELOPMENT AND CALIBRATION OF GENERALIZED SEVERITY RANKING

LIST OF TABLES

Table 2.1: Proposed Matrix for Numerical Modeling 4

ACRONYMS AND ABBREVIATIONS

DOT	Department of Transportation
FEA	Finite Element Analysis
PHMSA	US DoT Pipeline and Hazardous Materials Safety Administration
PRCI	Pipeline Research Council International
SN	Stress vs. number of cycles
ϵN	Strain vs. number of cycles
BMT	BMT Fleet Technology Limited

1 INTRODUCTION

Federal regulatory standards [1, 2] require repair of dents with depths exceeding 6% of the pipeline diameter and for dents exhibiting signs of mechanical damage interacting with secondary features. However, leaks have been known to occur at dents with depths less than 3% of the pipe diameter and dents interacting with secondary features have been known to survive in service for extended periods of time.

Engineering tools and empirical and mechanistic (numerical) models currently used for assessing the significance of mechanical damage are not able to accurately predict the strain state or fatigue life of the damage feature, as they are based on a number of assumptions (modeling and experimental data) rather than considering the anisotropy of the material properties, kinematic behavior of the materials, non-linear dent response to pressure and/or treating the dent solely as a geometric imperfection. This lack of accuracy can lead to either overly conservative assessments, promoting unnecessary maintenance, or the lack of required maintenance that could result in unexpected failures, which represent a significant environmental and safety concern and increases pipeline operating costs.

1.1 Project Objective

The objective of the current project is to develop a detailed dent assessment procedure based on three dimensional non-linear structural and material responses which will then lead to the development of criteria for ranking the severity of dents and develop a simplified methodology for estimating the remaining life of dent features.

1.2 Project Scope

This project will deliver three related approaches for assessing the fatigue life or cyclic loading dependent failure of pipeline dents (mechanical damage). All three integrity management tools draw upon pipeline operational, design and damage data. The methods provide a range of alternatives for integrity management, where the appropriate method for use is dependent on the desired outcome and the available information. The three methods are:

Level 1- Dent Geometric Severity Ranking: Develop Geometry based criteria to assess the relative severity of plain dent geometries or dent geometries interacting with secondary features. This would provide the user with a means of ranking the relative severity of dents in terms of the effect on the cyclic fatigue life of the pipeline, thus making it possible to prioritize response and remedial action/ actions in an informed manner.

Level 2 –Dent Geometry and Load Severity Ranking: Develop dent severity ranking criterion to assess the effects of geometry and line pressure spectra. This ranking criterion will improve on the Level 1 ranking by considering the operational pressure spectrum to include the effect of applied loading on severity ranking.

Level 3- Dent Fatigue Life Assessment Guidance Note: A detailed fatigue life assessment module (the detailed numerical (FEA) model underpinning the previous tools) – This model is intended to provide a life assessment for mechanical damage features. This model will likely only be used in fitness for purpose of unique or high consequence damage features. The approach will provide a detailed guidance note on the techniques used to assess the fatigue life of

a dented pipeline segment. This deliverable will permit others to apply the techniques used to develop life assessments and understand the development of the tools used to develop Level 1 and 2 ranking systems.

Eight interrelated tasks were defined in the proposal to accomplish the project scope and are identified below:

- Task 1: Project Kick-Off Meeting
- Task 2: State of Knowledge Review and Documentation
- Task 3: Documentation and Further Validation of Dent Modeling
- Task 4: Development and Validation of Fatigue Life Estimation Approach
- Task 5: Development and Calibration of Generalized Severity Ranking
- Task 6: Development of Critical Operational Stress/Strain Concept
- Task 7: Industry Workshop
- Task 8: Project Management and Reporting

2 PROJECT STATUS

2.1 Task 1: Kick-off Meeting

A teleconference was held with PHMSA and industry representatives and a presentation was made on the objectives, scope, deliverables and schedule. The presentation material was subsequently uploaded to the DOT website.

A meeting was also held in Montreal in October 2010 with pipeline industry representatives to go over in detail on the project scope and objective.

Another meeting in conjunction with PRCI technical meeting was held in Atlanta in February 2011 with PHMSA representative and broader pipeline industry representative to go over the project scope and progress to date was presented.

Status: Complete

2.2 Task 2: State of Knowledge Review and Documentation

Literature review was carried out to identify, gather and review past and current research into the behaviour of dented pipelines and a report has been prepared and included in Annex A of the present report.

Status: Complete

2.3 Task 3: Documentation and Further Validation of Dent Modeling

Detailed three dimensional non-linear finite element dent modeling was carried out. The validation was carried out using the data from the full scale experimental joint test program supported by PRCI and DOT (PRCI Project # MD-4-2, DOT 339), which uses rigid spherical indenters to create single peak dents for a variety of testing scenarios. The dent modeling validation results are included in the Annex B of the present report.

Status: Complete

2.4 Task 4: Development and Validation of Fatigue Life Estimation Approach

Three fatigue life estimation approaches, stress versus number of cycles (SN), strain versus number of cycles (ϵ N) and fatigue crack growth are being used to calculate the fatigue lives based on the stress and strain range output from the detailed finite element models developed in Task 3. The task includes the evaluation of the effect of mean stress on the estimated fatigue life. The predicted lives are being compared with the full scale test results generated under the joint project supported by PRCI and DOT (PRCI Project # MD-4-2, DOT 339).

The progress to date has been included in the Annex C of the present report.

Status: On-going

2.5 Task 5: Development and Calibration of Generalized Severity Ranking

In this task a generalized dent severity ranking criteria is being developed and calibrated. The dent severity criteria will take into account dent shape and size, pipe geometry (d/t), material grade and the effect of welds in order to relatively rank the potential severity of various dents with respect to the cyclic fatigue performance of the dented pipeline. This task will involve developing an extensive numerical modeling matrix (see Table 2.1) encompassing a wide range of dent scenarios and post processing the numerical/analytical results to develop a regression equation that is capable of ranking the relative severity of the dents based on the dent and pipe geometries and material grade.

Table 2.1: Proposed Matrix for Numerical Modeling

Parameters	Minimum Number of Variations
Pipe diameter /Wall thickness	3
Material Grade	2
Condition	2
Dent depth	5
Indenter Size	6

The progress to date has been reported in Annex D of the present report and involves the evaluation of the prior BMT dent assessment approach, selection of the dent geometric parameters, their effect on the fatigue life so that appropriate range of parameters can be selected for the numerical modeling matrix.

Status: On-going

2.6 Task 6: Development of Critical Operational Stress/Strain Concept

Status: To be carried out

2.7 Task 7: Industry Workshop

Status: To be carried out

2.8 Task 8: Project Management and Reporting

Monthly status updates and quarterly progress reports were prepared and delivered/uploaded to the DOT website.

2.8.1 Pipeline Safety Research Peer Review

Presentation was prepared as per the guidelines and template provided by DOT for the peer review meeting and presentation made in an on-line peer review meeting organized by DOT.

Status: On-going

3 SUMMARY AND RECOMMENDATIONS

The literature review task was completed with the objective of identifying, gathering and reviewing past and current research on the behaviour of dented pipelines. Based on the review some of the potential improvements that should be pursued in developing both a detailed fatigue life assessment methodology and the simplified assessment approach have been identified including:

- Dent depth alone is generally not an accurate predictor of the severity of the dent in terms of its impact on the fatigue life of a pipe. The dent fatigue response is affected by a number of parameters, including, dent depth, dent length, dent width, depth ratio (d/D) and length ratio (L/D). In line with these findings, the development of the simplified fatigue life assessment approach should consider the use of a wide variety of dent/pipe shape parameters. Therefore, a greater range of pipe geometries (i.e., D/t), material grades and dent geometries (i.e., dent length, width, depth) to be included in the development of the methodology.
- A nonlinear kinematic material model should be used to model the material response during dent formation, re-rounding and cyclic loading. This will result in a more accurate prediction of the strain response, particularly for scenarios where cyclic plasticity could play a significant role
- The dent validation methodology should not be just limited to a comparison of predicted and experimental fatigue lives. The reason for any discrepancies between the two, whether conservative or unconservative, could not then be explained i.e., was it due to inaccurate strain/stress estimates from the finite element analysis or inaccuracies in the damage accumulation/failure criteria.
- Dent response and therefore dent fatigue life is dependent on dent restraint condition. If different methodologies are developed for restrained and unrestrained dent then a methodology needs to be developed to help determine whether the dent is restrained or unrestrained.

The dent modeling task was completed where detailed three dimensional non-linear finite element dent modeling was carried out to further validate BMT dent model. The dent validation was carried out using data generated in the full scale dent fatigue test program supported by PRCI and DOT. The validation task included comparing load displacement data, dent formation strain data, cyclic strain data during pressure cycling and dent shape data as recommended in the path forward of the literature review task.

The dent validation task did not include complex shape dents and multi peak dents as detailed full scale experimental test data is not available. The future dent assessment program should therefore incorporate full scale dent fatigue test program incorporating complex dent shapes to validate the dent models against complex shapes.

The dent validation task also did not incorporate dent interaction with metal loss as experimental data for dent metal loss is very limited and it was beyond the scope of the present program. The dent assessment program should be expanded to include dent interaction with metal loss as the in line inspection techniques being currently used/developed are becoming better in detecting and accurately sizing metal loss features interacting with dents.

The parameters identified in the proposed numerical modeling matrix for developing dent severity ranking and life assessment may need to be increased, e.g., the number of d/t parameters may need to be increased to 5 (from 3 in the proposed matrix) and similarly dent depth and shape parameters may need to be increased so as to encompass a wide range of dent shapes and sizes in wide range of pipe geometries.

The current program does not define the dent weld interaction criteria, i.e., how close a dent has to be to a weld to be considered to be interacting with the weld. Therefore, it is recommended that dent assessment criteria should be expanded to include development of dent weld interaction criteria.

ANNEX A
TASK 2: STATE OF KNOWLEDGE REVIEW AND DOCUMENTATION

TABLE OF CONTENTS

ACRONYMS AND ABBREVIATIONS	iii
A.1 INTRODUCTION	1
A.1.1 Project Objective.....	1
A.2 REVIEW OF PREVIOUS DENT CHARACTERIZATION EFFORTS	2
A.2.1 Review of Historical Efforts	2
A.2.2 NG-18 Early Studies.....	6
A.2.3 Texas A&M Study	7
A.2.4 CSA Study on Dent Acceptance.....	11
A.2.5 Stress Engineering Services.....	12
A.2.6 Effect of Dents on Stress in Cylindrical Shells.....	16
A.3 DENT ASSESSMENT MODELS	17
A.3.1 Dent Re-rounding Behaviour	17
A.3.2 Dents on Girth Welds.....	18
A.3.3 Gaz de France	18
A.3.4 PDAM	19
A.3.5 Q - Factor.....	21
A.3.6 British Gas	22
A.3.7 Fatigue with Severe Mechanical Damage.....	22
A.3.8 EPRG Fatigue Life.....	23
A.3.9 EPRG Denting and Puncturing Models	24
A.3.10 Rinehart and Keating	25
A.3.11 Battelle Pipeline Technology	25
A.3.12 Summary	25
A.4 DENTED PIPELINE FATIGUE LIFE PREDICTION METHODOLOGIES.....	28
A.4.1 <i>Cyclic Pressure Fatigue Life of Pipelines with Plain Dents, Dents with Gouges, and Dents with Welds</i> , J.R. Fowler, et al [19].....	28
A.4.2 <i>Effect of Smooth and Rock Dents on Liquid Petroleum Pipeline (API 1156)</i> , C.R. Alexander, J.F. Kiefner, [24]	29
A.4.3 <i>Development of a Model for Fatigue Rating Shallow Unrestrained Dents</i> , M. J. Rosenfeld [27].....	30
A.4.4 <i>Guidelines for the Assessment of Dents on Welds</i> , M. J. Rosenfeld [29]	31
A.4.5 <i>EPRG Methods for Assessing the Tolerance and Resistance of Pipelines to External Damage Part 1 and 2</i> , R.J. Bood, et al [42].....	32
A.4.6 Comparison of Dented Pipeline Fatigue Life Assessment Methodologies	33
A.5 DEMONSTRATION OF FATIGUE LIFE ASSESSMENT METHODOLOGIES.....	34
A.5.1 Summary of Assumptions.....	34
A.5.2 Fatigue Life Assessment Results	34
A.5.3 Summary of Comparison	38
A.6 PATH FORWARD	39
A.6.1 Wider Range of Dent and Pipe Geometries.....	39
A.6.2 Improved Material Modeling.....	39
A.6.3 Validation of Intermediate Outputs	40

A.6.4	Restrained versus Unrestrained Dents	41
A.6.5	Parameters Governing Dent Fatigue Life	42
A.7	REFERENCES	43

APPENDIX 1 SUMMARY OF EXPERIMENTAL DATA USED IN FATIGUE LIFE METHODOLOGY DEMONSTRATION

LIST OF FIGURES

Figure A.1:	Typical Transverse Stress Distributions of Long and Short Dents [17] for (a) a Typical Dent as Formed, (b) Re-rounding at the Center of a Long Dent, and (c) Short Dents that Do Not Re-round with Tensile Stresses around the Periphery	Error! Bookmark not defined.
Figure A.2:	Comparison of Estimated and Experimental Fatigue Lives	Error! Bookmark not defined.
Figure A.3:	Comparison of Estimated and Experimental Fatigue Lives – Restrained vs Unrestrained Dents	Error! Bookmark not defined.
Figure A.4:	Material Hardening Models.....	Error! Bookmark not defined.

LIST OF TABLES

Table A.1:	Summary of Fatigue Results for NPS 12, 0.398 in. WT Pipe [19]	Error! Bookmark not defined.
Table A.2:	Theoretical Weld Correction Factors [19].....	Error! Bookmark not defined.
Table A.3:	Experimental Gouge Correction Factors [19]	Error! Bookmark not defined.
Table A.4:	Pipeline Defect Assessment Manual (PDAM) Recommended Methods to Predict Burst Strength, from [36]	Error! Bookmark not defined.
Table A.5:	Summary of Dent and Gouge Test Details.....	Error! Bookmark not defined.
Table A.6:	Average Dent Depths and Elastic Springback, 45,000 lb force, X52	Error! Bookmark not defined.
Table A.7:	Estimated and Experimental Fatigue Lives for MD4-2 [46] Specimens	Error! Bookmark not defined.
Table A.8:	Estimated and Experimental Fatigue Lives for Additional Specimens [17, 24]	Error! Bookmark not defined.

ACRONYMS AND ABBREVIATIONS

AE	Acoustic Emission
AGA	American Gas Association
ANG	Associated Natural Gas Corporation
ANSYS	Computer Based Engineering Simulation
ASME	American Society of Mechanical Engineers
ASME BPVC	ASME Boiler and Pressure Vessel Code
BG	British Gas
CANMET	Materials Technology Laboratory
CSA	Canadian Standards Association
CVN	Charpy Vee Notch
DIN	A list of standards published by the Deutsches Institut für Normung
DNV	Det Norske Veritas
DOT	US Department of Transportation
DOE	US Department of Energy
DSAW	Double Submerged Arc Welding
e-N	Strain-life
EPRG	European Pipeline Research Group
ERW	Electric Resistance Welded Pipe
FATT	Fracture Appearance Transition Temperature
FE	Finite Element
FEA	Finite Element Analysis
ID	Inside Diameter
IPC	International Pipeline Conference
IIW	International Institute of Welding
NPS	Nominal Pipe Size
OD	Outside Diameter
PDAM	Pipeline Defect Assessment Manual
PRCI	Pipeline Research Council International
Psi	Pounds per square inch
SCF	Stress Concentration Factor
SMLS	Seamless Steel Pipe
SMYS	Specified Minimum Yield Strength
S-N	Stress-Life
UTS	Ultimate Tensile Strength
WT	Weight

A.1 INTRODUCTION

Federal regulatory standards [1, 2] require repair of dents with depths exceeding 6% of the pipeline diameter and for dents exhibiting signs of mechanical damage interacting with secondary features. However, leaks have been known to occur at dents with depths less than 3% of the pipe diameter and dents interacting with secondary features have been known to survive in service for extended periods of time.

Engineering tools and empirical and mechanistic (numerical) models currently used for assessing the significance of mechanical damage are not able to accurately predict the strain state or fatigue life of the damage feature, as they are based on a number of assumptions (modeling and experimental data) rather than considering the anisotropy of the material properties, kinematic behavior of the materials, non-linear dent response to pressure and/or treating the dent solely as a geometric imperfection. This lack of accuracy can lead to either overly conservative assessments, promoting unnecessary maintenance, or the lack of required maintenance that could result in unexpected failures, which represent a significant environmental and safety concern and increases pipeline operating costs.

The objective of the current project is to develop a detailed dent assessment procedure based on three dimensional non-linear structural and material responses which will then lead to the development of criteria for ranking the severity of dents and develop a simplified methodology for estimating the remaining life of dent features.

A.1.1 Project Objective

The following report documents a state of knowledge literature review that has been carried out to identify, gather and review past and current research into the behaviour of dented pipelines. The objectives of the literature review include:

- Develop an understanding of the general behaviour of dented pipelines.
- Identify and review past efforts, whether experimental or analytically based efforts to characterize and evaluate the effect of a dent on the integrity of a pipeline.
- Develop a list of potential critical parameters that may be used to characterize the effect of a dent on the fatigue life of a pipeline,
- Identify, review and evaluate existing dented pipeline fatigue life prediction methodologies,
- Create a path forward in terms of developing an improved fatigue life prediction methodology for dented pipelines.

The literature review and its primary outcomes are presented in the following sections of this interim report.

A.2 REVIEW OF PREVIOUS DENT CHARACTERIZATION EFFORTS

Over the past 50 years considerable effort has been dedicated towards understanding problems associated with dents in pipelines, including their impact on the integrity of the pipeline system. The work has involved full scale pipe testing programs, laboratory testing of pipe ring samples containing dents, and finite element analysis based studies. The goal of the efforts has been to provide the necessary knowledge and background to allow for the development of guidelines for determining which dents can be left in service, and which ones should be removed to ensure the continued safe operation of the pipeline.

The pipeline industry standards, i.e. CSA Z662 [3] and ASME B31.4 [4], recognize the work undertaken to date in that dents are allowed to remain in service provided that they satisfy certain criteria. The dent characteristics that must be considered to determine whether the pipe should be repaired include the depth of the dent in relation to the diameter, whether the dent contains stress concentrators such as gouges, grooves, arc burns, or cracks, and whether the dent interacts with a mill or field weld.

The references presented in the following sections present a summary of the key features of previous investigations into the behavior of dents in pipelines. The references include historical discussions on dent behavior, small scale and full scale experimental test programs and numerical (i.e., finite element analysis) based investigations. They include discussions relating to the effect of dents, dent-gouge and dent-weld combinations in terms of both the burst pressure and the fatigue life of the pipeline. The references are organized into a number of sections. The first section presents a brief wide ranging review of historical dented pipeline research. This is followed by a number of sections that summarize research that has been carried out by various organizations/researchers over the years. The final section presents a summary of various dented pipeline assessment methodologies, covering both burst and fatigue life prediction methods.

The historical references and the various discussions and findings serve as a guide to developing more advanced dent characterization and fatigue life prediction methods.

A.2.1 Review of Historical Efforts

In a summary of pipeline failures spanning a period of 20 years, Eiber [5] noted that failures in the base metal of pipelines are usually associated with a gouge and a dent. This type of defect often results as a consequence of mishandling during construction, but most often is due to third party activity carried out around the buried pipeline. In these gouge and dent features there is typically a cold worked region at the base of the dent that has shallow surface cracks. In some cases, a 10-20 mil layer of martensite has resulted as a consequence of the impact, or even bits of foreign material have welded to the pipe surface. The internal pressure will attempt to reround the pipe to its original shape, but this in turn results in cyclic bending stresses in the deformed region. The presence of a crack and cyclic stresses can lead to fatigue crack growth and failure of the pipeline. Eiber [5] suggests that it is impossible to estimate the severity of mechanical damage defects on appearance alone, and suggests that they be considered on the verge of failure. The authors, of the failure reports, have similarly noted that dents will often contain some mechanical damage from which a failure has initiated. .

One of the first reported studies on dents was undertaken by Belonos and Ryan [6] in the 1950s as a result of growing interest in the gas pipeline industry with regards to the performance of pipelines containing dents. Their tests considered the effects of internal pressure, residual stress, and static internal pressure at failure for dented pipe. The residual stresses were obtained by strain gauging the dented pipe and recording the strain changes as the pipe was cut shorter.

Tests on an NPS 26, X52 pipe with a 3% oval dent ($l/w = 0.7$) showed that the external residual stresses were -45300 psi transverse and -20700 psi longitudinal. The tests on the NPS 20, X42 pipe used a 2% deep continuous dent for residual stress measurements and burst tests. The same pipe was not used for both as the residual stresses were obtained by cutting the length of the dented pipe and measuring relieved stresses. The transverse residual stresses in various portions of the dent were approximately the same absolute value, $24,694$ psi and $-23,938$ psi, and the maximum longitudinal stress of $23,053$ psi was noted at the centre of the dent. The stresses are reported at pressures of 1000 and 1200 psi (yield pressure of 1050 psi) and 5 test results showed that the pipe burst away from the dent at pressures between 1580 and 1725 psi (UTS pressure 1650 psi). They noted that the dents were completely removed during pressure testing at pressures between 850 and 1200 psi. The results include stresses calculated as the pressure was increased during testing for the different regions of the dent, and show how yielding occurs in some regions. It is suggested that residual stresses should be added algebraically to get the true stress. The authors conclude that dents, even though they can have high residual stresses, do not affect the service performance unless there is a notch or scratch, or metallurgical notch such as cold work, within the dent.

In the early 1980s, CANMET began a systematic series of studies to examine the behavior of dents under typical pipeline loading conditions. The first report [7] included 8 tests where four different round indenters were used to hydraulically form plain dents to a depth of 6% of the pipe OD (before rerounding). The pipe diameters ranged from 8 to 20 in, with wall thickness from 5.59 to 9.65 mm. The dents either simulated construction damage, i.e., dented and then hydrostatically tested, or in-service damage, i.e., formed after the hydrotest and then fatigue tested up to 12000 cycles at pressures corresponding to hoop stresses as high as 80% SMYS. The test results provide information on the strains on the inside and outside surface of the pipe wall in the dented region, during pressurization and during fatigue testing. An equation was developed relating the hoop strain in the dent to the dent depth at 110% of yield, i.e. during the initial pressure test. The final part of the test procedure was to pressurize the pipe to 110% SMYS. Cracks were observed in only one specimen near the ends of a long dent where rerounding was restricted; a repeat of the test failed to produce cracks. No cracking was observed in any of the other tests. The authors suggest that further studies would hopefully aid in explaining the reason for cracking at the end of this dent.

Tyson and Wang [8] summarized the laboratory work at CANMET related to dents, gouges, and gouges in dents; the damage was produced using 4 types of indenters and one gouging process on the following pipe:

- NPS 6, 6.86 mm WT;
- NPS 8, 8.0 mm WT;

- NPS 12, 9.70 mm WT; and
- NPS 20, 9.65 and 5.59 mm WT.

Formulae are presented to calculate the failure pressures for various forms of damage, comparing them to the experimental results. No reduction of failure pressures was observed for dents alone; however, in one case failure occurred by fatigue after 3000 cycles at the curved ends of a long dent. For gouges, a modified strip yield model using toughness estimated from Charpy data was able to conservatively estimate failure pressures. The case of a gouge in a dent can be analyzed by considering the bending component of the stress intensity factor and by calculating the collapse stress for a part-through surface crack. Gouges in dents result in lower failure pressures than either dents or gouges alone. This summary paper does not contain many experimental details, and one would need to go to the individual references by K.C. Wang for complete details.

A brief summary of research prior to 1987 is provided by Maxey [9], in which he summarizes work completed at British Gas and Battelle. British Gas tested rings cut from damaged pipe where the specimens were tested in a ring yield machine. The program also included tests on pipe that was damaged both before and after pressurization. The Battelle work included full-scale burst tests on pipe that was damaged both before and after pressurization, and investigated the influence of gouge length, a variable that could not be considered in the BG ring tests. The variables that were examined by BG and Battelle include the following:

- Gouge depth
- Gouge length
- Dent depth
- Pipe size
- Pipe toughness (Charpy upper shelf energy)
- Pipe yield strength
- Failure pressure

Maxey [10] expands on previous work to consider the effects of temperature on the failure characteristics of dented and gouged pipe, as well as the crack growth that occurs with different hold pressures. Pipe tested below the fracture appearance transition temperature (FATT) failed in a brittle manner, while above the FATT the pipe leaked after stable through-wall tearing. The hold experiments showed that crack growth did not occur until pressures over 70% of the final failure pressure were achieved. The dents in this case were 5% of the pipe wall; they rerounded immediately upon pressurization, and the recovery was linear up to the failure pressure. The concluding part of the article describes tests that were completed in which pressurized pipe (pressurized to 50, 60, or 72% of SMYS) was dynamically gouged and dented. In some cases the pipe failed immediately, while the majority of defects failed later during pressure testing. The details of the experiments noted that the pipe rerounds immediately following the passage of the denting tool, and that for long dents the centre portion rerounds and becomes almost flat, whereas the ends of the gouge and dent combination show less recovery to the original shape.

The variables that were included in the experiments are as follows:

- Pipe grade: X52 to X65
- Diameter: NPS 20 to NPS 42
- Wall thickness: 0.296 to 0.498 in.
- CVN upper shelf 2/3 size: 15 to 45 ft-lb.
- Gouge length: 7 to 24.5 in.
- Gouge depth: 0.010 to 0.100 in.
- Dent depth: 0.21 to 1.20 in.

A method is described by Maxey in the conclusion to the article [11] that can be used to determine the significance of dent/gouge combinations by calculating the expected failure pressure using a parameter, Q . This parameter includes pipe toughness (CVN), gouge length ($2c$), dent depth/pipe diameter ratio ($D/2R$), and gouge depth/pipe thickness (d/t), as follows:

$$Q = \frac{CVN}{\left(\frac{D}{2R}\right)\left(\frac{d}{t}\right)(2c)}$$

The gouge/dent details, material properties, and operating pressure are needed for the analysis. The paper includes results for two experiments that used acoustic emission (AE) to detect crack growth activity for pressurized pipe. The hold pressure was increased if the AE activity stopped, and showed that there was crack growth at each of the pressures until the crack led to failure. Maxey notes that for the case of longer dents (more than 8 in.), the middle of the dent will attempt to return to its original shape sooner than the ends of the gouged area, and that initial surface cracking will occur in the flexible centre of the gouge.

Bjornoy et al [12] completed 14 full-scale tests, 5 plain dent tests on X52 pipe and 9 gouged dents on X65 pipe with various repairs made to the gouges. The results included the dent depths, the loads used to produce the dents, including springback, the depth of grinding repair, and a brief description of each test. The dents with gouges had the lowest burst pressure, and it was shown that grinding below the depth of any cracks (and a bit further) was necessary to restore the full load carrying capacity of the pipe.

Lancaster and Palmer [13] describe experimental work completed using aluminum pipe to model steel pipelines. Short, smooth dents were made in unpressurized pipe to a nominal depth of 13%. The dents were strain gauged and tested to pressures as high as 1.1 yield pressure. The peak strains occurred along the pipe axis at the ends of the dents, in “crescent-shaped zones”. The strains, expressed as strain concentration factors, were greatest at intermediate pressures, p/p_y , of 0.35. The authors cite some of their other published work that showed that gouges placed on these regions of high strain resulted in significantly lower burst test pressures.

The results of the experiment are used by Lancaster and Palmer [14] and compared to full scale tests completed by Battelle, CANMET, and British Gas. The analysis includes machined gouges, but excludes cracking, tearing, and dynamic effects, and it is noted that these results are particularly relevant to the analysis of dents with a gouge where the gouge has been repaired by grinding to remove any cracks. For the case of gouged dents, the results show that the Battelle flow stress model accurately predicts the failure pressures, provided that the gouges are located away from the regions of high strain at the ends of the dents. The results also showed that the dent depth had little influence on the failure pressure, as it was influenced mainly by the gouge depth. When the gouge intersected the regions of high strain, the failure pressures were approximately 50 % of the pressures calculated by the Battelle model. The dent displacement behavior upon unloading was shown to be linear, and followed a line joining the maximum dent depth with the flow stress. Note that these dents were made at zero pressure. The implications here are that the previous loading history of the dent is important in assessing the damage to the pipe. The authors also noted that the gouge depth has no influence on the rerounding behavior.

Battelle [15] has reported on the results of the first year of a PRCI sponsored project looking at developing an improved criterion to assist in serviceability decisions for pipelines with dents and/or gouges. The intent is to extend the concepts of the ductile flaw growth model that has shown to accurately predict the behavior of axial flaws in pipelines. The discussion follows through experimental validation, pipeline support conditions, indenter considerations, pressure stiffening of the pipeline, rerounding, residual dent size, the effect of time and cycle dependent deformation, and line pipe grade. The results are presented primarily as load-displacement curves, showing the displacement as load increases, and then the rebound as the load is removed. The focus of this phase of the work was to investigate the deformation behavior of the pipe and the related changes in stresses and strains. Soil support, line pressure, whether the line was in tension or compression, and the nature of the outside force was seen to have a strong influence on the mechanical damage. The authors conclude that the ductile flaw growth model can be used to predict the serviceability of pipelines subject to mechanical damage.

A.2.2 NG-18 Early Studies

One of the earlier papers on dents was presented by Kiefner [16] at the 4th AGA Symposium on Line Pipe Research. This paper summarized the results from the Fracture Initiation phase of the NG-18 research committee. It goes through a general description of how defects become leaks or rupture, and presents the relationships between flaw size and failure stress.

Some results are presented for gouges in dents for both unpressurized and pressurized pipe. The results for unpressurized tests show that indented notches fail at lower pressures than notches alone, presumably because the pipe ‘unbends’ as it is being pressurized, causing high bending stresses. Also, the longer gouge and dent combinations fail at lower pressures. The results correlated with the depth of the dent and not the depth of the notch, suggesting that the failure pressure depends only on the length of the notch.

Four pressurized pipe tests were summarized where the indenter was pushed into the pipe until failure, using pipe with several wall thicknesses and different internal pressures. Curves are shown with the wedge load plotted against the wedge travel.

Strain gauge readings during pressurization indicated that “the principal effect of plain dents is to introduce highly localized longitudinal and circumferential bending stresses in the pipe wall”. It is also mentioned that “without a sharp stress concentrator in the dent, yielding occurs over large enough areas that no high stress gradients are present”.

A.2.3 Texas A&M Study

A study sponsored by the United States Department of Transportation by Keating and Hoffman [17] involved experimental and finite element modeling of dents in pipelines. Damage included dents due to rocks, dents formed with backhoe teeth, and short longitudinal dents with simulated gouges. The investigation included the effect of dent restraint and the rebound behavior of dents.

Their review of existing data included a study by Urednicek [18] on pipe that was statically pressurized to failure and work completed at Stress Engineering Services [19] where many of the tests included cyclic pressures to simulate field conditions. The authors concluded from their literature review that:

- The fatigue behavior of long, plain dents has been adequately studied experimentally by AGA.
- Short dents and dents restrained against elastic rebound need to be studied.
- Dent residual stresses are influenced by the denting process and the elastic-plastic dent rebound.
- Dent stiffness, which influences the denting process and rebound behavior, is a three-dimensional phenomenon, and 2-D modeling will not accurately represent dent behavior.

The experimental program developed at Texas A&M included 15 pipe specimens, with pipe ranging from NPS 12 to NPS 36, wall thickness of 6.25 and 9.53 mm, and with strengths ranging from Grade B to X60. Three different dent types were used, with the focus being on short dents and restrained dents:

- Type A – 6 in. long dent with simulated damage;
- Type BH-T or BH-L – simulated backhoe dents; and
- Type R – simulated rock dents.

The experiments included measuring the forces required to dent the pipe, the restraint load as the pipe was pressurized to the maximum pressure, and the elastic rebound. The denting force results showed a general trend in increasing force with greater dent depth, but the authors noted that the results did not show any correlation with D/t ratio.

The restraint force measurements showed a general increase with increasing internal pressure. The pipe with smaller D/t ratios showed a smaller change in restraint force with internal pressure, which was attributed to increased pipe stiffness compared to large D/t pipe. They

suggest that the restraint of the object will be lost when the force (due to pressure) exceeds the restraint force. This will cause the dent to rebound, changing the fatigue behavior of the dent and its mode of failure.

Dent rerounding behavior was measured extensively to determine how the dent shapes change as they are pressurized. It was found that with the unrestrained Type A dents, the center of the dent would bulge outward, which resulted in the outer surface being in tension and thus more likely to develop fatigue damage than a dent without a bulge. It is noted, however, that bulging was not observed with large diameter pipe. The change in rerounding behavior with larger diameter led to a difference in fatigue crack location. The larger diameter dents failed in the contact region at the centre of the dent, while cracks with the smaller dents were observed around the dent periphery. The authors suggest that increasing the dent depth and diameter results in an increased dent stiffness that limits rebound and thus limits the reversal of compressive residual stresses. The sketches in Figure 4.1 illustrate the differences with long and short dents with relation to the tensile stresses and crack locations. In Figure 2.1(a) the stresses are compressive below the indenter. Figure 2.1(b) shows that with pressurization on a long dent the center rebounds and becomes tensile, thus promoting crack growth in the center of the dent. With shorter dents the center does not rebound and the edges of the dent exhibit the highest tensile stresses as seen in Figure 2.1(c), thus promoting crack initiation in these regions.

A significant part of the study included an elastic-plastic 3-D finite element analysis to extend the experimental results, with the results reported in terms of displacement, stress, and strain. Displacement was used to predict rebound behavior, stress ranges at likely failure locations, and strain data is used to estimate a damage term for fatigue life. The authors describe the modeling process and techniques used to converge the models to a solution.

In the experimental program it was noted that Type A dents with different initial depths had the same depth (measured at the centre of the dent) following pressurization. This was due to bulging at the centre, as the ends of the dents did show differences. The FEA models showed similar behavior, and a 'rebound ratio' was introduced that can be used to describe the dent's initial depth from its final depth, or vice versa; this ratio is a constant for each combination of pipe diameter, thickness, and grade. Tables of rebound ratios are presented for Type A, BH, G, and H dents. The rebound is related to the stiffness of the pipe, D/t , and the depths of the dents, as the deeper dents tend to be stiffer. The larger diameter pipes tend not to rebound as much at the centre of the dent, thus leading to longer fatigue lives.

The discussion of the longitudinal stress results were similarly shown for each of the dent types. The type A dents list transverse OD surface stresses at locations along the pipe axis and a table is presented to predict where failure would be expected to occur for different pipe dimensions and dent depths, i.e. if they behave as long dents with cracking at the centre, or short dents with peripheral cracks. Similar results for BH cracks predict failures to be predominantly at the periphery of the dent. The Type G indenter results in primarily Mode 1 failures (at the centre of the dent), with Mode 2 failures occurring at large diameters and heavier wall thickness. Type H indenters exhibit behaviors between A and G due to the shorter contact area on the pipe.

The unrestrained rebound behavior of transverse dents was comparable to the longitudinal dents. Consideration needs to be given to the length of the indenter. Stress values around the dent are shown, indicating that cracks can form in the dent contact area or the periphery.

Spherical unrestrained dents behave similar to BH dents, with all failures located at the edges of the dent.

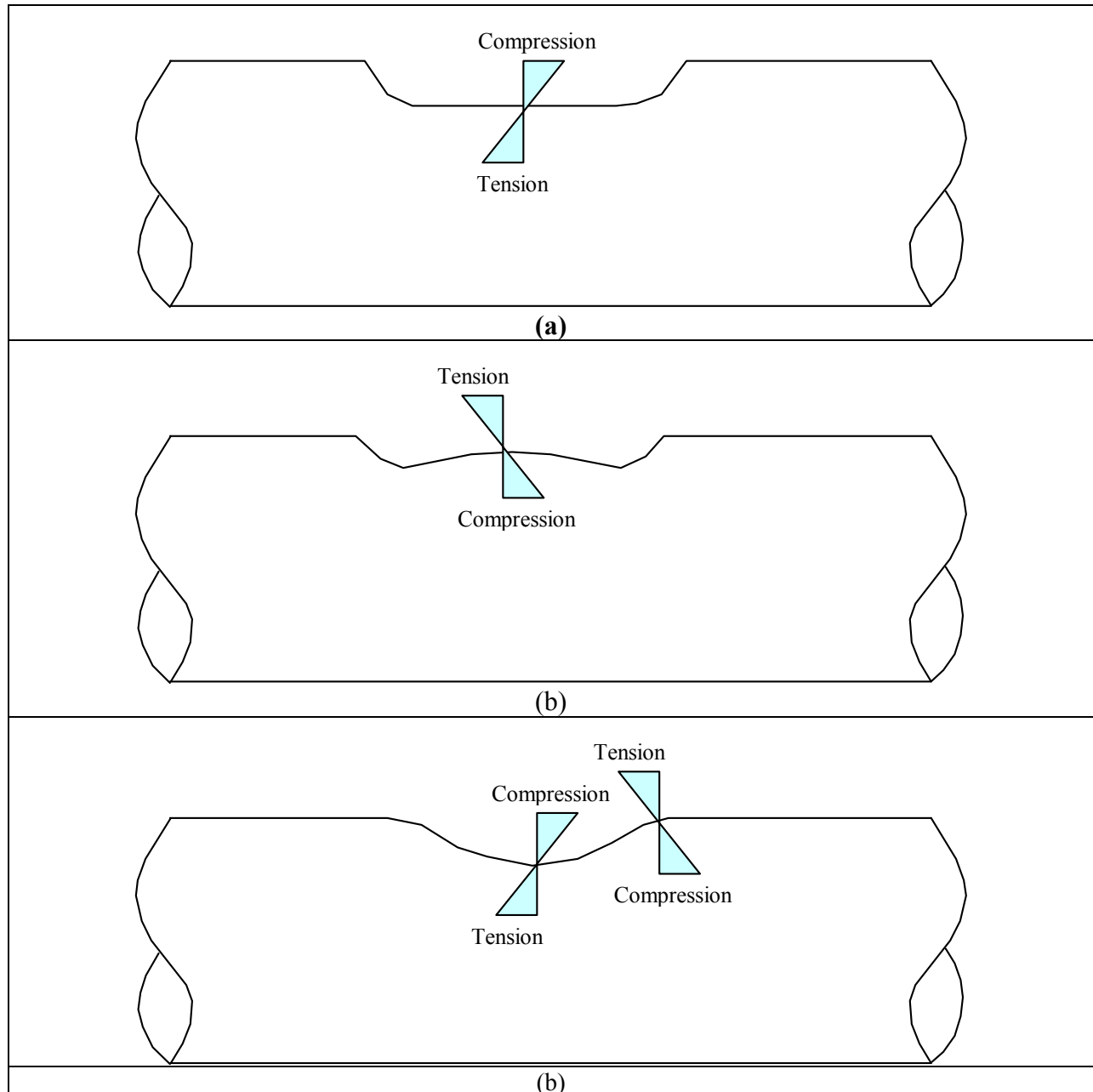


Figure A.1: Typical Transverse Stress Distributions of Long and Short Dents [17] for (a) a Typical Dent as Formed, (b) Re-rounding at the Center of a Long Dent, and (c) Short Dents that Do Not Re-round with Tensile Stresses around the Periphery

Results are also shown for plate indenters that are similar to Fowler's work [19], in that they behave as long dents but do not exhibit bulging.

Restraint was modeled for Types A, BH, and rock (R) dents, using both rigid and flexible restraint. The rigid case was modeled by forcing zero displacement, while the flexible case kept the restraining force constant while the pipe was allowed to rebound. It is expected that actual dents would be between these two cases. The Type A and BH dents all had peripheral cracks. The Type R dents exhibited cracking from the ID surface and transverse to the pipe axis for pipe 8 tests, during the experimental program and spherical indenters were used to model these tests. It was found that low pressure cycling caused high tensile bending stresses on the ID surface, leading to cracking. Shallow dents were seen to have a higher stress range and thus were more likely to fail before deeper restrained dents. The results are explained using the dent depth, restraint flexibility, and dent shape.

The crack locations were either single elliptical cracks in the contact region or multiple cracks on the periphery of the dent. The single elliptical cracks were found only with the Type A dents. The cracks outside of the contact region were found in all dents, but primarily with the BH dents and all restrained dents. The unrestrained Type A dents were observed to exhibit a change in failure mode to the periphery of the dent with larger diameter and depth, which the authors attributed to an increase in dent stiffness and limited rebound, and residual stresses in the contact region. The restrained Type A dents tended to fail at the periphery of the dent due to higher tensile stresses. All BH dents failed by periphery cracking, behaving similar to restrained dents as the sharp geometry prevents significant elastic rebound. Rock dents leaked at both the periphery of the dent and from the inside surface beneath the rock at low pressure.

Other variables that were studied include the influence of longitudinal stress, pipe grade and pressure history, support conditions during indentation, and pressure during indentation.

The model behavior was compared to the experimental results, and it was concluded that modeling could be successfully used instead of experimental testing for both rebound behavior and failure mode.

A general procedure for determining dent acceptance is discussed in Section 5 of Ref [17], describing how the current results can be used to predict dent failure. Keating and Hoffman [17] recommend that dent modeling should be continued to specifically extend the existing data to address the following:

- fatigue behaviour of dents not previously tested, such as transverse and unsymmetrical dents;
- finite element modeling of dents to understand strain data and residual stresses and apply these to damage factors;

- investigate the use of 3-D solid elements in the contact region to better model the stress behavior of the contact region; and
- modeling of soil interaction and restraint, with consideration of different restraint conditions.

A.2.4 CSA Study on Dent Acceptance

The work by Urednicek [18] that was referenced by Keating [17] had been prepared when the acceptance criteria for dents in gas pipelines (in CSA Z184-M1983, Gas Pipeline Systems) was at 2% of the pipe OD, i.e., the same as for new construction. (A comment in the summary suggests that it had already been changed to 6% of the OD in CSA Z183, Oil Pipeline Systems for operating pipelines).

An analysis of experimental work and Nova's operational experience was used to review the current guidelines regarding plain dents and dents with gouges. The data included dents with welds and dents with gouges, using some of the work completed at British Gas [20].

Information is provided in a summary table (Table A.6) on the results of four failure analyses of Nova/ANG dents with cracks. They were all rock induced damage and all had scoring on the ID surface. The dents ranged in depth from 30 to 44 mm, giving depth/diameter ratios from 3.3 to 4.81 %. Two of the dents had through-wall cracks, one was cracked to 70% WT, and no cracking was found on the remaining dent. The conclusion common to all of the failure investigations was that cracking resulted from "tensile overload resulting from a continuous rock penetration". Results are also presented for Nova tests on rock-induced plain dents and Columbia Gas [6] results for plain dents.

It was determined that plain dents up to 10% of the OD in depth could remain in service without an adverse affect on pipeline integrity, and it was recommended that the 6% criteria be adopted for plain dents in gas pipelines. The nominal hoop stress at failure in the data set analyzed exceeded the flow stress of the linepipe.

Full-scale tests of dents produced by rocks were removed from service and pressure tested. They behaved similar to plain dents, but there was a low risk of cracks forming within dents caused by large, sharp rocks. Urednicek [18] recommended that operators should confirm the absence of cracking by visual and nondestructive examination on a sample of the dent population when numerous dents are indicated from internal inspection in rocky terrain.

Urednicek [18] also recommended increasing the acceptance criterion for plain dents on in-service pipelines greater than NPS 12 from 2% to 6% of the pipe OD.

A.2.5 Stress Engineering Services

In the early 1990s, Stress Engineering Services undertook several studies of dented pipe for the American Gas Association [19]. Their work included a summary of the literature to date, followed by experimental and theoretical work to study the following variables:

- Dent shape: round bar pressed into pipe transverse to pipe axis, round bar parallel to pipe axis, and flat plate
- Diameter/wall thickness: 18 to 94
- Yield strength: 51 to 84 ksi
- Dent depth, d/D : 1% to 20%
- Dent length, L/D : 2 to 5
- Pressure Fluctuations: 700 to 1000 psi for gas, 550 to 1200 psi for oil
- Process of pipe manufacture: SMLS, ERW, DSAW
- Surface condition: smooth, rough, gouge, weld

The results are described as Phase I (no gouges) and Phase II (gouges). Phase I work showed that neither the dent type nor the dent length were important in terms of reducing the fatigue life, but the dent depth, D/t ratio, and weld type were important factors. In order to produce a dent with a given final depth, it was necessary to indent the pipe to about twice the desired depth. The rebound of the pipe following release of the indenter was greatest for thin-walled pipe. Their studies indicated that smooth dents less than 5% of the pipe OD should not pose a significant threat to the integrity of a pipeline unless it is subjected to severe pressure cycling. This is consistent with operating experience that suggests that shallow dents on the order of 2%-3% of the pipe OD can fail under the right combination of dent geometry, pipe dimensions and operating pressure spectrum. Similarly, gradual dents in excess of 6% of the pipe OD may pose no threat to integrity within the design life of a pipeline.

To provide guidance for cases that were not covered experimentally, Fowler et al [23] undertook finite element analyses to determine the important dent features. They used an elastic-plastic model using half symmetry and 3-D shell elements, and rigid elements for the indenters. The models were loaded using the same sequence as the experimental tests and then fatigued to failure. These results were used to develop dent stress concentration factors that could later be used to predict the life of a dented pipe. The stress concentration factors varied from 3 to 5 with different D/t ratios. Additional information on stress concentration factors is provided in a short information note to highlight the work that Stress Engineering Services had completed related to dents, with an emphasis of marine damage from keels and anchors. It provides some figures from other references plotting cycles to failure vs. D/t ratio and SCF vs. D/t ratio. In the first case, it is seen that a 15% WT gouge can fail after one cycle, while 10% and 5% gouges take approximately 100 cycles to fail. There is an improvement with grinding, and an indication that

D/t does not play much of a role in failure beyond a D/t of 40. This observation is supported by finite element analyses that show the SCF to increase rapidly from D/t ratios of 20, and peak at D/t of 50. The SCF is as high as 100 for a 5% dent.

Further work by Fowler et al [19] addresses dents, gouges, and weld effects, and includes both experimental and finite element analyses (elastic and plastic) on pipes with D/t ranging from 19 to 94 experimentally and 18 to 100 theoretically. All pipes were fatigue tested and a procedure was developed to predict the life for unrestrained plain dents.

The results indicated that plain smooth dents less than 5% should not be a problem unless subjected to severe cycling. Gouge depth had a significant impact on life, with unground gouges >10% having essentially no fatigue life. It was shown that grinding out gouges restored the fatigue life. The gouge depth is best described with respect to pipe WT. Dents on girth welds had considerably shorter lives than dents away from these welds. Dents with peaks positioned 71 degrees from the ERW long seam weld had virtually the same fatigue lives as dents centered on the long seam; these were the two regions of highest stress from the FEA results.

The details of testing and the experimental results are briefly described for each of the tests, and results are compared amongst the various tests. The results include the number of cycles to failure and the failure locations. Some of the results related to comparing smooth dents with dents associated with secondary effects are described in the following paragraphs.

A series of tests considered the influence of longitudinal seam welds and girth welds, as shown in Table 2.1. The first two dents at 5% depth did not fail, while all other dents failed at the cycles indicated. The next grouping of dents is 10% deep and shows the influence of the welds on both longitudinal welds and girth welds. Dent 7 on the pipe failed after 78,754 cycles and Dent 2 on the long seam failed at 61,218 cycles, which is a slight reduction, but Dent 2 had a slightly deeper final dent depth. In contrast, Dents 4 and 5 on the girth weld failed at 52,155 and 42,690 cycles, considerably less than the 78,754 cycles for Dent 7 on the pipe wall. The two 15% deep dents failed at similar numbers of cycles. The results support the conclusions that the dents on the pipe body did not have significantly greater lives than the dents on the high toughness ERW longitudinal welds, and that girth welds are important when considering a reduction in fatigue life.

Table A.1: Summary of Fatigue Results for NPS 12, 0.398 in. WT Pipe [19]

Dent No.	% Dent Depth, d/D		Dent Location Relative to Welds	Pressure Cycles, psi	
	Initial	Final		$\Delta P = 400$	$\Delta P = 900$
3	5	5.16	On longitudinal weld	49,331	29,423
6	5	5.40	71° off longitudinal weld	49,331	29,423
2	10	8.08	On longitudinal weld	49,331	11,887
4	10	7.11	On girth weld, 90° from long seam	49,331	2,824
5	10	6.66	On girth weld, 90° from long seam	42,690	-
7	10	7.94	71° off longitudinal weld	49,331	29,423
1	15	9.93	On longitudinal weld	49,331	-
8	15	9.75	71° off longitudinal weld	45,221	-

Fowler et al [19] also show that gouges (with and without dents) have a significant influence on fatigue life. For example, a 5% deep gouge has a fatigue life that is 3½ times greater than a 15% deep gouge. They also show that grinding out a gouge increases the fatigue life threefold compared to the same gouge without grinding due to the removal of microcracks.

The techniques used for FEA modeling are described, providing indications of some of the limitations on dent depths that could be achieved and the locations of maximum stresses. The maximum stress concentrations from FEA were reported at the dent centre on the OD surface at the top of the pipe and approximately 70 degrees off vertical on the ID surface. These locations corresponded to the crack locations in the experimental tests. The ratios of hoop stress to internal pressure were tabulated for all of the cases, as these are used to predict the fatigue life based on Miner's Law.

The predicted fatigue lives are based on using the results for plain dents and then multiplying the life extracted from an API X' curve by a correction factor for either gouges or welds. Examples of theoretical and experimental "Gouge Correction Factors" and "Weld Correction Factors" are shown in Table A.2 and Table A.3.

Table A.2: Theoretical Weld Correction Factors [19]

D/t	% Dent Depth	Dent Location Relative to Welds	Weld Correction Factor
32	10	On pipe body	3.26
32	10	On longitudinal weld	1.46
32	10	On girth weld	0.534

Table A.3: Experimental Gouge Correction Factors [19]

D/t	Dent d/D	Gouge Depth, % t	Weld Correction Factor
32	7.17	5	0.025
32	7.21	10	0.0096
32	7.06	15	0.0068

A more recent study on the effects of dents and mechanical damage on pipeline integrity [24, 25] was carried out by Stress Engineering Services under API sponsorship (API 1156). The first of two reports [24] summarizes the results of tests completed on NPS 12 pipe, with a few tests using NPS 24 and NPS 32 pipe. The results are comprehensive in that they include the indented shapes of the pipe, the total number of cycles to failure in fatigue tests, and details of any cracks in each of the tests. Tests to determine the puncture resistance of the pipe were also completed to find the dent depths that would cause the pipe to fail. With each of the sets of experiments, there is a discussion of the mechanics of the tests and the significant observations. The appendices contain techniques that allow one to determine the equivalent number of cycles to failure based on Miner's Rule, and has a literature review summary that highlights the investigations that have been completed to date. The second report in this investigation [25] addressed many of the questions that had been raised in the first part of the study, namely indenter diameter, additional puncture tests, corrosion within dents, interaction of closely-spaced dents, the timing of when the dents were introduced into the pipe and the pressures during rerounding, and three tests on buckled pipe.

Overall, API 1156 looked at a number of variables, which included dent depth, indenter type, pipe diameter, pipe wall thickness, smooth and sharp dents, both constrained and unconstrained, stress concentrations (corrosion, weld seams, and girth welds), and the effect of hydrostatic testing. Most dents were made without the pipe being pressurized, some tests were made with pressurized pipe, others were tested straight to failure by puncturing, and the remainder was fatigue tested. The main findings included the following:

- The pressure carrying capacity of the pipe was not affected by smooth dents without stress concentrators.
- The dents rerounded elastically up to 67% of the maximum depth upon removing the indenter, and rerounded up to 88% upon pressurization to 65% SMYS.
- For unconstrained smooth dents, the fatigue life was shorter for deeper dents.
- Minor stress concentrators such as girth welds reduced the fatigue life somewhat.
- Partially overlapping smooth dents have shorter fatigue lives than individual dents.
- Hydrostatic testing has a beneficial effect on fatigue life due to rerounding of the dent.
- Smooth dents failed by leaks in all cases, they were oriented longitudinally, and initiated on the OD surface. In most cases the cracks were located on the sloping transition on the ends of the dents. For constrained dents, the leaks were oriented transversely, and had initiated on the ID surfaces. All failures were ductile in nature.

A.2.6 Effect of Dents on Stress in Cylindrical Shells

A general investigation of the effect of localized geometric imperfections on the stress response of pipelines has been carried out by Rinehart [26]. The work covers a wide range of topics including 3D finite element analysis and 2D elastic semi-analytical analysis of dented cylindrical shells for a wide variety of dent shapes, with the aim of estimating stress concentration factors (SCFs) associated with dent shapes.

The work highlights a number of interesting findings in terms of the behavior of dents and the effect of the dent shape on the stress response of the pipe wall.

- Dent length plays a significant role in the detailed stress response for unrestrained dents.
- Short unrestrained dents have a peak stress range in the shoulder region of the dent.
- Long unrestrained dents exhibit a peak stress range in the centre of the dent.
- Dent restraint plays a role in the stress response and influences how short and long dents behave.
- Behaviour exhibited by dents is affected by the pipe diameter (i.e., relative dent depth).
- A relationship between the cyclic stress range and fatigue life with the non-dimensional volumetric parameter shown below:

$$\frac{L d_f w}{D^2 t}$$

Where:

- L = length of dent
- d_f = dent depth
- w = width of dent
- D = pipe outer diameter
- t = pipe wall thickness

A.3 DENT ASSESSMENT MODELS

The following section summarizes a variety of references which present different methods for assessing the effect of dents on the integrity of pipelines. In general the methods cover plain dents, and dent gouge combinations, and include methods to predict the burst pressure and the fatigue life of pipelines containing dents.

A.3.1 Dent Re-rounding Behaviour

Rosenfeld [27, 28] completed a study for the American Gas Association to develop a theoretical model to describe the re-rounding of a dent in pressurized pipe. The model was assumed to be long, so that only the cross-sectional shape was considered, and the analysis used a cyclic flow strength to account for the Baushinger effect and strain hardening.

The mechanics of dent re-rounding were described to show that it takes several cycles of pressure for the dent to become completely re-rounded. Other equations are presented to calculate the rebounded dent depth using the pipe dimensions, the initial dent depth, the width of the dent at half of the maximum dent depth, and the pressure in the pipe. Formulas for calculating the bending strains at the apex of the dent and the re-rounded dent width are provided and then used to determine the fatigue life of the dents, based on the number of cycles for fatigue crack initiation. The calculations are compared to results from other sources in the literature.

Some of the comments related to an analysis of the results include:

- Fatigue life is highest for low and high mean operating stress levels, as the low end stresses are not great enough to drive the crack, while on the high end the pipe is re-rounded so that the cyclic stress components are low.
- Fatigue life decreases with increasing D/t , presumably due to reduced stiffness.
- Fatigue life decreases with greater dent depths, due to greater damage upon initial re-rounding.
- Fatigue life increases with increasing d/w , as the wider dents have greater elastic stress ranges than narrow dents.
- Fatigue life decreases with increasing material grade because of less plastic re-rounding and larger elastic stress ranges.

The author then goes on to recommend how to remedy dents on oil and gas pipelines. As gas lines are unlikely to initiate fatigue cracks, the operator can excavate the pipe, then examine and/or repair the coating. For liquids lines, as the unrestrained dent is likely to initiate a fatigue crack, it might be better to leave the rock in place if the coating condition can be determined as adequate, or the pipe should be sleeved. One of the primary reasons for undertaking this study

was the general feeling that fatigue life may be a more rational basis for rating the severity of a dent than present criteria, which rely solely on dent depth with a maximum depth of 6% of the pipe diameter. It is suggested by Rosenfeld that in some cases, deeper dents might be permitted to remain in service, while in other cases, shallower dents should be repaired.

It is suggested that the model could be applied to dents with mechanical damage if a suitable crack propagation model is used.

A.3.2 Dents on Girth Welds

A procedure developed by Rosenfeld et al [29] to estimate the fatigue life of shallow dents on pipeline girth welds without mechanical damage is presented, and consists of the following steps:

1. Estimate a stress concentration factor from reported results (Fowler [19]).
2. Use pressure history to determine operating pressure histogram.
3. Select appropriate (IIW) S-N curve [30], considering weld quality based on API workmanship criteria.
4. Estimate fatigue life using Miner's Rule of Linear Cumulative Damage.

The procedure was demonstrated using test results from Fowler [19] and showed that the fatigue life depended to a large degree on the operating pressure history, and that for girth welds the most likely failure mode would lead to a leak.

A recent paper by Buitrago and Hsu [31] describes a linear elastic analysis of $\frac{1}{4}$ pipe shape for (1) a circular cross-section dent with sharp corners, and (2) an elliptical dent with rounded corners. The trough or bottom of the dents was flat and therefore the shapes do not represent typical dent shapes that one might find in the field. The peak stresses were found to lie in the center of the trough and moved to the sides at higher D/t ratios. The stress concentration factors were listed for axial and in-plane bending forces; they were proportional to pipe diameter, and inversely proportional to the square root of pipe wall thickness and dent length. In the dent description, they define the following parameters:

- pipe diameter to thickness, D/T, ratio;
- dent depth to length, d/l, or aspect ratio; and
- dent depth to pipe diameter, d/D, ratio.

A.3.3 Gaz de France

Gaz de France has been investigating damage to pipelines using both experimental and numerical means [32, 33]. One finite element model considers static denting, and the other addresses dynamic puncture, and they take into account large non-linearities: large displacements and strains, elastic-plastic material properties, contact between indenter and pipe, and the rupture process. Details are provided describing the mesh size selection and failure models, with failure models describing ductile rupture mechanisms such as softening and cavity growth. A separate

paper [34] describes the capabilities of the rig to produce mechanical damage type defects on pipe, and shows some preliminary results of gouge tests, both static and dynamic. The gouges are observed to have transverse lines at the bottom of the gouge that are characteristic of ‘stick-slip’ conditions during wear tests. The experimental results [35] address the static and dynamic puncture resistance of gas pipelines, using pipe with diameters from 8 to 48 in OD and new and worn excavator teeth. They confirm earlier findings that the puncture

A.3.4 PDAM

Cosham and Hopkins [36] recently completed a study (The Pipeline Defect Assessment Manual) to provide guidance to pipeline operators as to the best methods available to assess failure of pipeline defects that included corrosion, gouges, dents, cracks, weld defects, and combinations of these. The guidelines were based upon a critical review of literature and reanalysis of relevant published results, and describe the limitations of each of the analyses methods in terms of pipe dimensions, material properties, defect characteristics, and failure pressures. The range of applicability for each of the recommended methods is based upon the test data used to develop each of the assessment techniques. They provide methods to predict the burst pressure at failure due to static or cyclic internal loads, axial loads, and bending loads on the pipeline, noting that in some cases the loads on defects are not well understood.

The recommended methods from Cosham and Hopkins [36] to predict burst pressures of dents (plain and with other forms of damage) in piping subject to internal pressure are listed in Table A.4. The techniques listed in Table A.4 apply to longitudinal and circumferential defects, and assume that the pipe material fails by plastic collapse. The NG-18 equations have been found to be the best equations for predicting the failure pressures of part through-wall defects such as gouges in pressurized pipe. The solutions provided in PAFFC are noted to be a more sophisticated method of assessing part through-wall defects such as gouges. The empirical limits for plain dents are embodied in most pipeline standards and list a maximum depth of 6% of the pipe outside diameter. The dent-gouge fracture models are applicable to smooth dent and gouge (or other defects) combinations. The authors note that the general procedures of BS 7910 [37] (and API 579 [38]) can be applied (regardless of upper or lower shelf behavior), but that they are generally more conservative than the pipeline specific methods. ‘No method’ represents both limitations in existing knowledge and circumstances where the available methods were too complex for inclusion into the PDAM.

Cosham and Hopkins [36] have categorized the details of the full-scale tests that have been completed on dented and gouged pipe. The 242 experimental tests completed on dent and gouge combinations are broadly classified into 11 categories, as listed in Table A.5. The gouges are all longitudinally oriented, and in most of the tests the gouges are actually machined notches or slots. From this table, one can see that several sequences of denting and gouging have been used, both with and without pressure. They analyze the full scale results using the Q-factor model developed by Battelle and the British Gas dent-gouge fracture model (Section A.3.5), both using the dent depth after rebound measured when the pressure is reduced to zero.

With the dent-gouge model, a correction factor is used to recognize that in-service dents can be made with the pipe pressurized and that it is not always possible to depressurize the pipe completely to determine the dent depth. The predicted failure pressures for both methods are compared, and they show that the dent-gouge model is better. In their final recommendations, the authors suggest the use of a derived ‘model uncertainty’ to shift the data so that the predicted failure pressures are conservative, and to increase the gouge depth by 0.5 mm to account for uncertainties in depth measurements using ultrasonics.

Table A.4: Pipeline Defect Assessment Manual (PDAM) Recommended Methods to Predict Burst Strength, from [36]

Defect	Defect Orientation	
	Longitudinal	Circumferential
Gouges	NG-18 Equations PAFFC BS 7910 or API 579	Kastner local collapse solution BS 7910 or API 579
Plain dent	Empirical Limits	
Kinked dent	No method	
Smooth dents on welds	No method	
Smooth dents and gouges	Dent-gouge fracture model	No method
Smooth dents and other types of defects	Dent-gouge fracture model	No method

Note: The maximum pipe WT and minimum upper shelf energy for using the techniques listed in this table are as follows: Gouges - 21.7 mm WT and 14 joules; Dent and Gouge - 20 mm WT and 16 joules; Dent - 12.7 mm WT and 20 joules.

Table A.5: Summary of Dent and Gouge Test Details

Details	Pressures		No. of Tests
	Dent	Gouge	
Dent then machine a V-notch (artificial gouge) in the base of the dent	0	0	134
Machine a V-notch and then introduce the dent	0	0	47
Machine V-notch, then dent using a sharp steel triangle	0	0	1
Dent then scrape (gouge) pipe using a tool bit on a pendulum	0	0	11
Machine V-notch at 0 psi, then introduce dent at pressure	Pressure	0	14
Gouge at 0 psi, then dent at pressure	Pressure	0	8
Damage using 60° indenter	0, 150	0, 150	2
Dent and gouge simultaneously using special test rig	Pressure	Pressure	18
Dent at pressure, gouge at 0 psi with indenter in place	Pressure	0	10
Machine a blunt notch, then introduce dent at pressure	Pressure	0	20
Machine a 1 in. wide notch (simulated corrosion) then dent	0	0	3

In their general comments related to the tests, they note that internal pressure stiffens the pipe against indentation, and that a puncture is more likely on pressurized pipe with sharp indenters. They also note that introducing a dent following gouging increases the likelihood of cracking at the base of the gouge, but the more realistic tests are those where the dent and gouge are introduced at the same time on pressurized pipe.

It should be noted that the pipe wall thickness values used for this research are thicker than typical linepipe used in onshore applications, with the minimum thickness being 12.7 mm. Additionally, the minimum upper shelf Charpy energy values ranged between 14 and 20 joules which is below the minimum 27-joule value required at operating temperature in the CSA and API codes.

A.3.5 Q - Factor

Eiber and Bubenik [39] summarize the approaches used to address the various defects that are found on an operating pipeline. Fracture initiation control for an existing pipeline involves consideration of the pipe dimensions and properties to define the range of flaw sizes that can be tolerated under operating conditions.

Dents are usually found with some form of stress concentrator, and require the details of both the lengths and depths of the dent and gouge to predict the failure pressure; the equations to predict the tolerance to mechanical damage are as follows:

$$\sigma_h = \bar{\sigma} \left(\frac{(Q - 300)^{0.6}}{90} \right)$$

where: $\bar{\sigma}$ is the flow stress (yield strength + 10,000 psi)

$$Q = C_v^{(2/3)} \left(\frac{R t}{D d t} \right) [ft - lb/in.]$$

Where: $_{2/3}$ = 2/3 thickness upper shelf CVN energy, ft-lb
d = gouge and crack depth, in.
D = maximum dent depth at the time of defect introduction, in.

The equations are empirical and have a wide margin of error, which is related to the difficulty in defining the defect characteristics such as the maximum depth of the dent at the time that it is introduced and the depths of the gouge and associated cracking. The following equation is given for estimating the dent depth:

$$e^{-X/22} = \frac{\sigma_h}{\bar{\sigma}}$$

where X is the ratio of the dent depth at σ_h to the maximum initial dent depth.

A.3.6 British Gas

The results of early British Gas studies on the significance of dents and gouges have been summarized by Hopkins et al [40] and include tests that address the following:

- Straight to failure tests.
- Fatigue tests.
- Time dependent failure.
- Crack growth in dents with increasing pressure.
- Effect of introducing damage into pressurized pipe.

The following equation had been developed by British Gas to predict failure pressures:

$$\frac{\sigma_f}{SMYS} = \frac{C_v}{10^3} \left[15.35 - 0.71 \left(\frac{d}{t} \right) - 0.17 \left(\frac{2R}{D} \right) + 0.09 \left(\frac{2R}{D} \cdot \frac{t}{d} \right) \right]$$

where

- C_v = 2/3 Charpy energy
- σ_f = predicted failure stress
- $SMYS$ = specified minimum yield stress
- d/t = defect depth / wall thickness
- $d/2R$ = dent depth / pipe diameter

A.3.7 Fatigue with Severe Mechanical Damage

Hagiwara and Oguchi [41] built on some of their earlier work to extend the analysis for minor defects to the prediction of fatigue life of ERW pipe with severe defects, and to determine the influence of ERW pipe residual stresses on fatigue life.

The tests included a total of 20 fatigue tests on 216 and 324 mm OD, Grade 414 and Grade 483 MPa pipe, with long longitudinal dents in the base plate and the weld seam. Gouges, typically 0.2 mm wide and 168 mm long, with depths ranging from 1.8 to 3.2 mm, were machined following denting; two tests were completed with shorter, 84 mm long, gouges. The hoop stress varied between 15% and 30% of the yield stress of the pipe.

The authors used the two equations listed below to describe the behavior of gouges in dents, one by Mayfield et al [22] on failure pressures using a Q parameter, and a formula by Hagiwara (listed in ref. [41]) to describe the fatigue life of gouged dents:

$$Q = \frac{CVN}{(d/D)(t/T)(2c)}$$

$$N_{f \text{ predicted}} = C(d/D)^\alpha (t/T)^\beta (\Delta\sigma/E)^\nu$$

A threshold value of $Q = 9300 \text{ N}$ for $\sigma_{\max} = 0.3 \sigma_y$ was found that separated the results; below the threshold, crack propagation was initially associated with ductile growth and the fatigue life was less than 1000 cycles, while above the threshold the fatigue life could be predicted using equation [2]. The short fatigue lives on the weld seams were explained in relation to the CVN toughness, with ductile flaw growth occurring for the low toughness materials.

Residual stresses were measured on each pipe and one stress-relieved pipe. They ranged from 0.37 to 0.81 times the yield stress longitudinally and from 0.26 to 0.46 circumferentially. The residual stress did not seem to have an effect on the fatigue results; the authors attribute this to the fact that the plastic deformation associated with gouging was so much greater than the residual stress due to pipe manufacturing.

Regarding gouge dimensions, it was concluded that the gouge depth dominated both the initiation of a ductile crack and propagation of a fatigue crack, whereas the gouge length influenced only the initiation of a ductile crack but not propagation above a threshold Q value.

A.3.8 EPRG Fatigue Life

The EPRG [42] has developed an approach for predicting the fatigue life of a pipe containing a dent. The semi-empirical stress-life (S-N) approach has been developed using the DIN 2413 Part 1 S-N curve, where the dent is assumed to be unrestrained and the fatigue life (in terms of the number of cycles to failure) is calculated as follows:

$$N = \frac{5622}{S_L} \left(\frac{UTS}{2\sigma_A K_d K_g} \right)^{5.26}$$

Where S_L = desired factor of safety on fatigue life (suggested to be 10 for conservatism)
 UTS = the ultimate tensile strength of the pipeline material
 σ_A = the equivalent nominal fatigue stress amplitude
 K_d = the stress enhancement factor of the dent
 K_g = the stress enhancement factor of the gouge.

$$\sigma_A = \frac{\sigma_a}{1 - \left(\frac{\sigma_{\max} - \sigma_a}{UTS} \right)^2}$$

$$K_d = 1 + C_{s,p} \sqrt{\frac{H_o^{1.5} t}{D}}$$

Where: H_o = dent depth measured after damage at zero internal pressure (mm) = 1.43H
 H = the measured dent depth at pressure.
 C_p = 2 for smooth dents with radius $> 5t$
 C_s = 1 for sharp dents with radius $< 5t$

$$K_g = 1 + 9 \frac{d}{t}$$

Where d is the gouge depth.

This methodology results in very conservative estimates of the fatigue lives compared to experimental data.

A.3.9 EPRG Denting and Puncturing Models

Some of the earlier work [32] on denting and puncturing of pipelines was undertaken by the European Pipeline Research Group (EPRG), in which they had completed twenty-four quasi-static tests and sixteen impact tests on buried pressurized (102, 435, and 1015 psi) pipe. They used 0.375 and 0.5 in, X52 pipe and 0.5 in. X70 pipe for all tests, all NPS 36, measuring force, displacement, and springback for all tests. Their results for static tests with the ram vertical, see Table A.6, show that increasing the wall thickness has the most noticeable effect on suppressing dent formation.

Within the last decade, Gaz de France has completed numerical modeling and experiments to study static denting and dynamic puncture of gas pipelines, as reported by Zarea et al [32]. This particular paper deals mainly with a description of the analysis process and some examples to illustrate the agreement between calculations and experiments. The steps involved in the static denting model analysis include:

- Determine the dent depth based upon the applied force (from given equipment)
- Calculate total and residual dent depths including springback calculations
- Determine the residual stress variation between extreme pressure values
- Use the above information to calculate the remaining lifetime under fatigue loading conditions of a dent and gouge.

Table A.6: Average Dent Depths and Elastic Springback, 45,000 lb force, X52

Pressure	Dent Depth, in. (%OD) Before Springback		Elastic Springback, in. (%OD) ^a	
	0.375 in. WT	0.5 in. WT	0.375 in. WT	0.5 in. WT
102 psi	1.693 (4.7)	3.46 (2.05)	0.445 (1.24) 26	0.248 (0.689) 7
435 psi	0.945 (2.63)	0.531 (1.48)	0.287 (0.8) 30	0.228 (0.63) 43
1015 psi	0.689 (1.91)	0.374 (1.04)	0.248 (0.689) 36	0.161 (0.45) 43

(a) Numbers in bold are percentage springback.

The dynamic failure model is a void nucleation model that is based upon the chemistry of the steel to determine the total void fraction, followed by a cavity growth model and finally a failure criterion that is based upon a critical void fraction.

A.3.10 Rinehart and Keating

Rinehart and Keating have presented example fatigue life assessments for short [43] and long [44] dents. The fatigue life assessments utilized 3D elastic-plastic finite element analysis of the indentation and cyclic loading to predict the localized stress response in the pipe wall. These stresses were then used to predict both the crack initiation life, using an approach by Dowling, based on the change in local strain due to surface roughness, and the crack propagation life using a Paris Law fracture mechanics based approach.

The total estimated fatigue lives were then compared to available experimental data, where the predictions exhibited a range of possible values depending on the treatment of the compressive residual stresses that exist in the pipe wall.

A.3.11 Battelle Pipeline Technology

In work presented at IPC 2004, Leis [45] presents a wide ranging discussion on integrity analysis of dents in pipelines. In the paper, a fatigue life assessment methodology is described which utilizes a nonlinear large displacement elastic-plastic finite element analysis to predict the local pipe wall stress and strains during indentation and internal pressure cyclic for a range of restrained and unrestrained dent shapes. The elastic-plastic material response for a typical X42 grade steel was modeled using an isotropic hardening model.

Fatigue lives were estimated for a variety of operating pressure spectrums that represent typical operation for gas and liquid lines.

The fatigue life assessment for each of the scenarios was carried out based on the local stresses, strains and mean stress in terms of an energy based fatigue damage parameter, where the damage assessment and accumulation were based on strain-life fatigue data for vintage X42.

The results of the various analyses are presented and discussed in terms of the general trends exhibited, however limited validation or comparison to existing experimental data is presented in support of the method.

A.3.12 Summary

There has been considerable effort directed towards the understanding of dents and how they are affected by operating conditions on buried pipelines. The research has ranged from laboratory testing of dented pipe samples to dynamic puncture tests using backhoes. The details summarized below are considered to be relevant to the modeling activities that are to be undertaken in the subsequent tasks. While much of the work has included gouges, the results are still applicable to this phase of the modeling project as the literature also describes the response of the pipeline to external loading (denting).

Belonos and Ryan [6] suggested that residual stresses should be added algebraically to get the true stress, and they concluded that dents, even though they can have high residual stresses, do not affect the service performance unless there is a notch or scratch, or metallurgical notch such as cold work, within the dent.

Studies at CANMET [7] showed that there was no reduction of failure pressures for dents alone; however, in one case failure occurred by fatigue after 3000 cycles at the curved ends of a long dent. For gouges, a modified strip yield model using toughness estimated from Charpy data was able to conservatively estimate failure pressures. The case of a gouge in a dent can be analyzed by considering the bending component of the stress intensity factor and by calculating the collapse stress for a part-through surface crack. Gouges in dents result in lower failure pressures than either dents or gouges alone.

Maxey [11] considered the dynamic effects of gouging on pressurized pipes, as well as determining how crack growth is related to operating pressure. Tests on dynamically gouged and dented pipe resulted in immediate failure in some cases, while the majority of defects failed later during pressure testing. He noted that the pipe rerounds immediately following the passage of the denting tool, and that for long dents the centre portion rerounds and becomes almost flat, whereas the ends of the gouge and dent combination show less recovery to the original shape. The dents rerounded immediately upon pressurization, and the recovery was linear up to the failure pressure. The hold experiments showed that crack growth did not occur until pressures over 70% of the final failure pressure were achieved. Using the gouge/dent details, material properties, and operating pressure, Maxey provides a formula that can be used to determine the significance of dent/gouge combinations.

In experimental work on plain dents, Fowler [23] showed that neither the dent type nor the dent length were important in terms of reducing the fatigue life, but the dent depth, D/t ratio, and weld type (if present) were important factors. In order to produce a dent with a given final depth, it was necessary to indent the pipe to about twice the desired depth. The rebound of the pipe following release of the indenter was greatest for thin-walled pipe. The second phase of his work used finite element analyses to develop dent stress concentration factors to be used to predict the life of a dented pipe; these factors ranged in many cases from 3 to 5 with different D/t ratios. A method is described that can be used to predict the failure of dents on a pipeline.

The main findings of the work described in API 1156 [24, 25] showed that the pressure carrying capacity of the pipe was not affected by smooth dents without stress concentrators, dents rerounded elastically upon removing the indenter and upon pressurization, the fatigue life of unconstrained smooth dents decreased with increasing dent depth, stress concentrators such as girth welds reduced the fatigue life, partially overlapping smooth dents have shorter fatigue lives than individual dents, hydrostatic testing has a beneficial effect on fatigue life due to rerounding of the dent. Smooth dents failed by leaks in all cases, they were oriented longitudinally, and initiated on the OD surface. In most cases the cracks were located on the sloping transition on the ends of the dents. For constrained dents, the leaks were oriented transversely, and had initiated on the ID surfaces. All failures were ductile in nature.

The main finding of the work from Rinehart [26] showed that the pipe wall stress response in the presence of a dent is a function of the dent length, width, depth and the pipe outer diameter. For unrestrained dents, short dents exhibit peak stress ranges in the shoulder of the dent while long dents tend to exhibit stress range peaks in the centre of the dent. The restraint condition can also alter the behavior of dents with long restrained dents behaving similar to short restrained and unrestrained dents.

Several fatigue life assessment methodologies have been developed and presented. The majority of the approaches utilize finite element analysis methods to estimate the local stresses and strains in the pipe wall and relate them to the applied internal pressures. The types of finite element analyses used range from 3D linear elastic, to 2D elastic-plastic and full 3D nonlinear large displacement elastic-plastic methods, where in the elastic-plastic method the material response is modeled using isotropic material hardening. The damage accumulation and failure approaches utilized in the various methods include stress-life, strain-life and fracture mechanics. A more detailed discussion of some of the general fatigue life assessment approaches is presented in Section A.4 of this appendix.

A.4 DENTED PIPELINE FATIGUE LIFE PREDICTION METHODOLOGIES

The previous section presented a wide range of references regarding the behaviour and performance of dented pipelines. Included in the references were various assessment methods, developed to help estimate the impact of a plain dent, a dent/gouge or a dent on weld, on the integrity of the affected pipeline.

The following section presents a more detailed review of five of the methods developed for estimating the fatigue life of dented pipelines. These methods have been selected for more detailed discussion and demonstration because they are presented in a general form that allows them to be used to evaluate a variety of existing dent scenarios.

The review includes a summary of each of these methodologies, along with a discussion of the similarities and short comings of each. A demonstration of each of these methodologies is presented in Section 4 of this report, based on the full scale experimental data generated as part of a joint DOT/PRCI project (DOT #339, PRCI MD4-2) [46].

A.4.1 *Cyclic Pressure Fatigue Life of Pipelines with Plain Dents, Dents with Gouges, and Dents with Welds, J.R. Fowler, et al [19]*

The report documents a combined experimental and numerical project focused on understanding the fatigue life of dented pipelines when subjected to cyclic internal pressures. The effort initially focused on unrestrained plain dents and was later expanded to include both dents with gouges and dents on welds. The project included the use of both older existing experimental data and on experiments designed and carried out in the project itself.

The majority of the experimental program utilized NPS12 pipe specimens ranging in D/t from 18 to 64 but also included an NPS24 specimen with a D/t of 94.1. The experimental program involved indenting the specimens with long bar (oriented both parallel and perpendicular to the longitudinal axis of the pipe) and flat plate indenters, where numerous dents of varying depth were formed in each experimental specimen. Note that for all experimental specimens, the indenters were removed and the dents allowed to rebound elastically and reround under internal pressure, and therefore represent unrestrained dents.

The numerical portion of the project involved the use of finite element analysis to further investigate the performance of the dented specimens, in particular to estimate the stress levels and predict the fatigue life of the specimens. The finite element analysis was carried out in two stages; 3D elastic analysis and 2D elastic-plastic analysis. The 3D analysis was carried out using the indented shape as the starting point for the analysis (i.e., ignoring the stress state at the end of the indentation process) where the internal pressure was cycled in order to estimate the local $\Delta\sigma/\Delta P$ transfer functions. The 3D elastic analysis resulted in two primary conclusions:

1. The stresses are greater than yield and therefore the elastic assumptions were inappropriate.
2. Differences in stress state between various dent shapes were small, leading to the assumption that dent length is not significant in terms of fatigue life.

The 2D plastic analysis was used to more accurately estimate the $\Delta\sigma/\Delta P$ transfer functions in the vicinity of the dent and to better understand the re-rounding behavior of the dent. The 2D analysis used 3D shell elements, where one element was used in the longitudinal direction of the pipe, implying a dent length over depth (l/d) of infinity. Elastic-plastic material properties were used along with an isotropic hardening law. The results of the 2D plastic analysis were used to develop tables of $\Delta\sigma/\Delta P$ transfer functions which are then used in the fatigue life assessment.

The fatigue life assessment is a stress-life (i.e., S-N) based assessment approach based on either the API RP2A curve 'X' or the DOE curve B. The fatigue life is calculated using the following equation:

$$N = C \left(\frac{\Delta\sigma}{\Delta P} \right)^{-m}$$

Where for the API RP2A 'X' curve, $C = 2 \times 10^6$, $\Delta\sigma =$ pressure fluctuation $\times (\Delta\sigma/\Delta P)$, $\Delta\sigma_{ref} = 11,400$ psi and $m = 3.74$. The $\Delta\sigma/\Delta P$ transfer functions are presented in the form of tables as a function of d/D (dent depth over outer diameter), D/t , mean internal pressure and pipe grade. Note that the dent depth refers to the elastically rebounded dent depth after indenter removal.

The comparison of the experimental and the predicted results carried out by the report authors reveals that the API 'X' curve is extremely conservative (i.e. greatly under predicts the experimental fatigue life) and the DOE B curve is less conservative.

A.4.2 Effect of Smooth and Rock Dents on Liquid Petroleum Pipeline (API 1156), C.R. Alexander, J.F. Kiefner, [24]

The stress-life (S-N) based fatigue life methodology developed in the project was based on the results of detailed 3D elastic-plastic finite element analysis combined with the ASME BPVC Div 2 fatigue life curve.

The detailed finite element analysis utilized elastic-plastic shell elements with an isotropic material hardening model to develop the $\Delta\sigma/\Delta P$ transfer functions for the various dent configurations, including separate factors for restrained and unrestrained dent scenarios. The fatigue life equation developed in the project is summarized below:

$$N = \exp \left[43.944 - 2.971 \ln \left(\frac{\Delta\sigma}{2} \right) \right]$$

Where

$N =$ fatigue life in number of cycles

$\Delta\sigma =$ stress range in psi = $SCF \times \Delta P$

$SCF =$ stress concentration factor from tables based on indenter shape, D/t , d/D and mean pressure

The application of the method to two of the experimental specimens from the same project indicated varied results, with one result over predicting the fatigue life and one under predicting the fatigue life.

A.4.3 Development of a Model for Fatigue Rating Shallow Unrestrained Dents, M. J. Rosenfeld [27]

The focus of the project summarized in this paper was to investigate the rerounding behavior of unrestrained dents in pipelines. The project included developing equations relating the rebounded and rerounded dent shapes to the initial dent depth and shape (primarily the width) of the dent.

As part of the project, a method for estimating the cyclic fatigue life of unrestrained dents was developed, where the stress-life (S-N) based approach utilized the fatigue life curve from the ASME B31 Code for Pressure Piping where:

$$N = \left(\frac{6S_{CF}}{\Delta\sigma} \right)^5$$

Where: $\Delta\sigma$ = cyclic stress range
 S_{CF} = the cyclic flow strength of the material = $0.5(0.667S_Y + S_U)$
 S_Y = yield strength
 S_U = tensile strength

The cyclic stress range, $\Delta\sigma$, is calculated using the equation shown below, which has been developed to estimate the stress range at the peak of the dent.

$$\Delta\sigma = \left(\frac{\Delta p_a D}{2t} \right) \left(2 + \frac{6(\Delta d^+ + \Delta d^-)}{t} \right)$$

Where: ΔP_a = applied cyclic pressure range
 D = outer diameter
 t = wall thickness
 Δd^+ = outward dent displacement
 Δd^- = inward dent displacement

Application of the method to a number of scenarios (i.e. pipe geometries, dent depths, operating pressure spectra) was used to develop general trends in the behavior of unrestrained dents in pipelines.

A.4.4 Guidelines for the Assessment of Dents on Welds, M. J. Rosenfeld [29]

The fatigue life assessment method documented in this report is a stress-life (S-N) based approach to estimating the fatigue life of unrestrained dents on either long seam or girth welds.

The methodology considers the effect of dent size, weld quality and the applied pressure spectrum on the fatigue life of a dented pipeline. Similar to the first two methods summarized above, the method utilizes stress concentration factors (*SCFs*), calculated based on detailed finite element analysis, to estimate the stress range in the dent as a function of the applied pressure range, the initial (i.e., unrounded) dent depth d , outer diameter D , D/t and the mean pressure.

The stress concentration factors are presented in the form of a series of graphs where the initial dent depth is calculated as:

$$d_i = \frac{d_r}{fg}$$

Where: d_r = rebounded dent shape

$$f = \frac{1.04}{1 + 0.0875x^{-3/2}} - 0.052$$

$$x = \frac{(D/w)^{0.3}}{(D/t)^{0.7} (p/E)^{0.2}}$$

$$g = \frac{0.88(D/w)}{1 + 0.59(D/t) + 0.041(D/t)^2}$$

Where: w = width of dent measured between half depth points
 p = internal pressure
 E = Elastic modulus

The fatigue life is calculated using the following equation:

$$N = 7970 \left(\frac{Q}{\Delta\sigma} \right)^{2.865}$$

The parameter Q is the IIW numerical weld quality category which is a function of the allowable weld imperfections (according to API 1104). The parameter Q is presented as a series of curves, one for each type of allowable weld imperfection, and is a function of the pipe wall thickness being analyzed.

The fatigue life equation can be used in conjunction with a linear Miner's damage summation to account for the effect of variable amplitude pressure fluctuations on the fatigue life of the dented pipeline.

A.4.5 *EPRG Methods for Assessing the Tolerance and Resistance of Pipelines to External Damage Part 1 and 2, R.J. Bood, et al [42]*

The fatigue life assessment methodology provided by EPRG is applicable to smooth dents, sharp dents and smooth dent/gouge combinations in the pipe body only. Dents or dent/gouge combinations incorporating field or manufacturing welds are not permitted.

The semi-empirical stress-life (S-N) approach has been developed from the DIN 2413 Part 1 S-N curve, where the dent is assumed to be unrestrained and the fatigue life (in terms of the number of cycles to failure) is calculated as follows:

$$N = \frac{5622}{S_L} \left(\frac{UTS}{2\sigma_A K_d K_g} \right)^{5.26}$$

Where: S_L = desired factor of safety on fatigue life (suggested to be 10 for conservatism)
 UTS = the ultimate tensile strength of the pipeline material
 σ_A = the equivalent nominal fatigue stress amplitude
 K_d = the stress enhancement factor of the dent
 K_g = the stress enhancement factor of the gouge.

$$\sigma_A = \frac{\sigma_a}{1 - \left(\frac{\sigma_{\max} - \sigma_a}{UTS} \right)^2}$$

$$K_d = 1 + C_{s,p} \sqrt{\frac{H_o^{1.5} t}{D}}$$

Where: H_o = dent depth measured after damage at zero internal pressure (mm) = 1.43H
H = the measured dent depth at pressure.
 C_p = 2 for smooth dents with radius > 5t
 C_s = 1 for sharp dents with radius < 5t

$$K_g = 1 + 9 \frac{d}{t}$$

Where d is the gouge depth.

This methodology results in very conservative estimates of the fatigue lives compared to experimental data.

A.4.6 Comparison of Dented Pipeline Fatigue Life Assessment Methodologies

There are a number of similarities between the various fatigue life methodologies summarized in the previous sections.

- All of the methods identified utilize a stress-life (S-N) based approach to estimate the fatigue life of dented pipelines as opposed to other approaches such as strain-life (ϵ -N) or fracture mechanics based approaches. This may be partly due to the wide availability and wide variety of S-N curves available in both open literature and in the various international standards and regulations
- Four of the five methods assume the dent to be unrestrained, i.e. the indenter is not in contact with the pipe during cyclic pressure loading. This is generally conservative as unrestrained dents tend to have a lower fatigue life than equivalent or even deeper restrained dents. Only the method from Alexander [24] provides different SCFs for restrained and unrestrained dents. However, none of the methodologies provide guidance on estimating whether a dent is actually restrained or unrestrained.
- Four of the five methods utilize finite element analysis techniques to estimate the stress concentration factor (SCF) associated with a dent, i.e. the transfer function relating the change in stress in the vicinity of the dent to the change in internal pressure. The finite element analyses utilized by the various methods range from 2D linear elastic techniques to 3D nonlinear elastic plastic techniques. In all cases the nonlinear material properties used to model the cyclic material behavior were idealized using an isotropic material hardening model.
- The SCFs (or the resulting local stress range in a dented pipeline) for all the methods are a function of d/D and D/t , where for four of the methods the dent depth (d) is the taken as the rerounded dent depth after removal of the indenter. For three of the methods [19, 24, 42], the effect of the mean operating pressure is also accounted for in the SCFs.
- For two of the methods, Alexander [24] and EPRG [42], the SCFs take into account the dent shape, however only the EPRG method [42] provides the user with guidance on how to classify the dent shape based on the local dent radius. Although Alexander [24] provides different SCFs for restrained and unrestrained dome and long bar indenters, very little guidance is provided as to how to classify the shape of the dent being assessed.

As will be demonstrated in more detail in the following section, application of the methods to the available full scale experimental data developed as part of MD4-2, results in a wide range of scatter in terms of the predicted fatigue life.

A.5 DEMONSTRATION OF FATIGUE LIFE ASSESSMENT METHODOLOGIES

A demonstration of four of the five available fatigue life methodologies is presented in the following section. The demonstration was carried out using the experimental data from the joint PRCI/DOT full scale experimental project (PRCI MD4-2, DOT #339) along with a selected sample of experimental results from two of the other experimental programs for which the appropriate data was available [17, 24]. (Due to a lack of experimental information the fifth methodology, from Rosenfeld [5] has not been evaluated using the experimental data).

A.5.1 Summary of Assumptions

A summary of the experimental data used to estimate the fatigue lives (available at the time of finalizing the report) is presented in Appendix A.

The following represents a summary of the major assumptions and limitations encountered in applying the methodologies to the experimental specimens:

- Where necessary (i.e., methods [19], [29] and [42]) restrained experimental dents were assumed to be unrestrained with a depth equal to the maximum dent depth achieved during indentation.
- For [19] the curves for the SCFs provided do not cover the D/t ratios of the experimental specimens. The existing curves have therefore been extrapolated to suit. The accuracy of this assumption represents an unknown.
- For [29] plain dent specimens were assumed to represent a weld quality category (Q) of 100. For the specimens with dents interacting with girth welds, as each girth weld has been inspected using UT and been verified as having no unacceptable flaws, a weld quality category of 77 has been assumed.

A.5.2 Fatigue Life Assessment Results

The results of the fatigue life assessments for the specimens from MD4-2 [46] are summarized in Table A.7, which presents the experimental results and the results of the four assessment methodologies. Similarly the results for the specimens from [17] and [24] are shown in Table A.8. The agreement between the various methodologies and the experimental lives is presented graphically in Figures A.2 and A.3.

As shown in Tables A.7, A.8 and Figure A.2, there is a significant amount of scatter between the predicted and experimental fatigue lives, with some of the methodologies greatly overestimating and others under estimating the fatigue life.

Based on the summary presented in Tables A.7 and A.8, both Alexander [24] and Fowler [19] generally significantly overestimate the fatigue life. Conversely, the EPRG method [42] significantly under predicts the experimental results. Generally, the method developed by Rosenfeld [29] is in better agreement with the experimental results than the other methods, generally over predicting the fatigue lives by a factor of 1.8.

Table A.7: Estimated and Experimental Fatigue Lives for MD4-2 [46] Specimens

Specimen	Exp'mtl (Cycles)	API 1156 [24]		EPRG [42]		Rosenfeld [29]		Fowler [19]	
		(Cycles)	(Pred/Exp)	(Cycles)	(Pred/Exp)	(Cycles)	(Pred/Exp)	(Cycles)	(Pred/Exp)
1	6948	153715	22.1	19	0.003	8682	1.2	65147	9.4
2	38685	153715	22.1	19	0.003	8682	1.2	65147	9.4
3	6886	52579	7.6	4	0.001	2042	0.3	1768	0.3
4	16234	52579	7.6	4	0.001	2042	0.3	1768	0.3
5	2531	52579	7.6	4	0.001	2042	0.3	1768	0.3
6	3359	52579	7.6	4	0.001	2042	0.3	1768	0.3
7	21103	213900	30.8	2206	0.317	28511	4.1	158898	22.9
8	28211	109485	15.8	441	0.063	28511	4.1	158898	22.9
9	6825	87639	12.6	263	0.038	28511	4.1	119713	17.2
10	9116	97492	14.0	345	0.050	28511	4.1	158898	22.9
11	15063	108829	15.7	435	0.063	28511	4.1	158898	22.9
12	27575	166514	24.0	1155	0.166	28511	4.1	185055	26.6
13	13262	47400	6.8	212	0.031	16199	2.3	108675	15.6
14	15065	56896	8.2	322	0.046	16199	2.3	108675	15.6
15	4035	43930	6.3	179	0.026	16199	2.3	108675	15.6
16	4684	43562	6.3	176	0.025	16199	2.3	108675	15.6
17	11415	76236	11.0	641	0.092	21319	3.1	108675	15.6
18	15949	78904	11.4	690	0.099	21319	3.1	108675	15.6
19	32282	164668	23.7	68	0.010	4106	0.6	72877	10.5
20	24919	164668	23.7	68	0.010	4106	0.6	72877	10.5
21	66871	164668	23.7	70	0.010	13484	1.9	72877	10.5
22A	66429	122838	17.7	7	0.001	13484	1.9	81884	11.8
23	12722	52193	7.5	4	0.001	3137	0.5	53842	7.7
24	16278	52193	7.5	4	0.001	3137	0.5	53842	7.7
25	19063	48660	7.0	417	0.060	13484	1.9	72877	10.5
27	18633	47700	6.9	313	0.045	13484	1.9	72877	10.5
28	16107	47822	6.9	299	0.043	13484	1.9	72877	10.5
29	14400	48548	7.0	623	0.090	13484	1.9	92442	13.3
31	9890	21978	3.2	241	0.035	7661	1.1	89713	12.9
32	9506	22096	3.2	233	0.034	7661	1.1	89713	12.9
33	9386	22503	3.2	428	0.062	7661	1.1	108675	15.6
34	9871	22374	3.2	368	0.053	11342	1.6	133398	19.2
35	19959	24108	3.5	422	0.061	7661	1.1	133398	19.2
36	15568	24887	3.6	466	0.067	11342	1.6	145396	20.9
26	40832	123208	17.7	7	0.001	2596	0.4	6076	0.9
30	31179	123208	17.7	7	0.001	2596	0.4	6076	0.9
37	42159	93848	13.5	2	0.000	2596	0.4	6076	0.9
38	32963	175787	25.3	475	0.068	28511	4.1	158898	22.9
39	7559	71229	10.3	37	0.005	6634	1.0	21204	3.1
40	6504	64089	9.2	126	0.018	16199	2.3	133398	19.2
41	69099	202825	29.2	118	0.017	5472	0.8	84406	12.1
42	69393	145668	21.0	10	0.001	1358	0.2	2560	0.4
46	125525	202825	29.2	94	0.014	5175	0.7	84406	12.1
48	23482	131407	18.9	432	0.062	10989	1.6	185223	26.7
52	9226	113796	16.4	278	0.040	9217	1.3	185223	26.7
54	47702	351576	50.6	4393	0.632	31230	4.5	283815	40.8
56	15473	157840	22.7	624	0.090	13852	2.0	185223	26.7
57	14091	198927	28.6	1167	0.168	16209	2.3	283815	40.8
Max			50.6		0.632		4.5		40.8
Min			3.2		0.000		0.2		0.3
Average			14.6		0.057		1.8		14.3

Table A.8: Estimated and Experimental Fatigue Lives for Additional Specimens [17, 24]

Ref	Spec	Exp'mtl (Cycles)	Alexander [3]		EPRG [6]		Rosenfeld [5]		Fowler [2]	
			(Cycles)	(Pred/Exp)	(Cycles)	(Pred/Exp)	(Cycles)	(Pred/Exp)	(Cycles)	(Pred/Exp)
17	3D	89684	82889	11.9	349	0.050	4060	0.6	87514	12.6
	3E	80880	75623	10.9	232	0.033	2774	0.4	63402	9.1
	3F	100943	145906	21.0	27	0.004	945	0.1	9887	1.4
	5D	62970	89060	12.8	475	0.068	6799	1.0	195857	28.2
	5E	73977	109641	15.8	869	0.125	9683	1.4	269756	38.8
24	UD12A-	31045	78228	11.3	-146	-0.021	7315	1.1	393711	56.7
	CD24A'-	4687	61801	8.9	-1005	-0.145	-3047	-0.4	35506	5.1
	UL12A-	15213	171935	24.7	3773	0.543	23167	3.3	644451	92.8

Figure A.3 presents the same results, but separates out the restrained and unrestrained experimental specimens to illustrate the effect of the assumed restraint condition. As shown, there is generally large scatter and overlap in the predicted results for the restrained and unrestrained specimens, with the majority of the methods over predicting the fatigue lives of both restrained and unrestrained dents, even though the methods generally assume all dents to be unrestrained.

It is interesting to note that for the Rosenfeld method [29], the agreement between the experimental and predicted fatigue lives for the unrestrained specimens are much better than those for the restrained specimens, where the predictions are generally much less than the experimental lives (as would be expected).

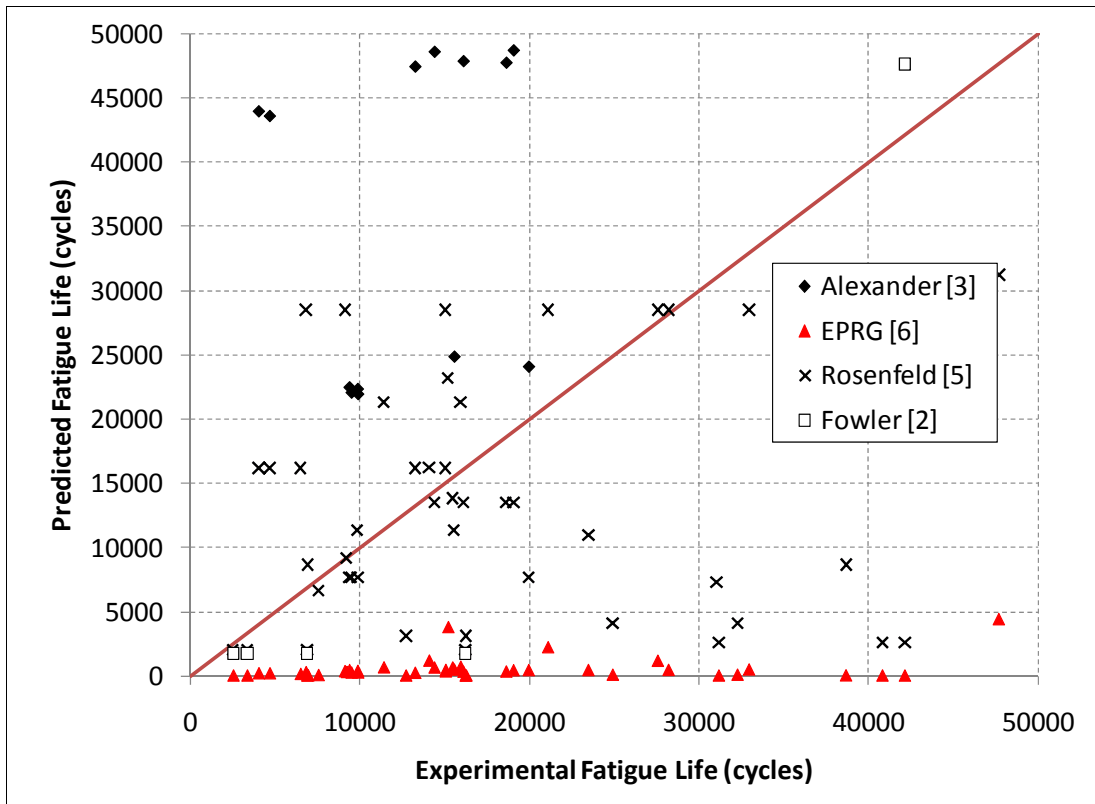
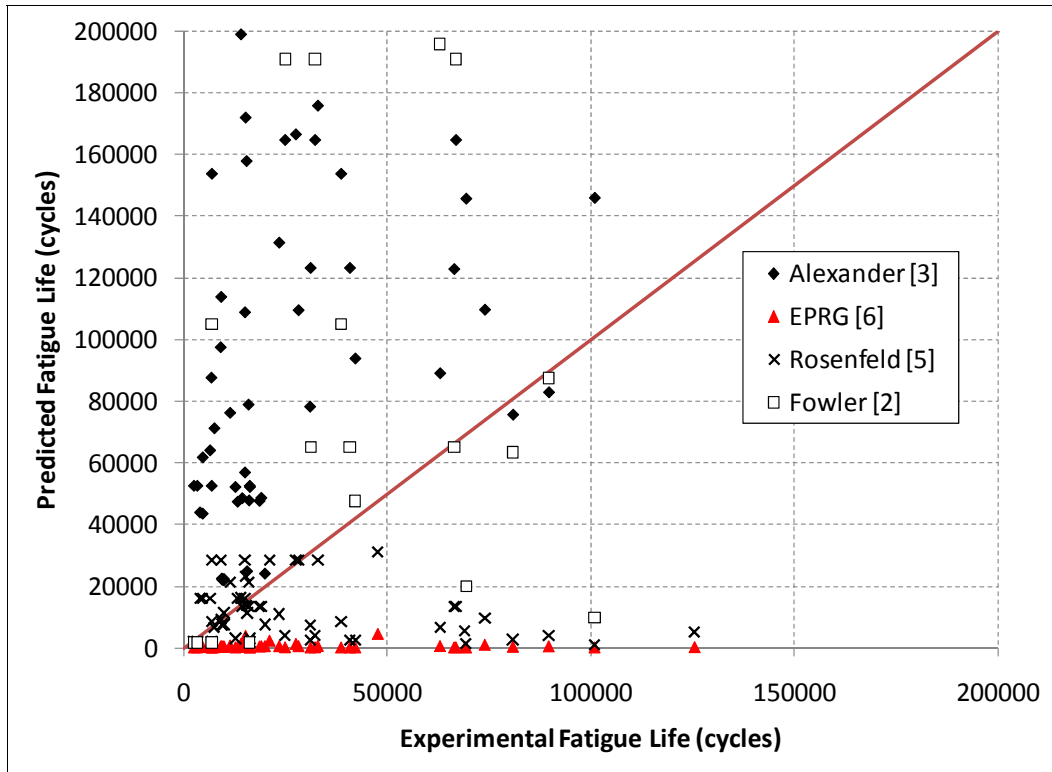


Figure A.2: Comparison of Estimated and Experimental Fatigue Lives

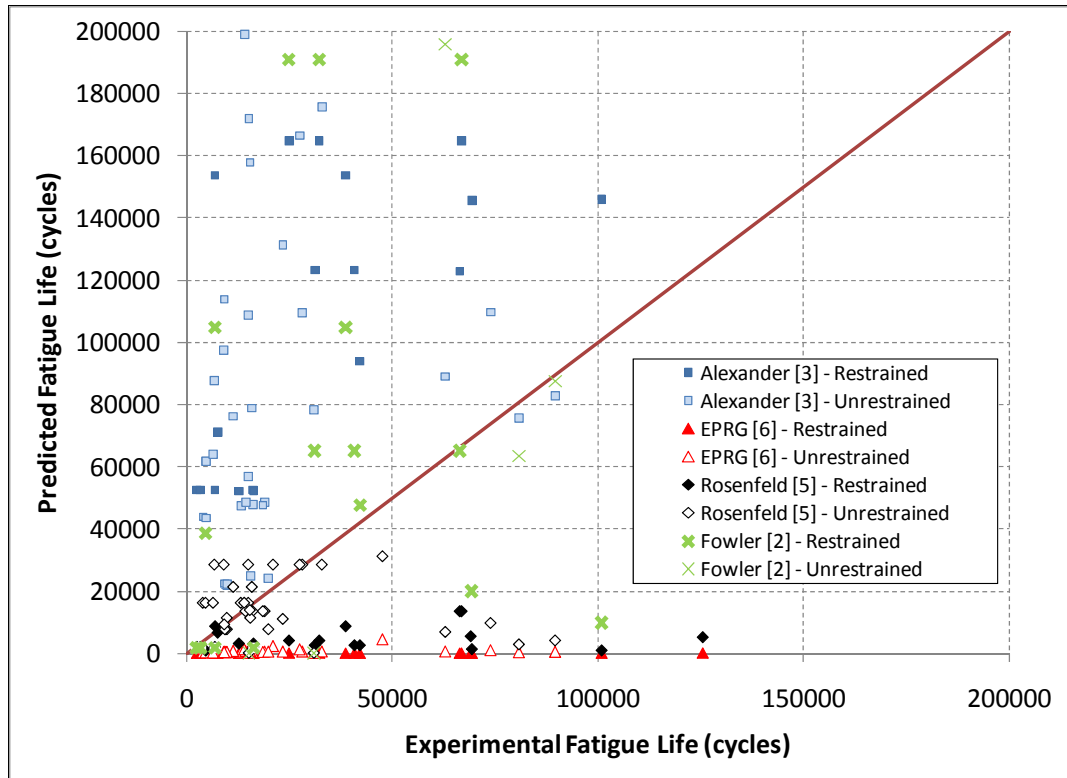


Figure A.3: Comparison of Estimated and Experimental Fatigue Lives – Restrained vs. Unrestrained Dents

A.5.3 Summary of Comparison

As shown in the previous section, there is a large amount of scatter in the accuracy of the four fatigue life prediction methodologies when compared to experimental data. This scatter can be attributed to a number of reasons, including:

- Differences in the S-N fatigue life curve used by each methodology.
- Differences in the detailed finite element analyses used to develop the stress concentration factors associated with the dents.
- Differences in the location of the peak stress range used to calculate the SCF's (i.e., dent peak, dent shoulder region).
- Three of the four methods [19, 29, 42] treat all dents as unrestrained.
- Two of the methods [19, 24] require extrapolation of the existing data to calculate SCF's for the range of D/t's associated with the experimental data.

Appropriately addressing these factors represents potential avenues for developing a more accurate fatigue life prediction methodology.

A.6 PATH FORWARD

The primary objectives of the current project are to develop a detailed validated fatigue life assessment methodology for dented pipelines and to use the detailed methodology to develop a simplified more rapid fatigue life assessment approach based on easily identifiable dent, pipe and the parameters.

The development of the detailed fatigue life assessment approach includes the use of a validated nonlinear finite element analysis model to accurately predict the stresses and strains in the dented pipeline, where the validation will be carried out using the full scale experimental data from DOT #339/PRCI MD4-2. This validated model will then be used along with a validated damage accumulation/failure model, in a wide ranging numerical modeling phase to estimate the fatigue life of many hypothetical dent scenarios. The results of the modeling phase will then be used to develop relationships between the various parameters and the estimated fatigue life.

The results of the literature review and the demonstration and comparison of the various fatigue life assessment methodologies presented in the previous sections provide a number of avenues for developing an improved fatigue life assessment methodology.

The following subsections present a brief summary of some of the potential improvements that will be pursued in developing both a detailed fatigue life assessment methodology and the simplified assessment approach.

A.6.1 Wider Range of Dent and Pipe Geometries

Increases in computing power and efficiency will be utilized to allow for detailed large displacement nonlinear elastic-plastic finite element analysis techniques to be applied to a greater number of dent scenarios. This will allow for a greater range of pipe geometries (i.e., D/t), material grades and dent geometries (i.e., dent length, width, depth) to be included in the development of the methodology. This will help to ensure that the method accounts for, and is applicable to, the wide a range of parameters that occur in operating pipelines.

A.6.2 Improved Material Modeling

As discussed in the previous sections, the existing dented pipeline fatigue life methodologies have used a variety of finite element analysis techniques to estimate the local pipe wall stresses and strains in the dent region. These all used an isotropic material hardening model to represent the cyclic behavior of the material.

An isotropic hardening model assumes that the yield surface is stationary and expands uniformly about the origin. The isotropic model does not account for the Baushinger effect as the stress-strain curve is considered to be symmetric about the origin. Thus, upon load reversal in cyclic loading, yielding occurs at a stress value equal to the maximum stress achieved in the previous reversal σ_{\max} , Figure A.4.

The kinematic hardening model assumes that the yield surface remains constant in size but is allowed to translate due to plasticity. The kinematic model accounts for the Baushinger effect in that upon load reversal, yielding is considered to occur at a stress value equal to $2\sigma_y$ less than the maximum stress reached in the previous reversal.

Under monotonic loading, the behaviors of isotropic and kinematic hardening models are essentially the same. The difference between the behaviors of the two models is evident following a load reversal. During the load reversal, yielding will occur much earlier in the kinematic model compared to the isotropic model. This earlier onset of yielding can have a significant effect on the predicted strain range during cyclic loading.

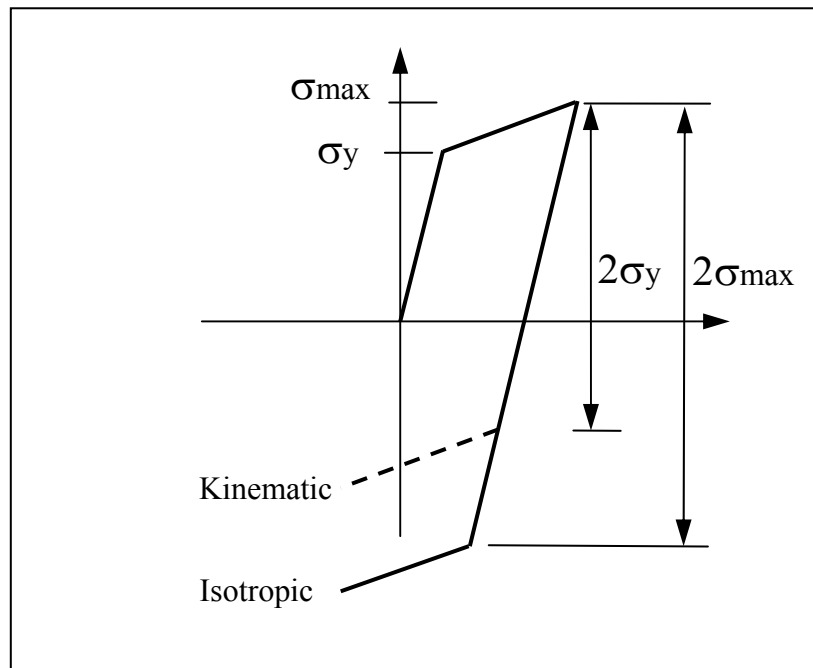


Figure A.4: Material Hardening Models

Therefore, a nonlinear kinematic material model will be used to model the material response during dent formation, re-rounding and cyclic loading. This will result in a more accurate prediction of the strain response, particularly for scenarios where cyclic plasticity could play a significant role.

A.6.3 Validation of Intermediate Outputs

The development of the existing fatigue life methodologies have all included validation efforts. However, due to a lack of detailed experimental data, the validation has been limited to a comparison of predicted and experimental fatigue lives. The reason for any discrepancies between the two, whether conservative or unconservative, could not be explained based on the available data, i.e., was it due to inaccurate strain/stress estimates from the finite element analysis or inaccuracies in the damage accumulation/failure criteria.

In the current project the full set of experimental data developed in DOT #339/PRCI MD4-2 will be utilized during the validation stage of the project. The validation of the finite element analysis models developed in this project will be carried out using the detailed experimental data including:

- Load versus displacement results during indentation,
- Detailed dent shape measurements at various stages of the testing,
- The pipe wall strains at various locations around the pipe OD.

Validating the models in this way provides a level of confidence in the accuracy of the detailed stresses and strains predicted in the dent region.

Once the finite element models have been validated, various damage accumulation/failure criteria will be explored and validated separately. The methods considered will include:

- Stress-life (S-N) approaches based on a variety S-N curves available in literature and in various industry standards and codes.
- Strain-life (e-N) approaches based on experimental curves developed for various pipe grade steels and various rules-of-thumb approaches.
- Fracture mechanics based approaches, involving calibrated initial flaw sizes and crack growth rate parameters.

This two stage validation approach will allow for a more thorough understanding of the accuracy of the different aspects of the fatigue life assessment methodology.

A.6.4 Restrained versus Unrestrained Dents

As discussed previously, four of the five existing methodologies presented in Section 4 assume all dents to be unrestrained. This is generally a conservative assumption as unrestrained dents generally experience greater stress and strain ranges during internal pressure cycling, and therefore generally exhibit lower fatigue lives than due similar restrained dents. However, adoption of such a conservative assumption for all dents could result in overly conservative (i.e., low) fatigue life estimates, which could lead to unnecessary remediation costs if the predicted lives were considered too low. Therefore properly accounting for the restraint condition while estimating the fatigue life of a dent, is considered important in estimating accurate fatigue lives.

In order to properly account for the restraint condition, a methodology will be developed to help estimate whether the dent is restrained or unrestrained. The methodology will make use of a number of parameters, including dent location, dent depth and dent shape.

A.6.5 Parameters Governing Dent Fatigue Life

As discussed in Section A.4, all of the five fatigue methodologies account for the effect of dent depth (i.e., relative dent depth d/D), pipe geometry (i.e. D/t) and mean pressure, on the estimated fatigue life of a dented pipe. In addition, the methods from Alexander [24] and EPRG [42] provide some method of accounting for the effect of the dent shape on the estimated fatigue life of the dent. Alexander [24] provides different tables of stress concentration factors for dome and long bar shaped indenters, however, no guidance is provided on determining whether a given dent shape falls into a dome or long bar type of indenter scenario. The EPRG method [42] provides a different factor depending on whether the dent is smooth or sharp and provides some guidance to determine smooth from sharp dents, based on the local radius of the dent.

As presented previously, dent depth alone is generally not an accurate predictor of the severity of the dent in terms of its impact on the fatigue life of a pipe. As presented in the literature review in Section A.3, the local stress-strain response in the pipe wall, and hence fatigue life, is affected by a number of parameters, including:

- Dent depth
- Dent length
- Dent width
- Depth ratio (d/D)
- Length ration (L/D)

In line with these findings, the development of the simplified fatigue life assessment approach will consider the use of a wide variety of dent/pipe shape parameters. The development of the detailed parameters that will be considered and the evaluation of the parameters will be carried out during Task 5 of the current project.

A.7 REFERENCES

- [1] Federal Regulations, Title 49 CFR §192 – Transportation of Natural and Other Gas by Pipeline: Minimum Federal Safety Standards.
- [2] Federal Regulations, Title 49 CFR §195 – Transportation of Hazardous Liquids by Pipeline.
- [3] CSA Z662-99, “Oil and Gas Pipeline Systems”, Canadian Standards Association, Etobicoke, Ontario, April 1999.
- [4] ASME B31.4, “Liquid Transportation Systems for Hydrocarbons, Liquid Petroleum Gas, Anhydrous Ammonia, and Alcohols”, The American Society of Mechanical Engineers, New York, New York, January 1993.
- [5] Eiber, R.J., “Causes of Pipeline Failures Probed”, Oil & Gas Journal, Vol. 77, No. 51, December 24, 1979, pp. 80-88.
- [6] Belonos, S.P, and Ryan, R.S., “Dents in Pipe”, The Oil & Gas Journal, Vol. 56, No. ? , November 17,1958, pp.151-161.
- [7] Wang, K.C. and Smith, E.D., “The Effect of Mechanical Damage on Fracture Initiation in Line Pipe: Part 1 – Dents”, Report ERP/PMRL 82-11(TR), Physical Metallurgy Research Laboratories, CANMET, January 1982.
- [8] Tyson, W.R. and Wang, K.C., “Effects of External Damage (Gouges and Dents) on Performance of Linepipe. A Review of Work at MTL, CANMET”, Report MTL 88-34(OP), Metals Technology Laboratories, CANMET, May 1988.
- [9] Maxey, W.A., “Analysis made of outside-force damage to pipelines, Defect behavior – 1”, Oil & Gas Journal, Vol. 85, No. 20, May 18, 1987, pp. 33-42.
- [10] Maxey, W.A., “Outside-force damage of pipe analyzed, Defect behavior – 2”, Oil & Gas Journal, Vol. 85, No. 21, May 25, 1987, pp.74-76.
- [11] Maxey, W.A., “Serviceability of damaged line pipe rated, Defect behavior – Conclusion”, Oil & Gas Journal, Vol. 85, No. 24, June 15, 1987, pp. 41-50.
- [12] Bjornoy, O.H., Rengard, O., and Bruce, P., “Residual Strength of Dented Pipelines, DNV Results”, Proceedings of the Tenth (2000) International Offshore and Polar Engineering Conference, Seattle.
- [13] Lancaster, E.R., and Palmer, S.C., “Experimental Study of Strains Caused by Pressurization of Pipes with Dents”, Fourth International Offshore and Polar Engineering Conference, Osaka, Japan, April 1994, The International Society of Offshore and Polar Engineers.

- [14] Lancaster, E.R., and Palmer, S.C., “Assessment of Mechanically Damaged Pipes Containing Dents and Gouges”, PVP-Vol. 261, Service Experience and Life Management: Nuclear, Fossil, and Petrochemical Plants, ASME, July 25-29, 1993, pp. 61-68.
- [15] Leis, B.N., Francini, R.B., Mohan, R., Rudland, D.L., and Olson, R.J., “The Pressure-Displacement Response of Gas-Transmission Pipelines Under Outside Forces – Towards a Serviceability Criterion for Mechanical Damage”, Paper 25, EPRG/PRC 11th Biennial Joint Technical Meeting on Line Pipe Research, April 1997, Washington, USA.
- [16] J.F. Kiefner, “Fracture Initiation”, 4th Symposium on Line Pipe Research, Dallas Texas, 18-19 November 1969.
- [17] Peter B. Keating and Roger L. Hoffmann, “Fatigue Behavior of Dented Petroleum Pipelines”, Texas Transportation institute, Texas A&M University System, College Station, Texas, May 1997.
- [18] M. Urednicek, “Effects of Dents on Failures of Gas Transmission Pipelines”, Report #14032, Materials Engineering Services, Nova An Alberta Corporation, September 1986.
- [19] J.R. Fowler, C.R. Alexander, P.J. Kovach, and L.M. Connelly, “Cyclic Pressure Fatigue Life of Pipelines With Plain Dents, Dents With Gouges, and Dents With Welds”, Report PR-201-927 and PR-201-9324, American Gas Association, June 1994.
- [20] D.G. Jones, “The Significance of Mechanical Damage in Pipelines”, American Gas Association – European Pipeline Research Group Line Pipe, Research Seminar IV, Duisburg, 22-24 September 1981, also 3R International, July 1982, pp 347-354.
- [21] R.J. Eiber, et al, “The Effects of Dents on Failure Characteristics of Line Pipe”, Battelle-Columbus Laboratories Report to the American Gas Association, AGA Catalogue No. L51403, May 1981.
- [22] M.E. Mayfield, W.A. Maxey, and G.M. Wilkowski, “Fracture Initiation Tolerance of Line Pipe”, AGA 6th Symposium on Line Pipe, 1979.
- [23] Fowler, J.R., Alexander, C.R., Kovach, P.J., & L.M. Connelly, “Fatigue Life of Pipelines with Dents and Gouges Subjected to Cyclic Internal Pressure”, PD Vol. 69, Pipeline Engineering, ASME 1995.
- [24] Alexander, C.R., & J.F. Kiefner, “Effects of Smooth and Rock Dents on Liquid Petroleum Pipelines”, American Petroleum Institute, API Publication 1156, November 1997.
- [25] Kiefner, J.F. and Alexander, C.R., , “Effects of Smooth and Rock Dents on Liquid Petroleum Pipelines (Phase II)”, American Petroleum Institute, Addendum to API Publication 1156, October 1999.

- [26] A.j. Rinehart, "Effects of Localized Geometric Imperfections on the Stress Behavior of Pressurized Cylindrical Sheels", Dissertation, Texas A&M University, August, 2003.
- [27] M.J. Rosenfeld, "Development of a Model for Fatigue Rating Shallow Unrestrained Dents", Final Report for Contract PR-281-9405, 19 Sept 1997, American Gas Association, Arlington, VA.
- [28] M.J. Rosenfeld, D.J. Warman, and R.C. McGregor, "Toward an Acceptance Criterion for Shallow Dents Affecting Girth Welds in Gas Transmission Pipelines", 1997 PVP conference in Orlando proceedings PVP Vol-353 "Pressure Vessel and Piping Codes & Standards".
- [29] M.J. Rosenfeld, "Guidelines for the Assessment of Dents on Welds", Final Report for Contract PR-218-9822, December 22, 1999, Pipeline Research Council International, Catalog Number L51810.
- [30] "IIW Guidance on Assessment of the Fitness for Purpose of Welded Structures", International Institute of Welding, IIW/IIS-SST-1157-90, 1990.
- [31] Buitrago, J., and Hsu, T.M., "Stress Concentration Factors for Dented Tubular Members", 1996 OMAE Conference, Volume 1 - Part A, Offshore Technology, pp 291-296.
- [32] M.F. Zarea, D.N. Toumbas, C.E. Philibert, and I. Deo, "Numerical Models for Static Denting and Dynamic Puncture of Gas Transmission Linepipe and Their Validation", International Pipeline Conference, Volume 2, ASME, 1996.
- [33] S. Hertz-Clemens, "Experimental and Numerical Modelling of Pipeline Denting", International Pipeline Conference, ASME, 2006.
- [34] Zarea, M., Champavere, R., Dezobry, J., Philibert, C., Cappanera, A., Dodi, F., Linke, G., and Engel, A., "The Pipe Agression Rig : A Comprehensive Means for Studying Pipe Resistance to Third Party Damage", Paper 22, EPRG/PRC 11th Biennial Joint Technical Meeting on Line Pipe Research, April 1997, Washington, USA.
- [35] Zarea, M., Deo, I., Philibert, C., "Full Scale Experimental Approach of Gas Transmission Pipeline Resistance to Dynamic Puncture", Paper 23, EPRG/PRC 11th Biennial Joint Technical Meeting on Line Pipe Research, April 1997, Washington, USA.
- [36] A. Cosham and P. Hopkins, "The Pipeline Defect Assessment Manual", Proceedings of 4th International Pipeline Conference, September 29 – October 3 2002, Calgary, AB, The American Society of Mechanical Engineers, New York, NY, pp 1565-1581.
- [37] BS 7910:1999, Guide on methods for assessing the acceptability of flaws in metallic structures, Incorporating Amendment No. 1, British Standards Institution, London, U.K., 1999.

- [38] Fitness-for-Service, API Recommended Practice 579, First Edition, American Petroleum Institute, Washington, DC, January 2000.
- [39] R.J. Eiber and T.A. Bubenik, "Fracture Control Plan Methodology", 8th Symposium of Line Pipe Research, Houston, TX, 26-29 September 1993, American Gas Association, Arlington, VA.
- [40] P. Hopkins, D.G. Jones, and A. Clyne, "Recent Studies of the Significance of Mechanical Damage in Pipelines", AGA/EPRG Seminar V, San Francisco, CA, September 1983, Paper 2.
- [41] N. Hagiwara and N. Oguchi, "Fatigue Behavior of Line Pipes Subjected to Severe Mechanical Damage", International Pipeline Conference, 11-17 June 1996, Calgary, AB, The American Society of Mechanical Engineers, New York, NY, 1998, pp 291-298.
- [42] R.J. Bood, M.R. Galli, U. Marewski, P. Roovers, M. Steiner, M. Zaream "EPRG Methods for Assessing the Tolerance and Resistance of Pipelines to External Damage Part 1+2", #R International, 1999.
- [43] A.J. Rinehart, P.B. Keating, "Fatigue Life Prediction of Short Dents in Petroleum Pipelines", Proceedings of the 2002 ASME pressure Vessels and Piping Conference, ASME, 2002, PVP2002-1268.
- [44] A.J. Rinehart, P.B. Keating, "Predicting the Fatigue Life of Long Dents in Petroleum Pipelines", Proceedings of the 21st International Conference on Offshore Mechanics and Arctic Engineering, 2002.
- [45] B.N. Leis, T.P. Forte, Z. Zhu, "Integrity Analysis for Dents in Pipelines", International Pipeline Conference, 2004, IPC04-0061.
- [46] PRCI MD4-2/DOT #339, Ongoing Full Scale Pipe Experimental Fatigue Life Program.

APPENDIX 1
SUMMARY OF EXPERIMENTAL DATA USED IN
FATIGUE LIFE METHODOLOGY DEMONSTRATION

Table A.1-1: Summary of Experimental Fatigue Life Specimens – MD4-2 [46]

#	Pipe	Nominal Diameter	Nominal Thickness	Nominal		Nominal Indenter Diameter	Initial Dent Depth	Dent Condition	Interacting with	Cyclic PressOre Range (%SMYS)	Experimental Cycles to Failure
				SMYS	UTS						
				(MPa)	(MPa)						
1	A	609.6	7.8994	358	455	2	7.5	R	Plain	10%-80%	6948
2	A	609.6	7.8994	358	455	2	7.5	R	Plain	10%-80%	38685
3	B	609.6	8.89	482	565	4	10	R	Plain	10%-80%	6886
4	B	609.6	8.89	482	565	4	10	R	Plain	10%-80%	16234
5	B	609.6	8.89	482	565	4	10	R	Plain	10%-80%	2531
6	B	609.6	8.89	482	565	4	10	R	Plain	10%-80%	3359
7	A	609.6	7.8994	358	455	2	15	U	Plain	10%-80%	21103
8	A	609.6	7.8994	358	455	2	15	U	Plain	10%-80%	28211
9	A	609.6	7.8994	358	455	2	15	U	Plain	10%-80%	6825
10	A	609.6	7.8994	358	455	2	15	U	Plain	10%-80%	9116
11	A	609.6	7.8994	358	455	4	15	U	Plain	10%-80%	15063
12	A	609.6	7.8994	358	455	4	15	U	Plain	10%-80%	27575
13	B	609.6	8.89	482	565	2	15	U	Plain	10%-80%	13262
14	B	609.6	8.89	482	565	2	15	U	Plain	10%-80%	15065
15	B	609.6	8.89	482	565	2	15	U	Plain	10%-80%	4035
16	B	609.6	8.89	482	565	2	15	U	Plain	10%-80%	4684
17	B	609.6	8.89	482	565	4	15	U	Plain	10%-80%	11415
18	B	609.6	8.89	482	565	4	15	U	Plain	10%-80%	15949
19	A	609.6	7.8994	358	455	2	5	R	Long Seam	10%-80%	32282
20	A	609.6	7.8994	358	455	2	5	R	Long Seam	10%-80%	24919
21	A	609.6	7.8994	358	455	2	5	R	Girth Weld	10%-80%	66871
22A	A	609.6	7.8994	358	455	4	10	R	Girth Weld	10%-80%	66429
23	B	609.6	8.89	482	565	4	10	R	Girth Weld	10%-80%	12722
24	B	609.6	8.89	482	565	4	10	R	Girth Weld	10%-80%	16278
25	A	609.6	7.8994	358	455	2	15	U	Girth Weld	10%-80%	19063
27	A	609.6	7.8994	358	455	2	15	U	Girth Weld	10%-80%	18633
28	A	609.6	7.8994	358	455	2	15	U	Girth Weld	10%-80%	16107

Table A.1-1: Summary of Experimental Fatigue Life Specimens – MD4-2 [46] – continued

#	Pipe	Nominal Diameter	Nominal Thickness	Nominal		Nominal Indenter Diameter	Initial Dent Depth	Dent Condition	Interacting with	Cyclic Pressure Range (%SMYS)	Experimental Cycles to Failure
				SMYS	UTS						
				(mm)	(mm)						
29	A	609.6	7.8994	358	455	4	15	U	Girth Weld	10%-80%	14400
31	B	609.6	8.89	482	565	2	15	U	Girth Weld	10%-80%	9890
32	B	609.6	8.89	482	565	2	15	U	Girth Weld	10%-80%	9506
33	B	609.6	8.89	482	565	4	15	U	Girth Weld	10%-80%	9386
34	B	609.6	8.89	482	565	4	15	U	Girth Weld	10%-80%	9871
35	B	609.6	8.89	482	565	4	15	U	Girth Weld	10%-80%	19959
36	B	609.6	8.89	482	565	4	15	U	Girth Weld	10%-80%	15568
26	A	609.6	7.8994	358	455	4	10	R	Metal Loss	10%-80%	40832
30	A	609.6	7.8994	358	455	4	10	R	Metal Loss	10%-80%	31179
37	A	609.6	7.8994	358	455	4	15	R	Metal Loss	10%-80%	42159
38	A	609.6	7.8994	358	455	4	15	U	Metal Loss	10%-80%	32963
39	B	609.6	8.89	482	565	4	5	R	Offset Metal Loss	10%-80%	7559
40	B	609.6	8.89	482	565	4	15	U	Offset Metal Loss	10%-80%	6504
41	C	457.2	7.9248	358	455	2	5	R	Plain	10%-80%	69099
42	C	457.2	7.9248	358	455	4	10	R	Plain	10%-80%	69393
46	C	457.2	7.9248	358	455	12	5	R	Plain	10%-80%	125525
48	C	457.2	7.9248	358	455	2	15	U	Plain	10%-80%	23482
52	C	457.2	7.9248	358	455	4	15	U	Plain	10%-80%	9226
54	C	457.2	7.9248	358	455	12	15	U	Plain	10%-80%	47702
56	C	457.2	7.9248	358	455	4	20	U	Plain	10%-80%	15473
57	C	457.2	7.9248	358	455	12	20	U	Plain	10%-80%	14091

Table A.1-2: Summary of Experimental Fatigue Life Specimens – [17]

#	Pipe	Nominal Diameter	Nominal Thickness	Nominal		Nominal Indenter Diameter	Initial Dent Depth	Dent Condition	Interacting with	Cyclic PressOre Range (%SMYS)	Experimental Cycles to Failure
				SMYS	UTS						
		(mm)	(mm)	(MPa)	(MPa)	(in)	(%)				
3D		324	6.35	289	413		12.5	U	BH-T	73%	89684
3E		324	6.35	289	413		15	U	BH-T	73%	80880
3F		324	6.35	289	413		12.5	R	Long Bar	73%	100943
5D		406	6.35	289	413			U	BH-T	72%	62970
5E		406	6.35	289	413			U	BH-T	72%	73977

Table A1-3: Summary of Experimental Fatigue Life Specimens – [24]

#	Pipe	Nominal Diameter	Nominal Thickness	Nominal		Nominal Indenter Diameter	Initial Dent Depth	Dent Condition	Interacting with	Cyclic PressOre Range (%SMYS)	Experimental Cycles to Failure
				SMYS	UTS						
		(mm)	(mm)	(MPa)	(MPa)	(in)	(%)				
UD12A-3		324	4.78	358	455	8	12%	U	Dome	36%/72%	26463/31045
CD24A'-26		324	4.78	358	455	8	24	R	Dome	36%/72%	23491/4687
UL12A-38T		324	4.78	358	455		12	U	Long Bar T	36%/72%	23159/15213

ANNEX B
TASK 3- DOCUMENTATION AND FURTHER VALIDATION OF DENT MODELLING

TABLE OF CONTENTS

ACRONYMS AND ABBREVIATIONS	iii
B.1 DEVELOPMENT AND VALIDATION OF DENT MODEL	1
B.1.1 Finite Element Model	1
B.1.2 Validation of Finite Element Model	3
B.1.2.1 Detailed Comparison – Specimen 27 (Batch A) and Specimen 24 (Batch B)	3
B.1.2.2 Summary of All Experimental Specimens	13

LIST OF FIGURES

Figure B.1: Finite Element Model (a) Pipe Specimen (b) Rigid Indenter	1
Figure B.2: Nonlinear Kinematic Hardening Material Model	2
Figure B.3: Comparison of Predicted and Experimental Stress-Strain Hysteresis Loops	2
Figure B.4: Comparison of Experimental and FE Results – Indentation Load vs. Indenter Travel	5
Figure B.5: Comparison of Experimental and FE Results – Pipe Wall OD Strains During Indentation	7
Figure B.6: Comparison of Experimental and FE Results – Specimen 27 – Axial Dent Profiles After Indenter Removal	8
Figure B.7: Comparison of Experimental and FE Results – Specimen 27 – Axial Dent Profiles After Second Pressure Cycle	9
Figure B.8: Comparison of Experimental and FE Results – Axial Dent Profiles At Completion of Test	10
Figure B.9: Comparison of Experimental and FE Results – Cyclic Strain Ranges During Internal Pressure Cycling	12
Figure B.10: Comparison of Experimental and FE Results – All Specimens – Indentation Load	15
Figure B.11: Comparison of Experimental and FE Results – All Specimens – Dent Depths after Completion of Testing	16
Figure B.12: Comparison of Experimental and FE Results – All Specimens – Internal Pressure Range	17
Figure B.13: Comparison of Experimental and FE Results – All Specimens – Hoop Strain Range	18
Figure B.14: Comparison of Experimental and FE Results - Specimen 27 – Axial Cyclic Strain Range	20

LIST OF TABLES

Table B.1: Specimen 27 (Batch A) and Specimen 24 (Batch B) Parameter Summary	4
Table B.2: Summary of Experimental Specimens used in Validation	13

B.1 DEVELOPMENT AND VALIDATION OF DENT MODEL

The development and validation of the numerical dent model has been completed. The validation was carried out using the data from the full scale experimental joint test program being carried out by PRCI and DOT (PRCI Project # MD-4-2, DOT 339), which uses rigid spherical indenters to create single peak dents for a variety of testing scenarios.

B.1.1 Finite Element Model

The numerical dent model developed as part of this project is a nonlinear finite element analysis model created and analyzed using the ANSYS 12.1 software package. The fully nonlinear model includes large displacements, large strains and nonlinear material behavior to accurately predict the behavior of a dented pipeline specimen.

The generic finite element model, shown in Figure B.1 below, consists of the experimental specimen including the pipe body and the hemispherical end caps, which are both modeled using 8-noded quadratic shell elements. The indenters are modeled using rigid contact elements where the shape of each of the indenters is based on the detailed geometry of the actual indenters used in the experiments. The rig plating at the center span of the model is modeled using contact elements with the rig surface being held rigidly in all degrees of freedom. The end supports are modeled as linear elastic plates which are rigidly fixed along the centerline of the pipe, to attempt to account for the leaf spring effect the end support jacks have in the actual test.

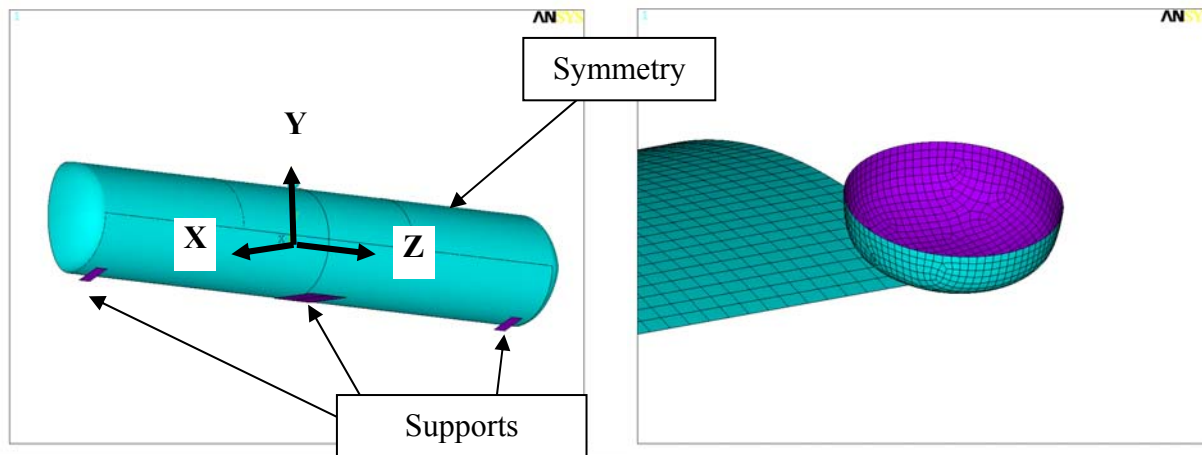


Figure B.1: Finite Element Model (a) Pipe Specimen (b) Rigid Indenter

A nonlinear kinematic hardening material model (CHABOCHE) was developed for each of the three pipe materials used in the experimental program. A sample curve fit to the monotonic stress-strain curve for the X70 material is shown in Figure B.2. The accuracy of the material model was assessed as shown in Figure B.3 which presents the stress-strain hysteresis loops predicted using a finite element analysis model compared against the experimental cyclic stabilized hysteresis loop generated for a typical round bar strain life test specimen.

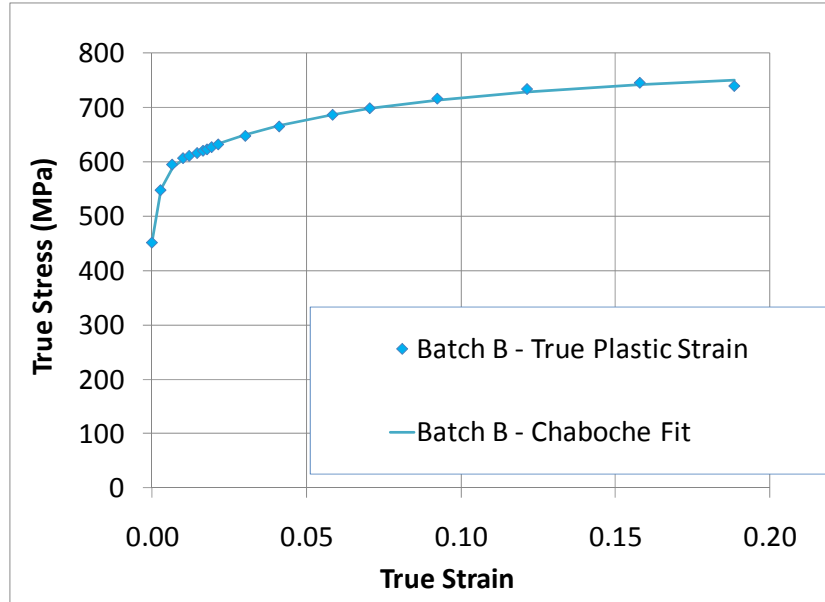


Figure B.2: Nonlinear Kinematic Hardening Material Model

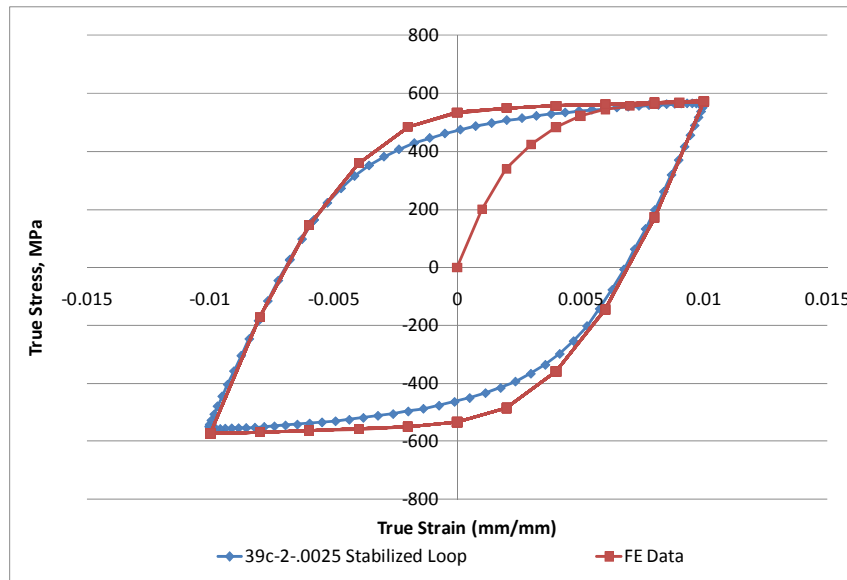


Figure B.3: Comparison of Predicted and Experimental Stress-Strain Hysteresis Loops

Material anisotropy (i.e., longitudinal versus circumferential) was modeled where applicable using a Hill plasticity model.

The loading procedure used in the finite element analysis closely matched the sequence used during the actual experiments and includes the following steps:

1. Displacement of the indenter into the pipe body to the specified depth with zero internal pressure.
2. If the specimen being modeled is unrestrained, the indenter is withdrawn until no contact exists between it and the pipe body. If the specimen being modeled represents a restrained indenter, the indenter is rigidly held in place at the specified depth throughout the remainder of the analysis.
3. Apply the first maximum internal pressure cycle (either 100% SMYS or 80% SMYS depending on the specimen).
4. Apply the second maximum internal pressure cycle (80% SMYS).
5. Apply three cycles of the cyclic pressure range (from 10% to 80% SMYS).

B.1.2 Validation of Finite Element Model

A summary of the finite element model validation efforts are presented in the following section. The validation is presented in two sections where the first section, (Figures B.4 through B.9) presents a detailed comparison of the experimental and FE model results for Specimens 27 and 24 (the parameters for Specimens 27 and 24 are summarized in Table 1) and the second section (Figures B.10 through B.15) presents a summary of the comparison of all the experimental specimens.

B.1.2.1 Detailed Comparison – Specimen 27 (Batch A) and Specimen 24 (Batch B)

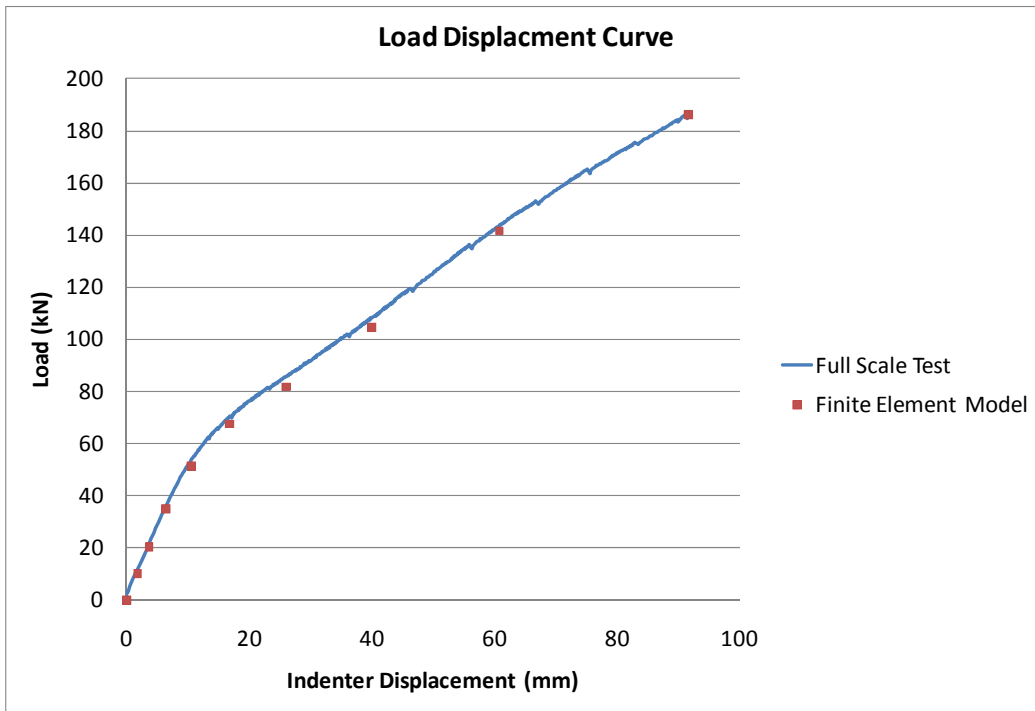
The detailed validation presented for Specimen 27 (Batch A, Unrestrained) and Specimen 24 (Batch B, Restrained) present a comparison of the results in terms of:

- The indentation load versus indenter travel during dent formation,
- The pipe wall strains experienced during indentation,
- The dent shapes at various stages of testing, and
- The cyclic pipe wall strain ranges experienced during the internal pressure cycling phase of the test.

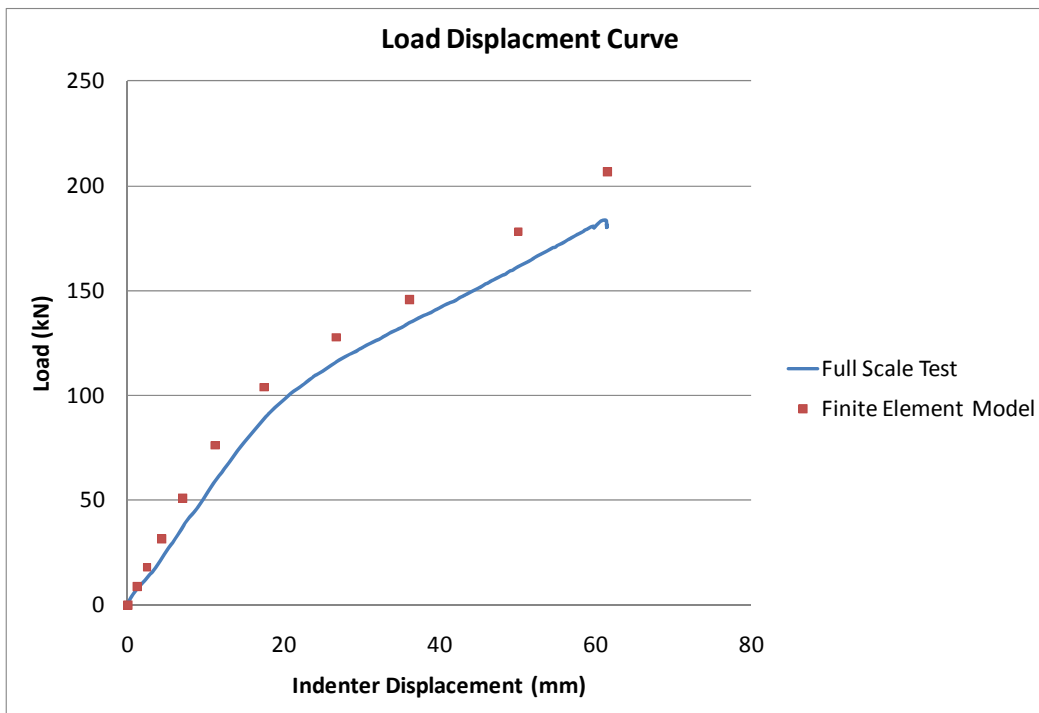
Table B.1: Specimen 27 (Batch A) and Specimen 24 (Batch B) Parameter Summary

Pipe Batch		A (Grade X52)	B (Grade X70)
Diameter	(mm)	609.6	609.6
Nominal Thickness	(mm)	7.8994	8.8900
SMYS	(MPa)	358	482
UTS	(MPa)	455	565
Indenter Nominal Diameter	(in)	2	4
Initial Dent Depth	(%)	15	10
Dent Condition		Unrestrained	Restrained
Interacting with		Girth Weld	Girth Weld
Initial Press. Cycle	(%SMYS)	100%	100%
Second Press. Cycle	(%SMYS)	80%	80%
Cyclic Press. Range	(%SMYS)	10%-80%	10%-80%

Figures B.4(a) and B.4(b) present a comparison of the experimental and FE model indentation load versus indenter travel for Specimens 27 and 24, respectively. As shown, the FE prediction of the load-displacement behavior is in good agreement with the experimental measurements.



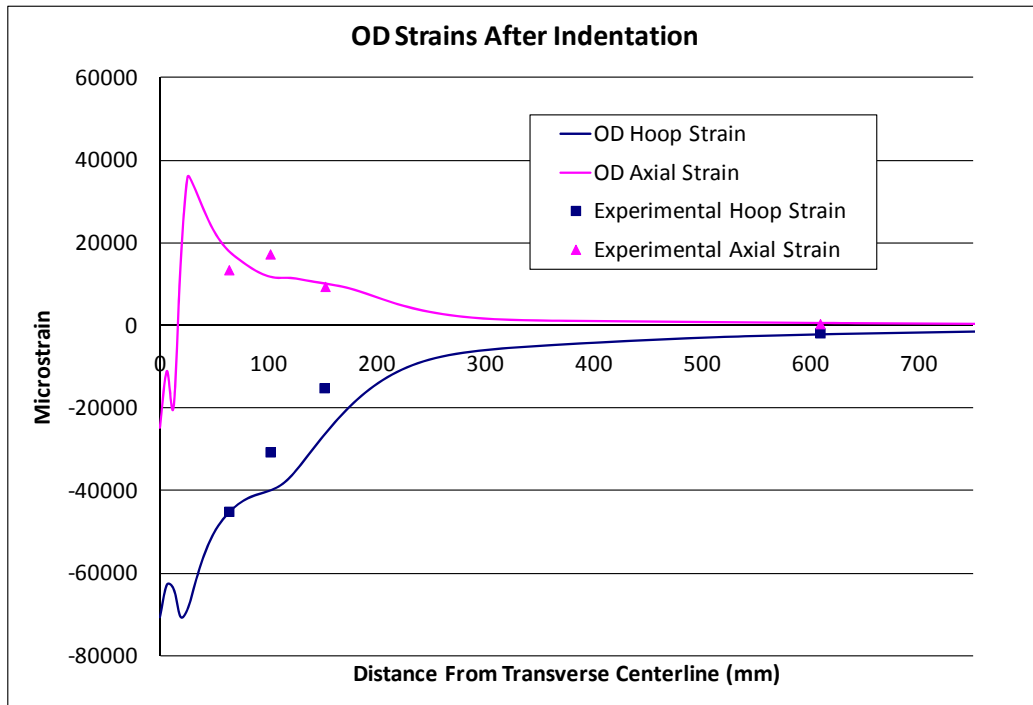
(a) Specimen 27



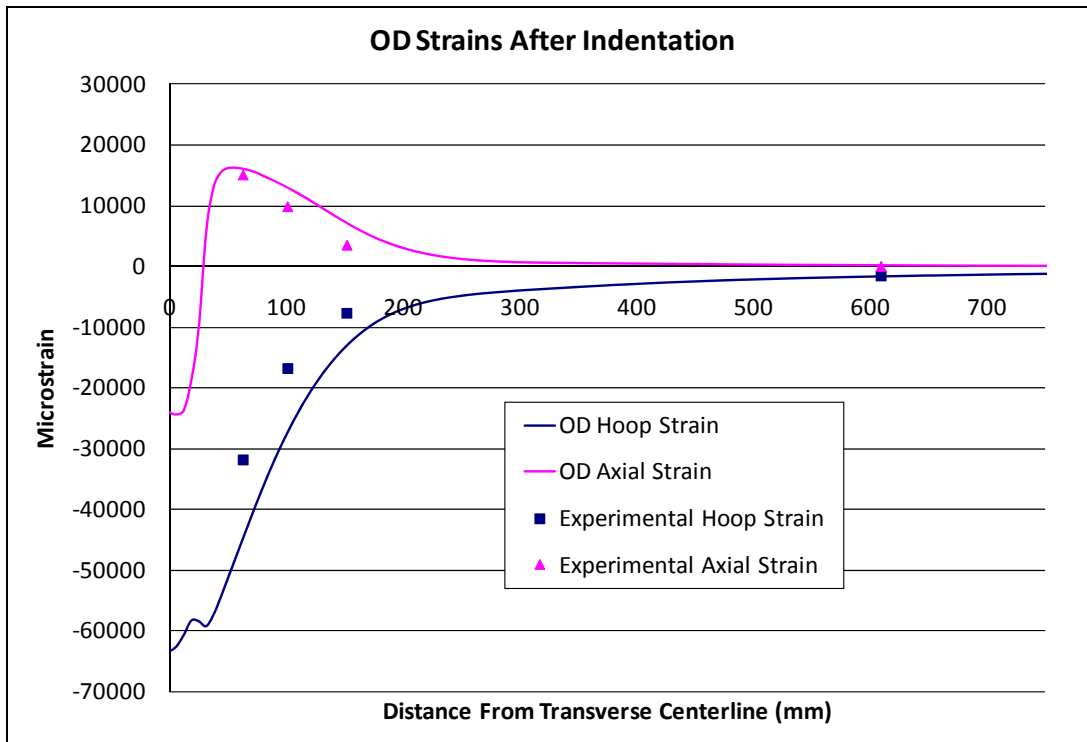
(b) Specimen 24

Figure B.4: Comparison of Experimental and FE Results – Indentation Load vs. Indenter Travel

Figures B.5(a) and B.5(b) present a comparison of the experimental hoop and axial strains during indentation versus the FE model predictions for Specimens 27 and 24, respectively. Although some differences between the experimental and predicted indentation strains are evident, the predicted results match both the trends and the strain magnitudes exhibited by the experimental results.



(a) Specimen 27



(b) Specimen 24

Figure B.5: Comparison of Experimental and FE Results – Pipe Wall OD Strains During Indentation

Figures B.6 through B.8 present a comparison of the experimental and predicted dent shapes at three different stages of the experimental process for Specimen 27, where the dent shapes are presented as axial profiles through the peak of the dent:

1. After the formation of the dent and removal of the indenter (allowing for elastic rebound).
2. After the second full scale pressure cycle (i.e., following both the first 100% SMYS pressure cycle and the 80% SMYS pressure cycle).
3. At the conclusion of the test.

As Specimen 24 is a restrained test, only the final dent shape is available for comparison with the finite element model. As such, Figure B.8(b) presents a comparison of the experimental and predicted dent shapes at the conclusion of the test.

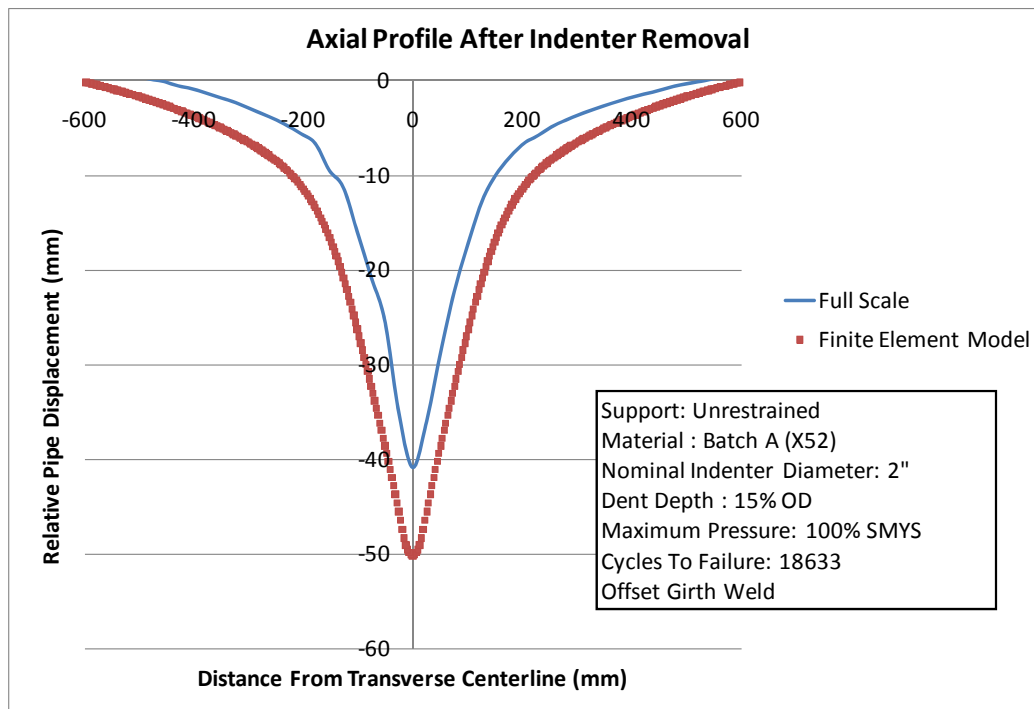


Figure B.6: Comparison of Experimental and FE Results – Specimen 27 – Axial Dent Profiles After Indenter Removal

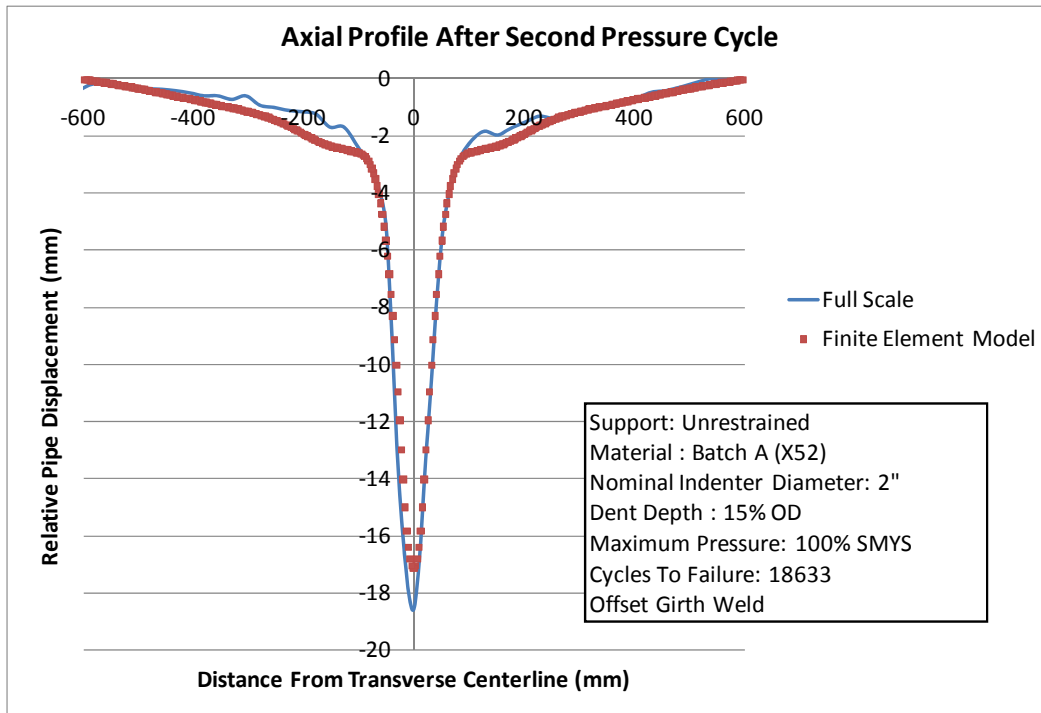
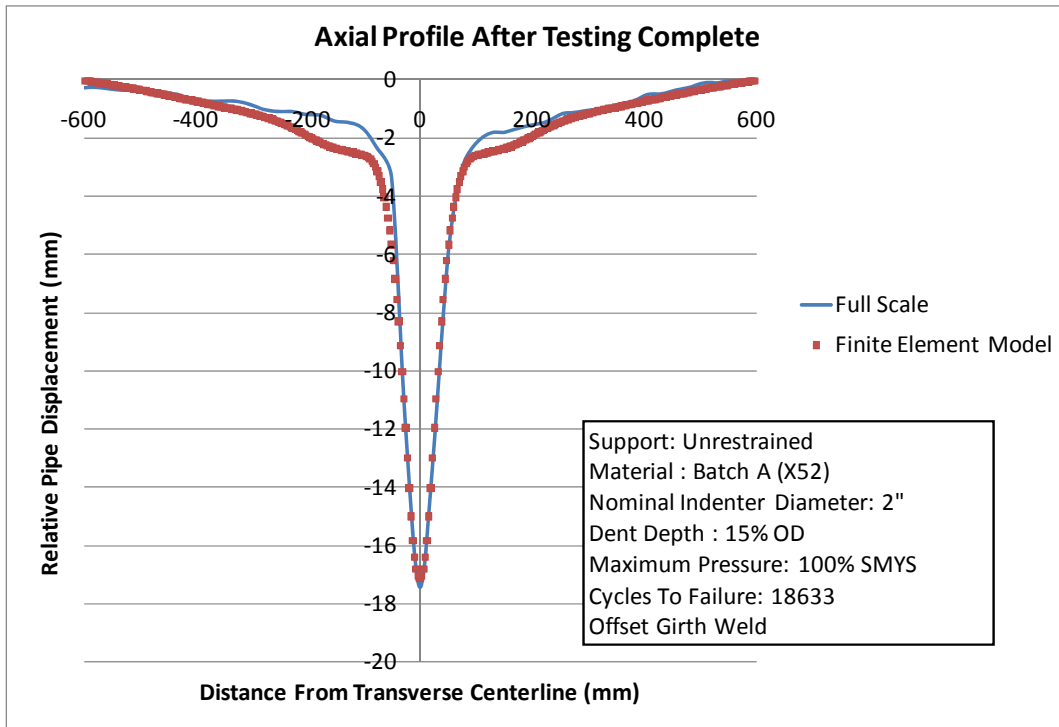
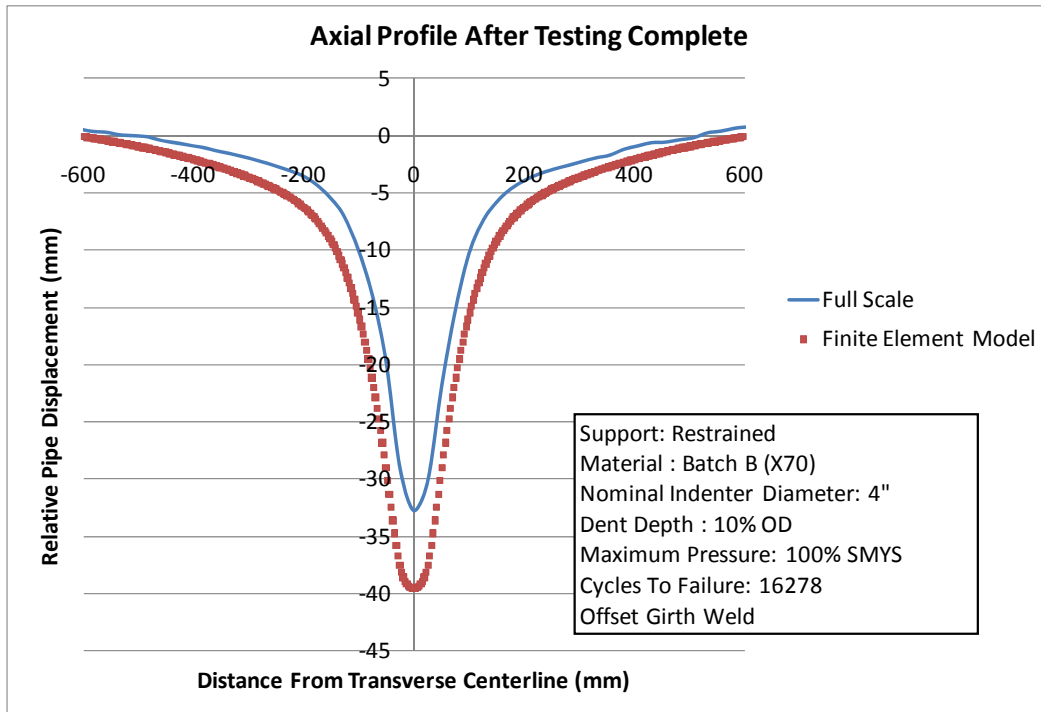


Figure B.7: Comparison of Experimental and FE Results – Specimen 27 – Axial Dent Profiles After Second Pressure Cycle



(a) Specimen 27



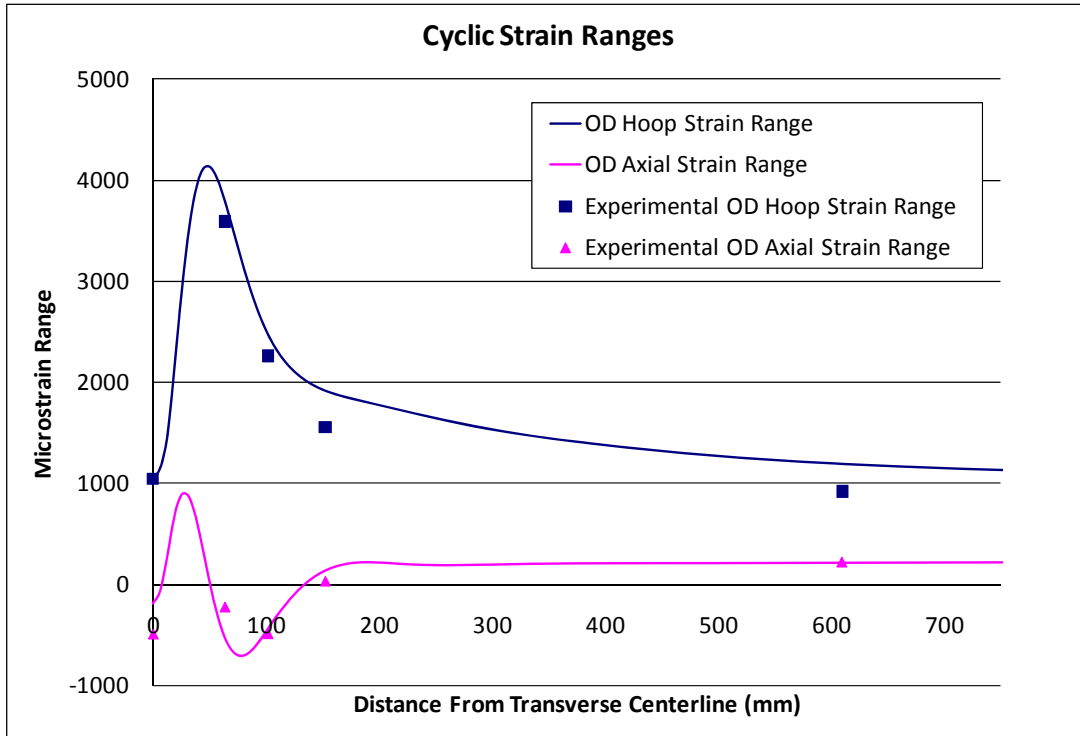
(b) Specimen 24

Figure B.8: Comparison of Experimental and FE Results – Axial Dent Profiles At Completion of Test

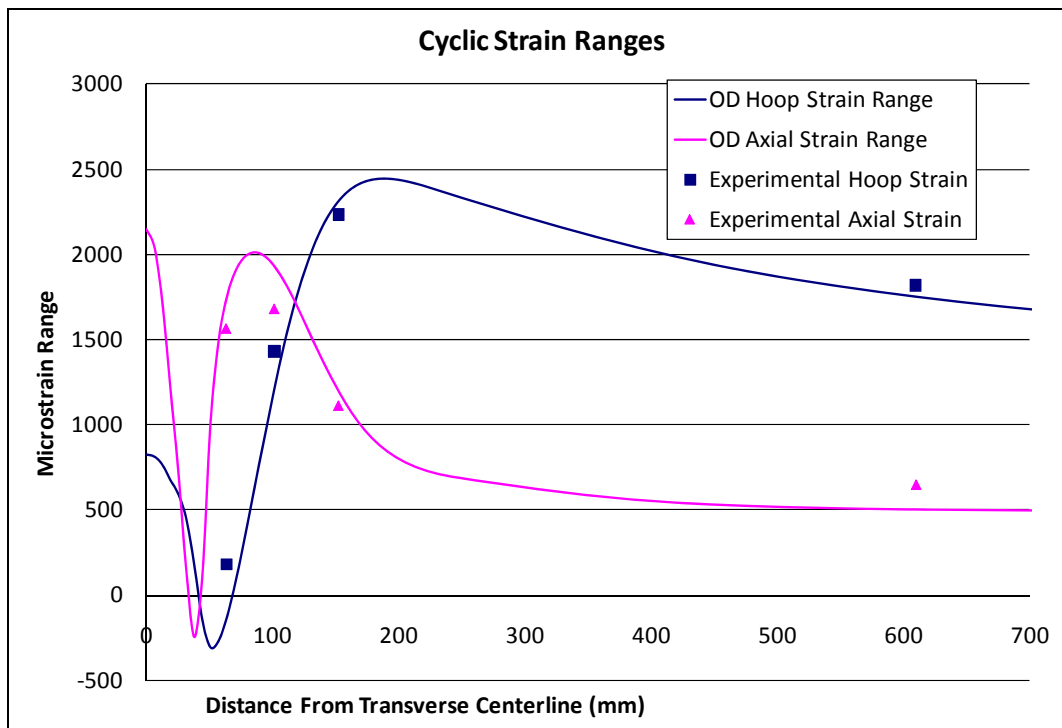
As shown in Figure B.6, the FE model dent shape under predicts the elastic rebound of the unrestrained dent (Specimen 27), such that the residual dent shape following the removal of the indenter is slightly deeper in the FE model than in the experiment. Figures B.7 and B.8 indicate that the agreement between the experimental and predicted dent shapes improves following the full scale pressure cycles and at the completion of the testing.

Figure B.8(b) shows that in the case of the restrained dent (Specimen 24), the FE model dent shape under predicts the final rebound of the dent, such that the dent shape following the removal of the indenter is slightly deeper in the FE model than in the experiment.

Figures B.9 and B.9(b) presents a comparison of the experimental and FE model cyclic strain ranges experienced at the pipe wall OD for Specimens 27 and 24, respectively. As shown, in general the FE predictions are in good agreement with the experimentally measured cyclic strain ranges for all the gauges along the axial centerline of the pipe specimen.



(a) Specimen 27



(b) Specimen 24

Figure B.9: Comparison of Experimental and FE Results – Cyclic Strain Ranges During Internal Pressure Cycling

B.1.2.2 Summary of All Experimental Specimens

The following section presents a summary of the comparisons between the experimental and predicted results for all of the experimental specimens available at the time of this report.

A summary of the experimental specimens included in the validation efforts is presented in Table B.2.

The validation results are presented as scatter plots comparing the FE model predictions against experimental results, for the following parameters:

1. Indentation loads,
2. Initial dent depths,
3. Internal pressure ranges,
4. Hoop and axial strain ranges for the gauges located at 2” and 4” from the centre of the dent.

Each data point in the plot represents a single experimental specimen. The plots include lines representing perfect agreement (1:1) between the experimental and predicted results (the solid red diagonal line), along with upper and lower 10% bounds (the dashed red diagonal lines).

Table B.2: Summary of Experimental Specimens used in Validation

Spec #	Pipe	Nominal Pipe Diameter	Nominal Thickness	Grade	Nominal Indenter Diameter	Initial Dent Depth	Dent Restraint	Interac.	Initial Press Cycle	Cyclic Press Range
		(mm)	(mm)	SMYS (MPa)	(in)	(%)			(%SMYS)	(%SMYS)
1	A	609.6	7.8994	X52	2	5	R	Plain	100%	10%-80%
2	A	609.6	7.8994	X52	2	5	R	Plain	100%	10%-80%
3	B	609.6	8.89	X70	4	10	R	Plain	100%	10%-80%
4	B	609.6	8.89	X70	4	10	R	Plain	100%	10%-80%
5	B	609.6	8.89	X70	4	10	R	Plain	80%	10%-80%
6	B	609.6	8.89	X70	4	10	R	Plain	80%	10%-80%
7	A	609.6	7.8994	X52	2	15	U	Plain	100%	10%-80%
8	A	609.6	7.8994	X52	2	15	U	Plain	100%	10%-80%
9	A	609.6	7.8994	X52	2	15	U	Plain	80%	10%-80%
10	A	609.6	7.8994	X52	2	15	U	Plain	80%	10%-80%
11	A	609.6	7.8994	X52	4	15	U	Plain	100%	10%-80%
12	A	609.6	7.8994	X52	4	15	U	Plain	100%	10%-80%
13	B	609.6	8.89	X70	2	15	U	Plain	100%	10%-80%
14	B	609.6	8.89	X70	2	15	U	Plain	100%	10%-80%
15	B	609.6	8.89	X70	2	15	U	Plain	80%	10%-80%
16	B	609.6	8.89	X70	2	15	U	Plain	80%	10%-80%
17	B	609.6	8.89	X70	4	15	U	Plain	100%	10%-80%
18	B	609.6	8.89	X70	4	15	U	Plain	100%	10%-80%

Table B.2: Summary of Experimental Specimens used in Validation (continued)

Spec #	Pipe	Nominal Pipe Diameter	Nominal Thickness	Grade	Nominal Indenter Diameter	Initial Dent Depth	Dent Restraint	Interac.	Initial Press Cycle	Cyclic Press Range
		(mm)	(mm)	SMYS (MPa)	(in)	(%)			(%SMYS)	(%SMYS)
19	A	609.6	7.8994	X52	2	5	R	LS	100%	10%-80%
20	A	609.6	7.8994	X52	2	5	R	LS	100%	10%-80%
21	A	609.6	7.8994	X52	2	5	R	GW	100%	10%-80%
22A	A	609.6	7.8994	X52	4	10	R	GW	100%	10%-80%
23	B	609.6	8.89	X70	4	10	R	GW	100%	10%-80%
24	B	609.6	8.89	X70	4	10	R	GW	100%	10%-80%
25	A	609.6	7.8994	X52	2	15	U	GW	100%	10%-80%
27	A	609.6	7.8994	X52	2	15	U	GW	100%	10%-80%
28	A	609.6	7.8994	X52	2	15	U	GW	100%	10%-80%
29	A	609.6	7.8994	X52	4	15	U	GW	100%	10%-80%
31	B	609.6	8.89	X70	2	15	U	GW	100%	10%-80%
32	B	609.6	8.89	X70	2	15	U	GW	100%	10%-80%
33	B	609.6	8.89	X70	4	15	U	GW	100%	10%-80%
34	B	609.6	8.89	X70	4	15	U	GW	100%	10%-80%
35	B	609.6	8.89	X70	4	15	U	GW	100%	10%-80%
36	B	609.6	8.89	X70	4	15	U	GW	100%	10%-80%
41	C	457.2	7.9248	X52	2	5	R	Plain	100%	10%-80%
42	C	457.2	7.9248	X52	4	10	R	Plain	100%	10%-80%
46	C	457.2	7.9248	X52	12	5	R	Plain	100%	10%-80%
48	C	457.2	7.9248	X52	2	15	U	Plain	100%	10%-80%
52	C	457.2	7.9248	X52	4	15	U	Plain	80%	10%-80%
54	C	457.2	7.9248	X52	12	15	U	Plain	100%	10%-80%
56	C	457.2	7.9248	X52	4	20	U	Plain	100%	10%-80%
57	C	457.2	7.9248	X52	12	20	U	Plain	80%	10%-80%

Figure B.10 presents the global comparison of the indentation load. As shown, there is good agreement between the experimental and FE predictions, with the majority of the indentation loads falling within the upper and lower 10% bounds.

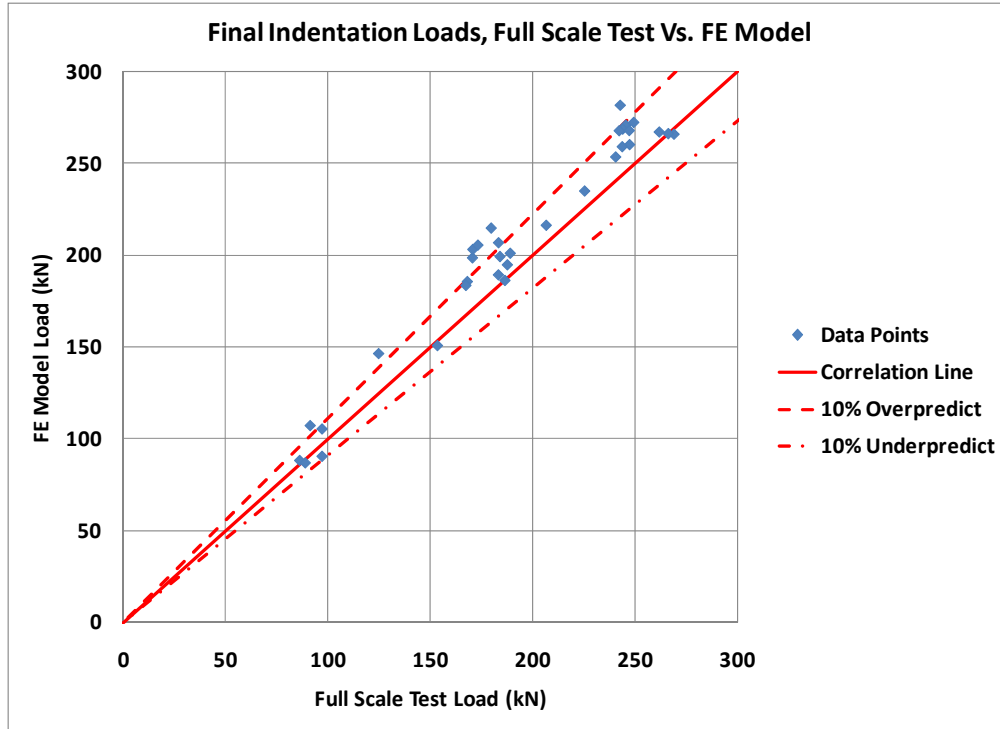


Figure B.10: Comparison of Experimental and FE Results – All Specimens – Indentation Load

Figure B.11 presents the comparison of the dent depth after completion of the testing, showing the general agreement between the experimental and predicted depths for both restrained and unrestrained specimens.

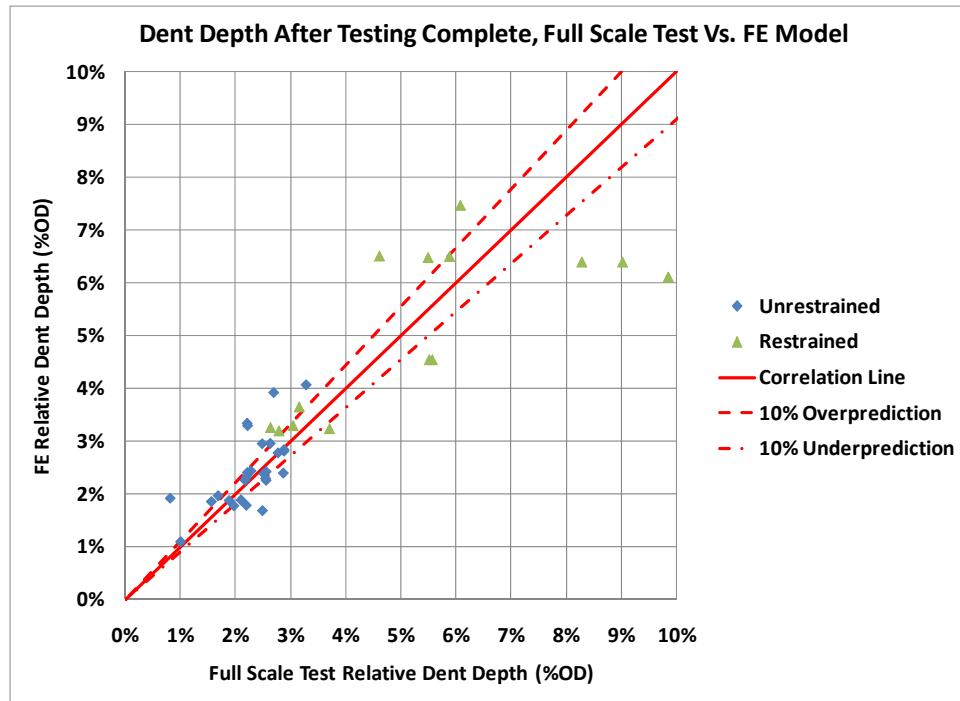


Figure B.11: Comparison of Experimental and FE Results – All Specimens – Dent Depths after Completion of Testing

In Figure B.11, the three restrained dents lying below and to the right of the agreement line represent experimental specimens that, due to the combination of small indenter radius and deep initial dent depths, exhibited significant localized plastic flow underneath the indenter, resulting in a significant localized indentation in the pipe wall. This degree of localized plasticity was not evident in other specimens.

Figure B.12 presents a comparison of the actual experimental internal pressure range (i.e., difference between maximum and minimum internal pressures) at the 200 cycle count point against the average pressure range used in the FE models. The plot helps to illustrate how accurately the internal pressure range used in the FE models approximates the actual pressure ranges applied in the experimental testing. Slight differences between the experimental and FE pressure ranges can help to explain some of the differences between the experimental and predicted pipe wall strains shown in Figure B.13.

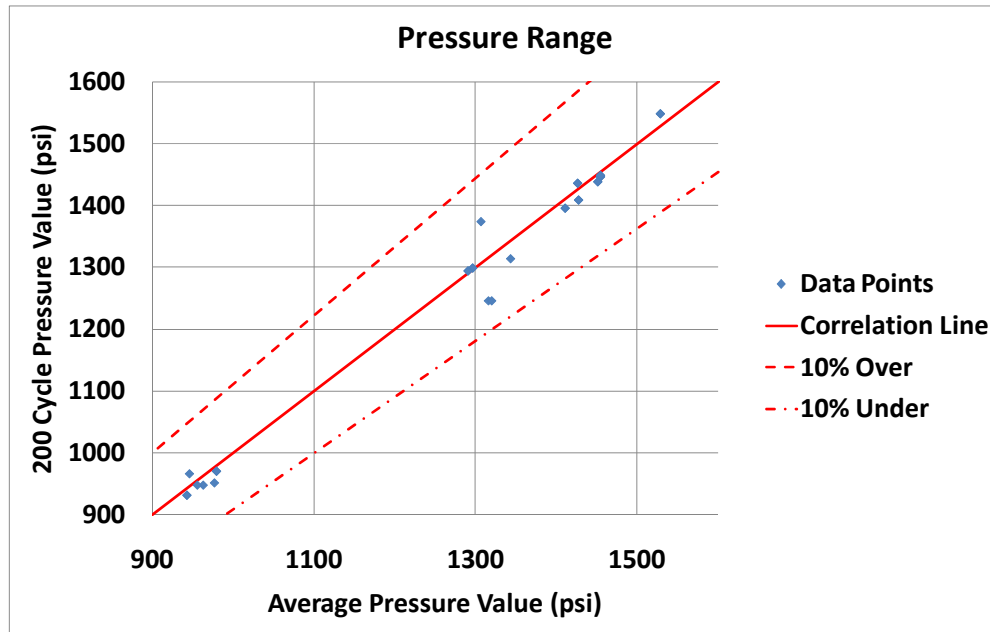
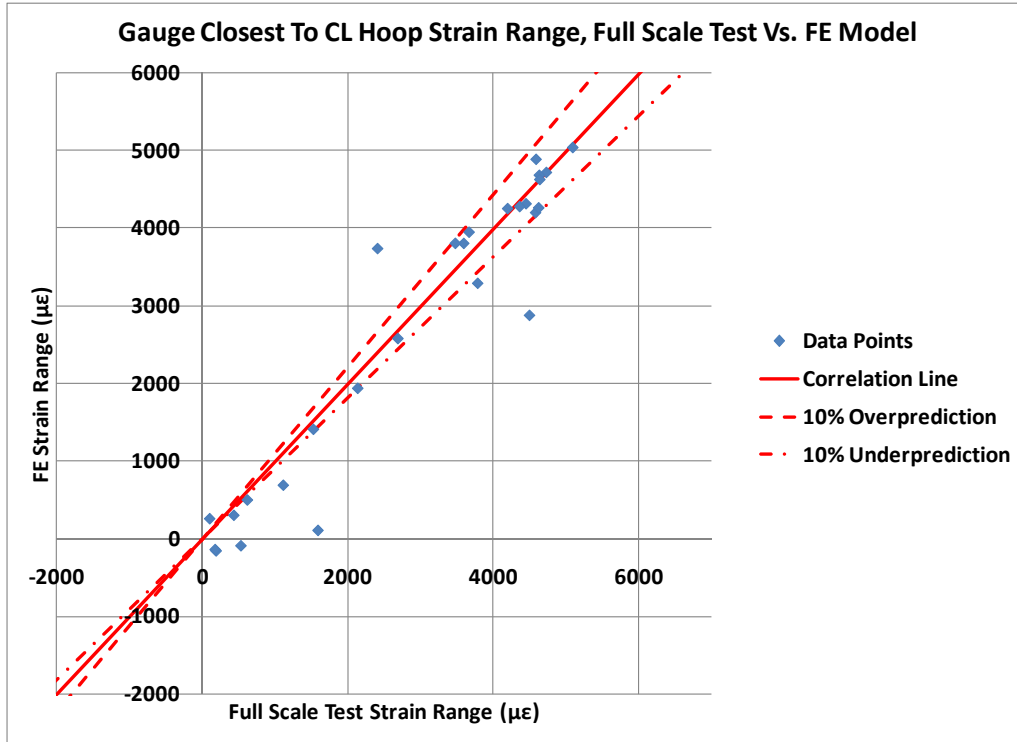


Figure B.12: Comparison of Experimental and FE Results – All Specimens – Internal Pressure Range

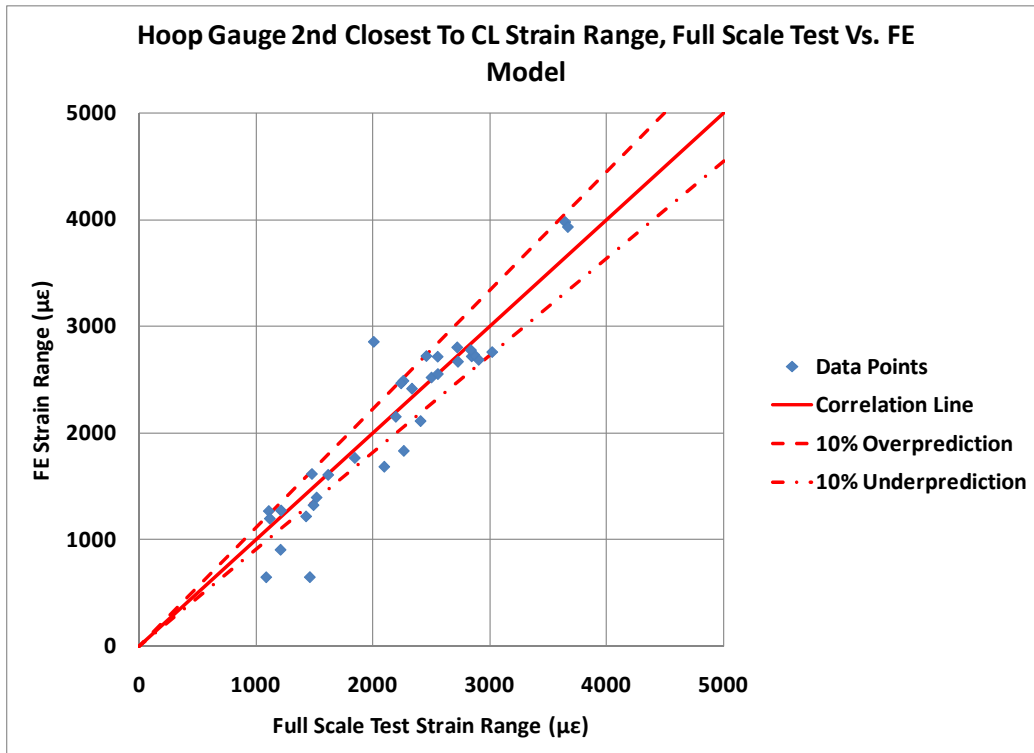
Figure B.13 presents the comparison of the hoop strain ranges during the cyclic internal pressure loading, for the gauge located closest to the dent peak and for the next closest gauge. Similarly, Figure B.14 presents a comparison of the axial strain ranges during the cyclic internal pressure loading.

As shown in Figure B.13, the predicted hoop strain ranges are in good agreement with the experimental results, with the majority of the predicted ranges falling within the 10% bounds of the experimental data. A more detailed analysis of the outliers will be used to identify possible reasons for the lack of agreement between the predicted and experimental results. The outcome of the detailed analysis will be presented in the full report documenting the development and validation of the finite element model.

The results shown in Figure B.14 indicate that the predicted axial strain ranges are also in good agreement with the experimental measurements. The differences in the axial strains at the gauge located closest to the dent peak, highlighted by the red circle in Figure B.14(a) may be due to the significant strain gradients that exist in this area. This strain gradient is illustrated in Figure B.15, which presents the axial strain plot from Figure B9 on a smaller scale. As shown in Figure B.15, a slight change in the axial location of the strain gauge can result in significant changes in the measured strains.

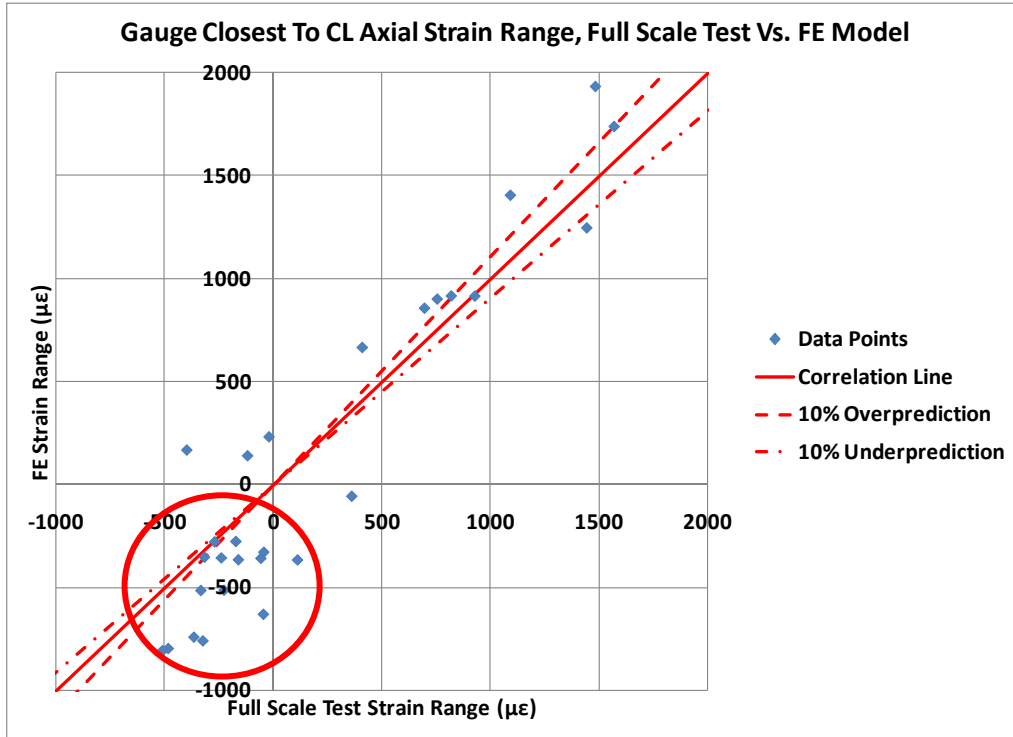


(a) Gauge Closest to Dent Peak

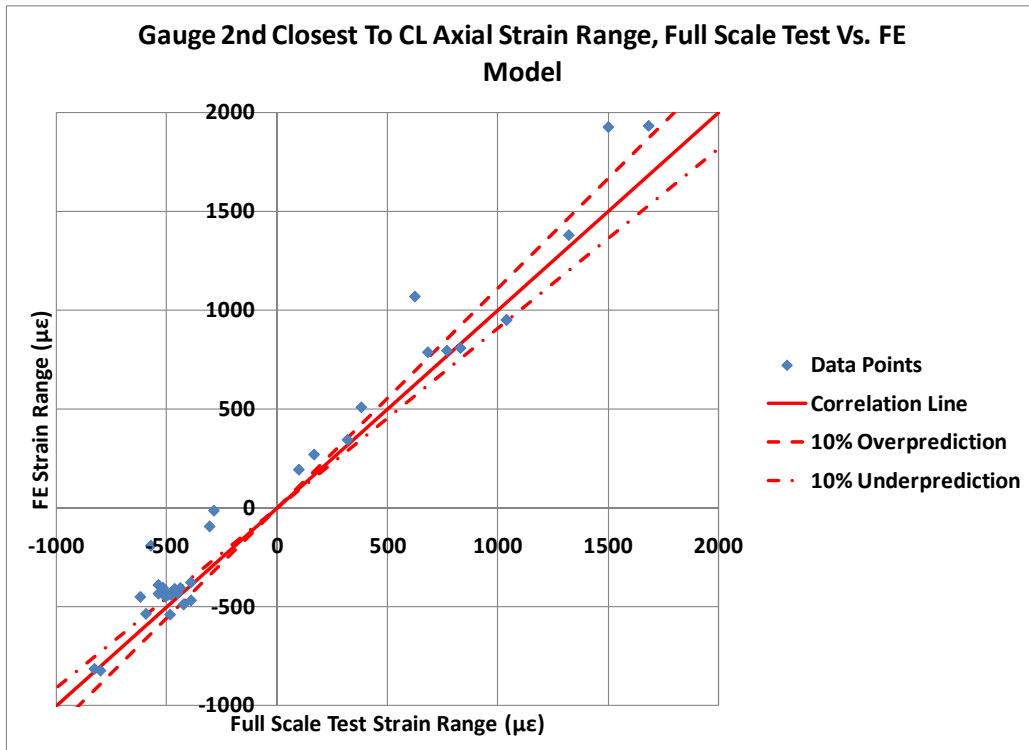


(b) Gauge 2nd Closest to Dent Peak

Figure B.13: Comparison of Experimental and FE Results – All Specimens – Hoop Strain Range



(a) Gauge Closest to Dent Peak



(b) Gauge 2nd Closest to Dent Peak

Figure B.14: Comparison of Experimental and FE Results – All Specimens – Axial Strain Range

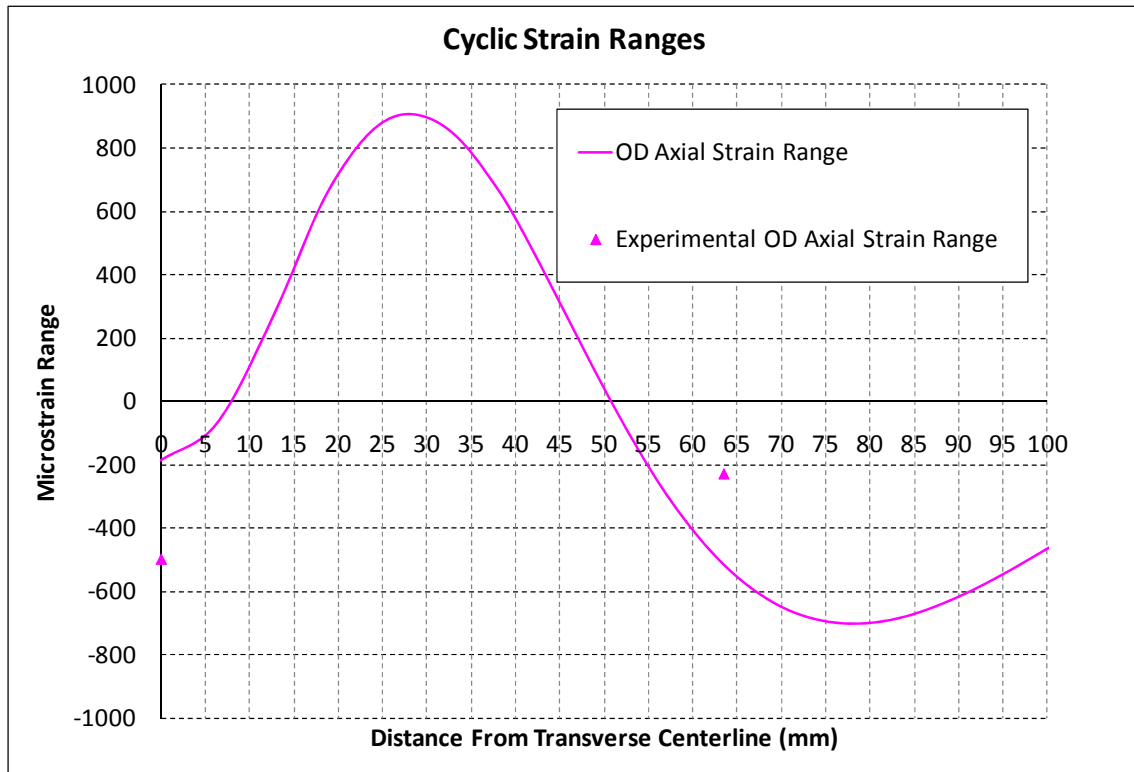


Figure B.15: Comparison of Experimental and FE Results – Specimen 27 – Axial Cyclic Strain Range

ANNEX C
TASK 4- DEVELOPMENT AND VALIDATION
OF FATIGUE LIFE ESTIMATION APPROACH

TABLE OF CONTENTS

ACRONYMS AND ABBREVIATIONS	iii
C.1 INTRODUCTION	1
C.2 STRESS LIFE (S-N) ANALYSIS	2
C.3 STRAIN LIFE.....	9
C.4 FRACTURE MECHANICS CRACK GROWTH ANALYSIS	18

LIST OF FIGURES

Figure C.1: Example S-N Curve Relating Stress Range ($\Delta\sigma$) to Cycles to Failure (N)	Error! Bookmark not defined.
Figure C.2: Comparison of Experimental Fatigue Lives and Industry Standard S-N Curves	Error! Bookmark not defined.
Figure C.3: Experimentally Derived S-N Curves.....	Error! Bookmark not defined.
Figure C.4: Generic Strain-Life Curve	Error! Bookmark not defined.
Figure C.5: Morrow Strain Life Curves	Error! Bookmark not defined.
Figure C.6: Manson-Halford Strain Life Curves.....	Error! Bookmark not defined.
Figure C.7: Smith-Watson-Topper Strain Life Curves.....	Error! Bookmark not defined.
Figure C.8: Effect of Surface Finish on Fatigue Strength	Error! Bookmark not defined.
Figure C.9: Experimental Strain-Life Curves – X52, X52 Vintage and X70....	Error! Bookmark not defined.
Figure C.10: Comparison of Experimental Strain Life Curves and Experimental Fatigue Lives	Error! Bookmark not defined.
Figure C.11: Comparison of X52 Modified Experimental Strain Life Curves and Experimental Fatigue Lives	Error! Bookmark not defined.
Figure C.12: Comparison of X52 Vintage Modified Experimental Strain Life Curves and Experimental Fatigue Lives.....	Error! Bookmark not defined.
Figure C.13: Comparison of X70 Modified Experimental Strain Life Curves and Experimental Fatigue Lives	Error! Bookmark not defined.

LIST OF TABLES

Table C.1: Industry Standard S-N Curves Considered.....	Error! Bookmark not defined.
Table C.2: Summary of BS 7608 and Experimental S-N Curve Parameters ...	Error! Bookmark not defined.
Table C.3: Comparison of Experimental and Predicted Fatigue Lives – BS 7608	Error! Bookmark not defined.
Table C.4: Summary of Calibrated Initial Flaw Sizes.....	Error! Bookmark not defined.
Table C.5: Summary of Initial Flaws Sizes Considered	Error! Bookmark not defined.

Table C.6: Comparison of Experimental and Predicted Fatigue Lives – Fracture Mechanics
.....**Error! Bookmark not defined.**

C.1 INTRODUCTION

The following section presents a discussion of the following three fatigue life assessment approaches investigated as part of the project:

- Stress Life (S-N);
- Strain Life (e-N); and
- Fracture mechanics based crack growth

The discussion focuses on using the detailed finite element analysis results (taken from the modeling efforts described in the previous annex) along with each of the fatigue life assessment approaches to predict the fatigue life for the full scale experimental specimens from MD-4-2 (DOT Project Number 339).

C.2 STRESS LIFE (S-N) ANALYSIS

The stress life (S-N) approach to fatigue life assessment utilizes a curve relating the stress range ($\Delta\sigma$) to the number of cycles to failure (N) as shown in Figure C.1 below. The typical stress life curve is described using the following equation:

$$\log N = \log C + m \log(\Delta\sigma) \quad (\text{C.1})$$

where $\log C$ and m are constants dependent on material and detailed geometry.

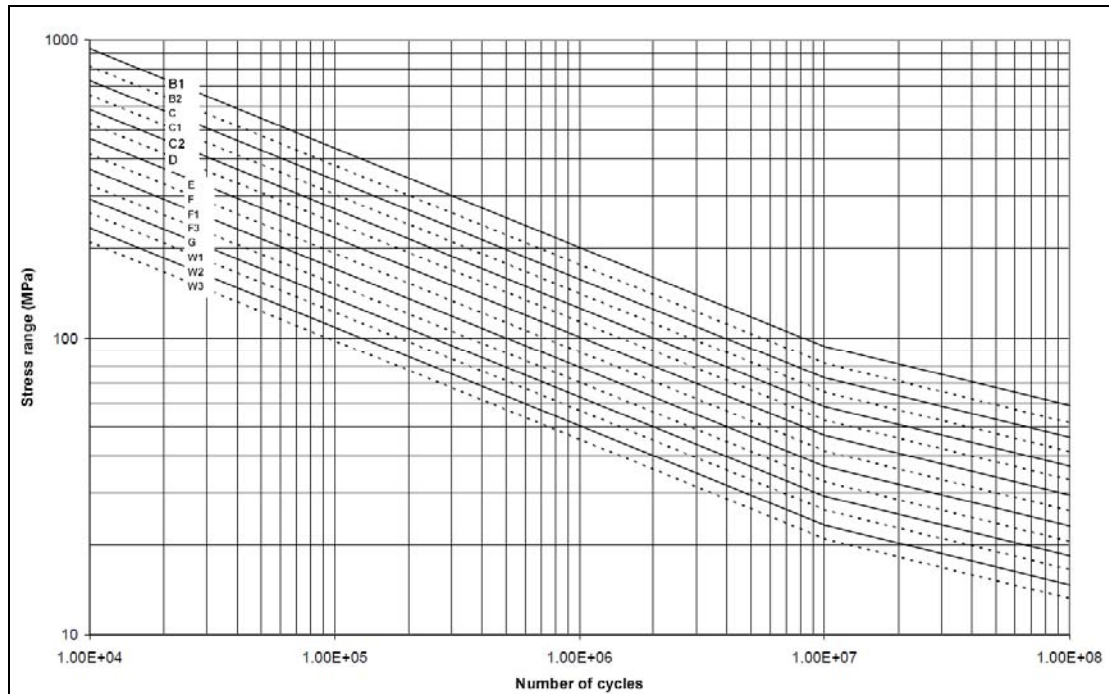


Figure C.1: Example S-N Curve Relating Stress Range ($\Delta\sigma$) to Cycles to Failure (N)

A range of industry standard S-N curves were compared to the fatigue life data from the full scale experimental specimens, where the number of cycles to failure (N) for each specimen was taken from the actual experimental data and the applied stress range ($\Delta\sigma$) was taken as the maximum stress range in the specimen predicted using the detailed finite element analysis. The industry standard curves considered in the assessment are summarized in Table C.1 and includes both base metal and typical butt weld curves.

Table C.1: Industry Standard S-N Curves Considered

Industry Standard	Base Metal	Weld Joint
BS 7608	Mean A	Mean D
BS 7608	Design A	Design D
IIW XIII-1965-03 / XV – 1127 - 03	160	90
DNV RP-C203	B1	D
API RP2	X	X'
AWS D1.1	A	C

Note that all of the curves represent design curves (generally the mean curve minus two standard deviations). In addition the mean curves from BS 7608 are also included.

A comparison of the experimental data and a selection of industry standard curves is shown in Figure C.2. To be consistent with how the industry standard S-N curves are presented, the experimental data is presented in two groups, one for plain dents and one for dents interacting with weld features. Note that the BS 7608 D Design curve is virtually identical to the similar curves used in the other codes (i.e. IIW 90 and DNV RP-C203 D).

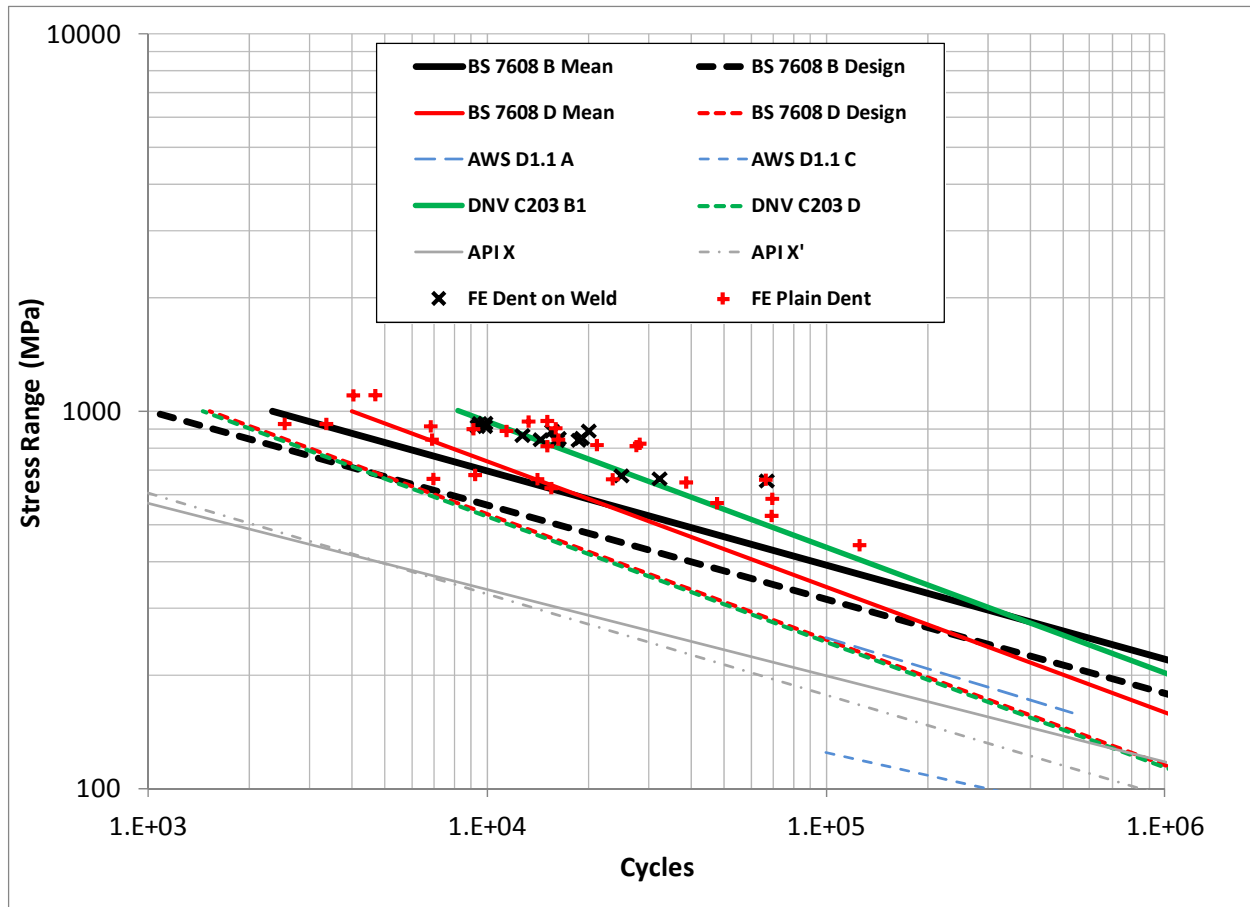


Figure C.2: Comparison of Experimental Fatigue Lives and Industry Standard S-N Curves

As shown in Figure C.2 the experimental data generally falls above the majority of the industry standard curves, except for the DNV X203 B1 curve. From the comparison it can also be seen that the slope of the BS 7608 B curve (i.e. $m = 4.0$) follows the experimental data better than do the slopes of the remaining curves (generally $m = 3.0$).

As BS 7608 is a widely used and reviewed S-N fatigue life standard, and the BS 7608 Class D Design curve is the same as several other standards, the BS 7608 B and D curves were chosen as the most suitable for use in estimating the fatigue life of the dent features. A comparison of the fatigue lives predicted using the various BS 7608 curves can be found later in the annex. A summary of the BS 7608 S-N curve parameters is presented in Table C.2.

“Experimental” S-N curves were also developed based on the experimental full scale data, a set of curves for plain dents and for dents interacting with weld features. Both mean and mean minus three standard deviation curves were developed for each scenario. The experimentally determined curves are presented in Figure C.3. A summary of the resulting experimental S-N curve parameters is also presented in Table C.2.

Table C.2: Summary of BS 7608 and Experimental S-N Curve Parameters

Curve	Detail	Type	Log C	m
BS 7608	B	Mean	15.3697	4.00
		Mean – 2sd	15.0055	4.00
	D	Mean	12.6007	3.00
		Mean – 2sd	12.1817	3.00
Experimental	Plain Dents	Mean	20.5146	5.65
		Mean – 3sd	20.0109	5.65
	Dents / welds	Mean	18.5482	4.90
		Mean – 3sd	18.3026	4.90

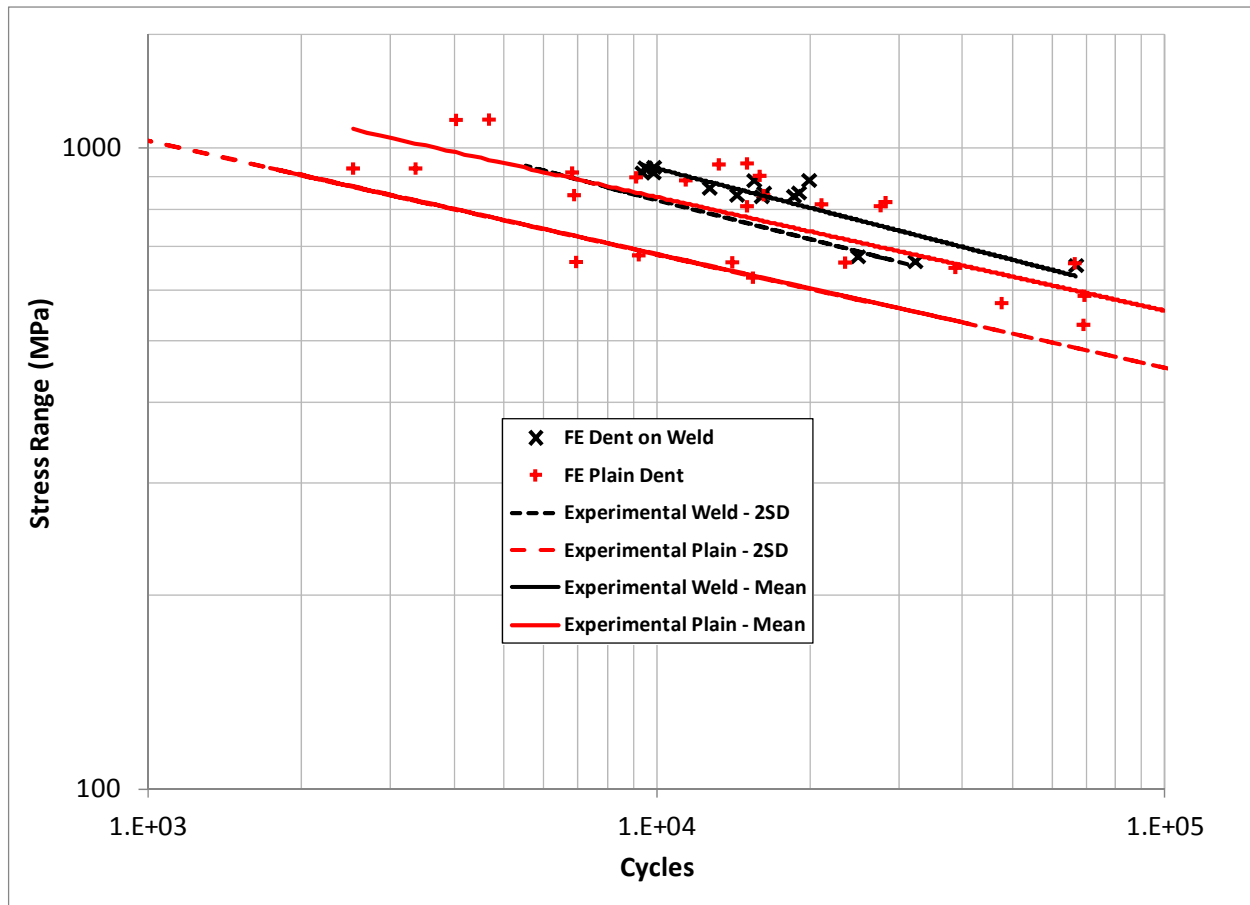


Figure C.3: Experimentally Derived S-N Curves

A comparison of the experimental and the predicted fatigue lives (based on the BS 7608 curves) is presented in Table C.3. The table presents the ratio of the predicted to the actual fatigue lives for both the mean and the design S-N curves, for each of the experimental specimens. The table

also presents a summary of the average ratio, and the maximum and minimum ratios, across all the experimental specimens along with the number of specimens where the predicted life is greater than the experimental life (i.e., the prediction is unconservative).

As shown in Table C.3, using the BS 7608 mean curves (Curve B for plain dents and Curve D for dents interacting with weld features) results in an average predicted/experimental fatigue life ratio of approximately 0.488, with a maximum ratio of 1.708 and over predicted fatigue lives for three out of the 41 specimens considered (approximately 7.3%). Using the BS 7608 design curves results in an average ratio of 0.203, a maximum ratio of 0.739 and no over predictions for fatigue lives.

A similar comparison for the experimentally developed S-N curves is presented in Table C.4. As shown in Table C.4, using the mean experimental S-N curves result in an average predicted to experimental life ratio of 1.279, a maximum ratio of 5.227 and over predicted lives for 21 of the 41 specimens. These results are not surprising for the mean S-N curves. Using the mean minus three standard deviation experimental S-N curves results in an average ratio of 0.493, a maximum ratio of 1.605 and over predicted lives for 4 of the 41 specimens (9.8%) of the specimens.

Table C.3: Comparison of Experimental and Predicted Fatigue Lives – BS 7608

Spec.	Pipe Mat	Indent. Dia (inches)	Indent. Depth (%OD)	Rest	Inter	Exp Life Ne (cycles)	Mean		Mean – 2sd	
							Pred Life Np (cycles)	Np/Ne	Pred Life Np (cycles)	Np/Ne
21	A	2	5	R	G. Weld	66871	13990	0.209	5331	0.080
23	B	4	10	R	G. Weld	12722	6085	0.478	2319	0.182
24	B	4	10	R	G. Weld	16278	6406	0.394	2441	0.150
25	A	2	15	U	G. Weld	19063	6400	0.336	2439	0.128
27	A	2	15	U	G. Weld	18633	6633	0.356	2528	0.136
28	A	2	15	U	G. Weld	16107	6674	0.414	2543	0.158
29	A	4	15	U	G. Weld	14400	6571	0.456	2504	0.174
31	B	2	15	U	G. Weld	9890	4857	0.491	1851	0.187
32	B	2	15	U	G. Weld	9506	4880	0.513	1859	0.196
33	B	4	15	U	G. Weld	9386	5157	0.549	1965	0.209
34	B	4	15	U	G. Weld	9871	5158	0.523	1966	0.199
35	B	4	15	U	G. Weld	19959	5594	0.280	2132	0.107
36	B	4	15	U	G. Weld	15568	5602	0.360	2135	0.137
19	A	2	5	R	L.S. Weld	32282	13438	0.416	5121	0.159
20	A	2	5	R	L.S. Weld	24919	12727	0.511	4850	0.195
1	A	2	5	R	Plain	6948	11870	1.708	5132	0.739
2	A	2	5	R	Plain	38685	12927	0.334	5588	0.144
3	B	4	10	R	Plain	6886	4545	0.660	1965	0.285
4	B	4	10	R	Plain	16234	4545	0.280	1965	0.121
5	B	4	10	R	Plain	2531	3099	1.224	1340	0.529
6	B	4	10	R	Plain	3359	3099	0.923	1340	0.399
7	A	2	15	U	Plain	21103	29274	0.424	12655	0.183
8	A	2	15	U	Plain	28211	19298	0.278	8343	0.120
9	A	2	15	U	Plain	6825	59872	0.477	25884	0.206
10	A	2	15	U	Plain	9116	5186	0.246	2242	0.106
11	A	4	15	U	Plain	15063	5020	0.178	2170	0.077
12	A	4	15	U	Plain	27575	3282	0.481	1419	0.208
13	B	2	15	U	Plain	13262	3517	0.386	1521	0.167
14	B	2	15	U	Plain	15065	5328	0.354	2303	0.153
15	B	2	15	U	Plain	4035	5321	0.193	2301	0.083
16	B	2	15	U	Plain	4684	2922	0.220	1263	0.095
17	B	4	15	U	Plain	11415	2881	0.191	1246	0.083
18	B	4	15	U	Plain	15949	1541	0.382	666	0.165
41	C	2	5	R	Plain	69099	1534	0.327	663	0.142
42	C	4	10	R	Plain	69393	3676	0.322	1589	0.139
46	C	12	5	R	Plain	125525	3442	0.216	1488	0.093
48	C	2	15	U	Plain	23482	11970	0.510	5175	0.220
52	C	4	15	U	Plain	9226	10790	1.170	4665	0.506
54	C	12	15	U	Plain	47702	21426	0.449	9263	0.194
56	C	4	20	U	Plain	15473	14859	0.960	6424	0.415
57	C	12	20	U	Plain	14091	11928	0.846	5157	0.366
							Average	0.488	0.203	
							Max	1.708	0.739	
							Min	0.178	0.077	
							# > 1.0	3	0	

Table C.4: Comparison of Experimental and Predicted Fatigue Lives – Experimental Curves

Spec.	Pipe Mat	Indent. Dia (inches)	Indent. Depth (%OD)	Rest	Inter	Exp Life Ne (cycles)	Mean		Mean – 2sd	
							Pred Life Np (cycles)	Np/Ne	Pred Life Np (cycles)	Np/Ne
21	A	2	5	R	G. Weld	66871	54770	0.819	31114	0.465
23	B	4	10	R	G. Weld	12722	14062	1.105	7988	0.628
24	B	4	10	R	G. Weld	16278	15294	0.940	8688	0.534
25	A	2	15	U	G. Weld	19063	15268	0.801	8674	0.455
27	A	2	15	U	G. Weld	18633	16188	0.869	9196	0.494
28	A	2	15	U	G. Weld	16107	16350	1.015	9288	0.577
29	A	4	15	U	G. Weld	14400	15941	1.107	9056	0.629
31	B	2	15	U	G. Weld	9890	9731	0.984	5528	0.559
32	B	2	15	U	G. Weld	9506	9804	1.031	5570	0.586
33	B	4	15	U	G. Weld	9386	10730	1.143	6095	0.649
34	B	4	15	U	G. Weld	9871	10736	1.088	6099	0.618
35	B	4	15	U	G. Weld	19959	12257	0.614	6963	0.349
36	B	4	15	U	G. Weld	15568	12284	0.789	6978	0.448
19	A	2	5	R	L.S. Weld	32282	51284	1.589	29134	0.902
20	A	2	5	R	L.S. Weld	24919	46931	1.883	26661	1.070
1	A	2	5	R	Plain	6948	36314	5.227	11152	1.605
2	A	2	5	R	Plain	38685	40962	1.059	12580	0.325
3	B	4	10	R	Plain	6886	9358	1.359	2874	0.417
4	B	4	10	R	Plain	16234	9358	0.576	2874	0.177
5	B	4	10	R	Plain	2531	5448	2.152	1673	0.661
6	B	4	10	R	Plain	3359	5448	1.622	1673	0.498
7	A	2	15	U	Plain	21103	11274	0.534	3462	0.164
8	A	2	15	U	Plain	28211	10767	0.382	3307	0.117
9	A	2	15	U	Plain	6825	5907	0.866	1814	0.266
10	A	2	15	U	Plain	9116	6515	0.715	2001	0.219
11	A	4	15	U	Plain	15063	11714	0.778	3597	0.239
12	A	4	15	U	Plain	27575	11693	0.424	3591	0.130
13	B	2	15	U	Plain	13262	5014	0.378	1540	0.116
14	B	2	15	U	Plain	15065	4915	0.326	1509	0.100
15	B	2	15	U	Plain	4035	2031	0.503	624	0.155
16	B	2	15	U	Plain	4684	2018	0.431	620	0.132
17	B	4	15	U	Plain	11415	6933	0.607	2129	0.187
18	B	4	15	U	Plain	15949	6320	0.396	1941	0.122
41	C	2	5	R	Plain	69099	129956	1.881	39910	0.578
42	C	4	10	R	Plain	69393	72143	1.040	22155	0.319
46	C	12	5	R	Plain	125525	357049	2.844	109650	0.874
48	C	2	15	U	Plain	23482	36745	1.565	11284	0.481
52	C	4	15	U	Plain	9226	31736	3.440	9746	1.056
54	C	12	15	U	Plain	47702	83630	1.753	25683	0.538
56	C	4	20	U	Plain	15473	49872	3.223	15316	0.990
57	C	12	20	U	Plain	14091	36563	2.595	11229	0.797
							Average	1.279		
							Max	5.227		
							Min	0.326		
							# > 1.0	21	4	

C.3 STRAIN LIFE

In the strain-life approach to fatigue analysis, the relationship between the applied strain levels and the number of cycles to failure is represented by a superposition of two curves, one describing the elastic strain portion of the fatigue life (governing high cycle fatigue), the other describing the plastic strain portion of the fatigue life (governing low cycle fatigue).

The most familiar strain-life relationship is described using the Coffin – Manson equation:

$$\Delta\varepsilon / 2 = (\sigma_f' / E)(2N_f)^b + \varepsilon_f'(2N_f)^c \quad (C.2)$$

where

- $\Delta\varepsilon$ = strain range
- σ_f' = fatigue strength coefficient
- E = modulus of elasticity
- b = fatigue strength exponent
- ε_f' = fatigue ductility coefficient
- c = fatigue ductility exponent
- N_f = cycles to failure

The first term on the right hand side of equation (C.2) represents the elastic strain-life curve, while the second term represents the plastic strain-life curve. The Coffin-Manson strain-life curve is shown schematically in Figure C.4.

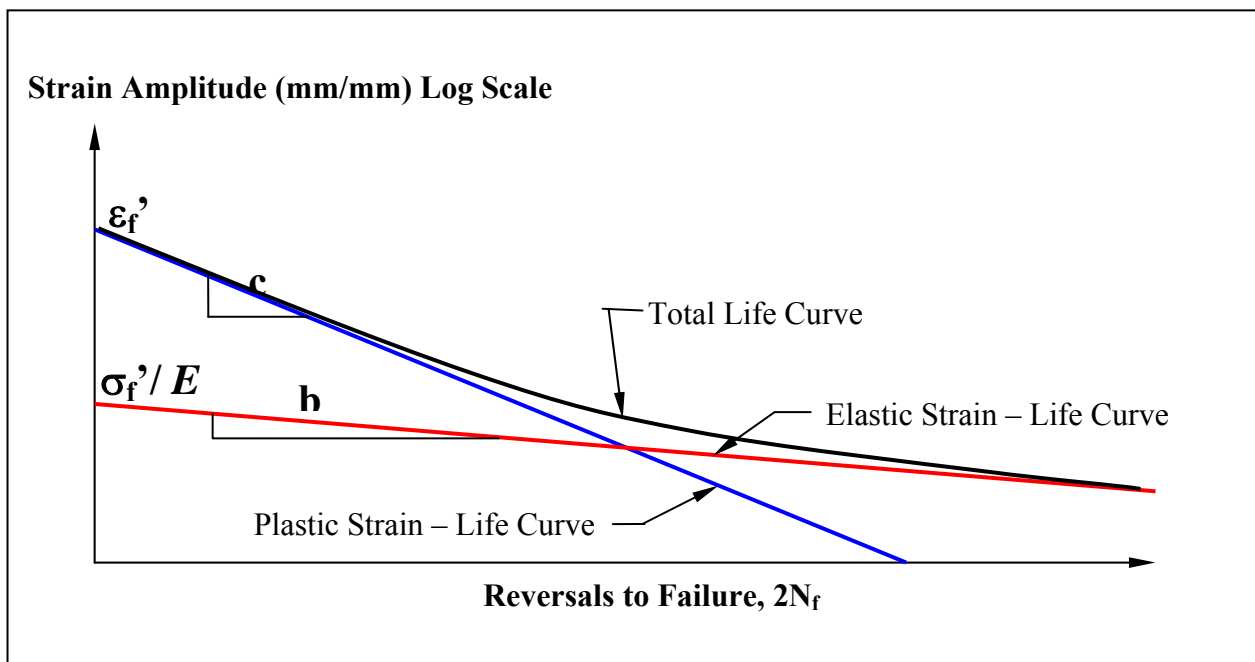


Figure C.4: Generic Strain-Life Curve

The strain life curve data is generated usually for fully reversed loading (i.e., stress ratio, $R = -1$). The test data thus generated would need to be modified to account for the effect of mean stress. Several researchers have proposed solution to account for the effect of mean stress on the strain life equation.

Morrow proposed a correction for mean stress (σ_o) by modifying the elastic term of the equation and the modified strain life equation takes the form as

$$\Delta\epsilon/2 = (\sigma_f' - \sigma_o)/E (2N_f)^b + \epsilon_f' (2N_f)^c \tag{C.3}$$

Manson and Halford modified both the elastic and plastic terms of the strain life equation as shown below:

$$\Delta\epsilon/2 = (\sigma_f' - \sigma_o)/E (2N_f)^b + \epsilon_f' ((\sigma_f' - \sigma_o) / (\sigma_f'))^{c/b} (2N_f)^c \tag{C.4}$$

The above equation, however, overestimates the effect of mean stress on life in the low cycle fatigue regime.

Smith, Watson and Topper (SWT) have proposed the following equation to account for the effect of mean stress.

$$\sigma_{max} (\Delta\epsilon/2) = (\sigma_f')^2 / E (2N_f)^{2b} + (\sigma_f' \epsilon_f') (2N_f)^{b+c} \tag{C.5}$$

where, $\sigma_{max} = \Delta\sigma/2 + \sigma_o$

Figures C.5 through C.7 illustrate the effect each of these equations has on the strain life curves.

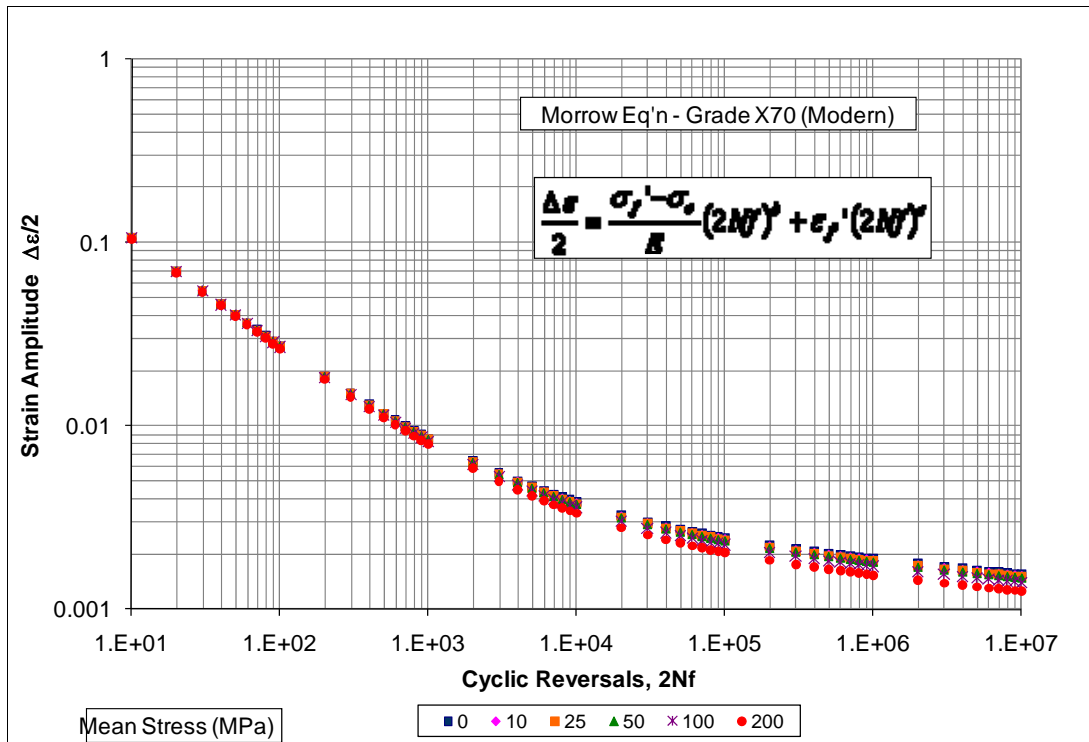


Figure C.5: Morrow Strain Life Curves

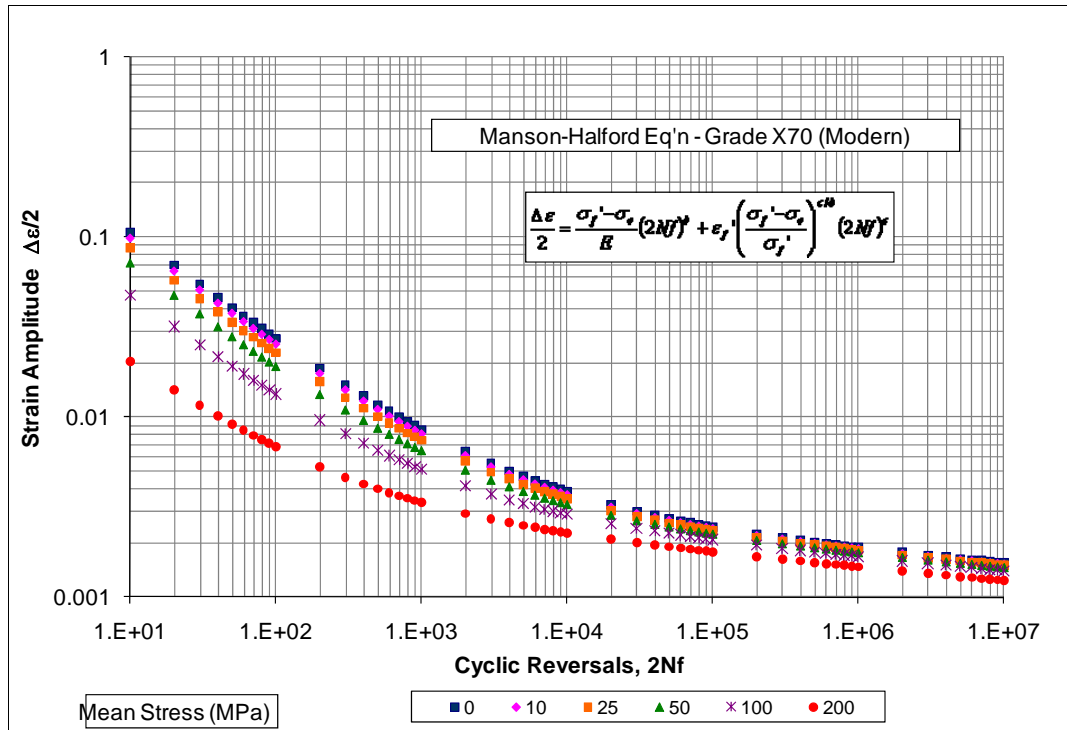


Figure C.6: Manson-Halford Strain Life Curves

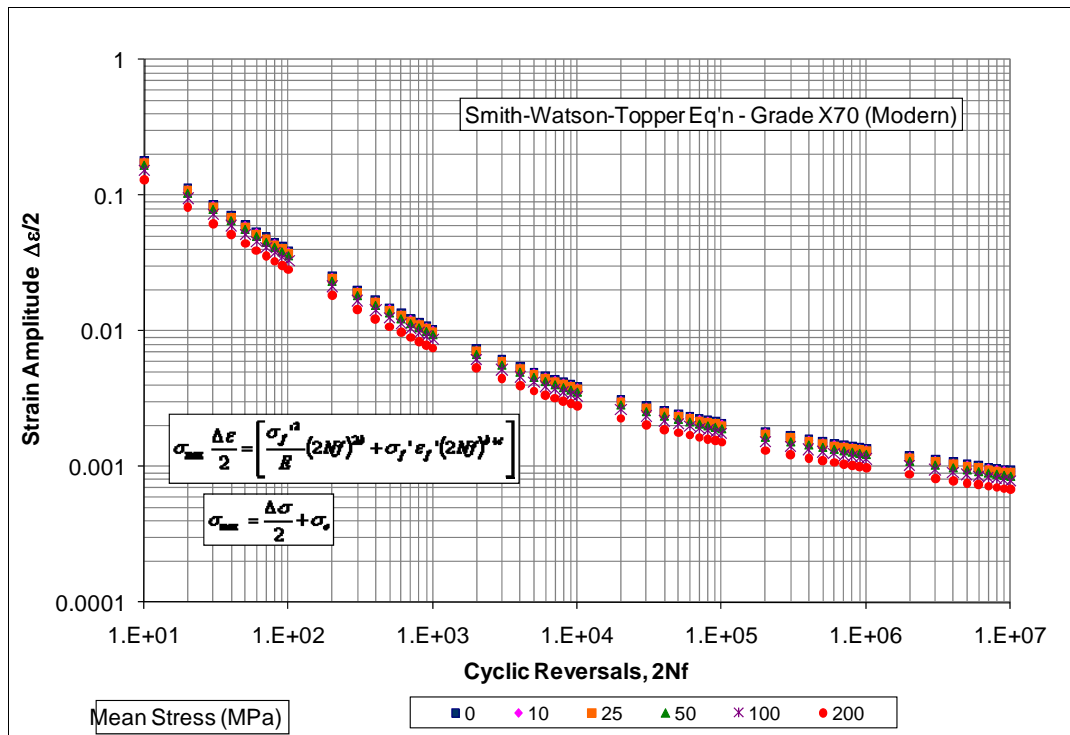


Figure C.7: Smith-Watson-Topper Strain Life Curves

Besides the mean stress effect strain life data can also be affected by the surface finish of the component. The experimental strain life curves are generated using specimens with a smooth polished surface whereas typical real world components have a comparably rougher surface which will generally result in a decrease in fatigue life, particularly at in the high cycle regime. Figure C.8 illustrates the effect different surface finishes have on the fatigue strength. Unfortunately the figure does not directly show the correlation of drop in fatigue life versus surface finish but shows the drop in the fatigue strength due to the surface finish. Again, the surface finish effects will have much more pronounced effect in the high cycle fatigue regime as compared to the low cycle fatigue life.

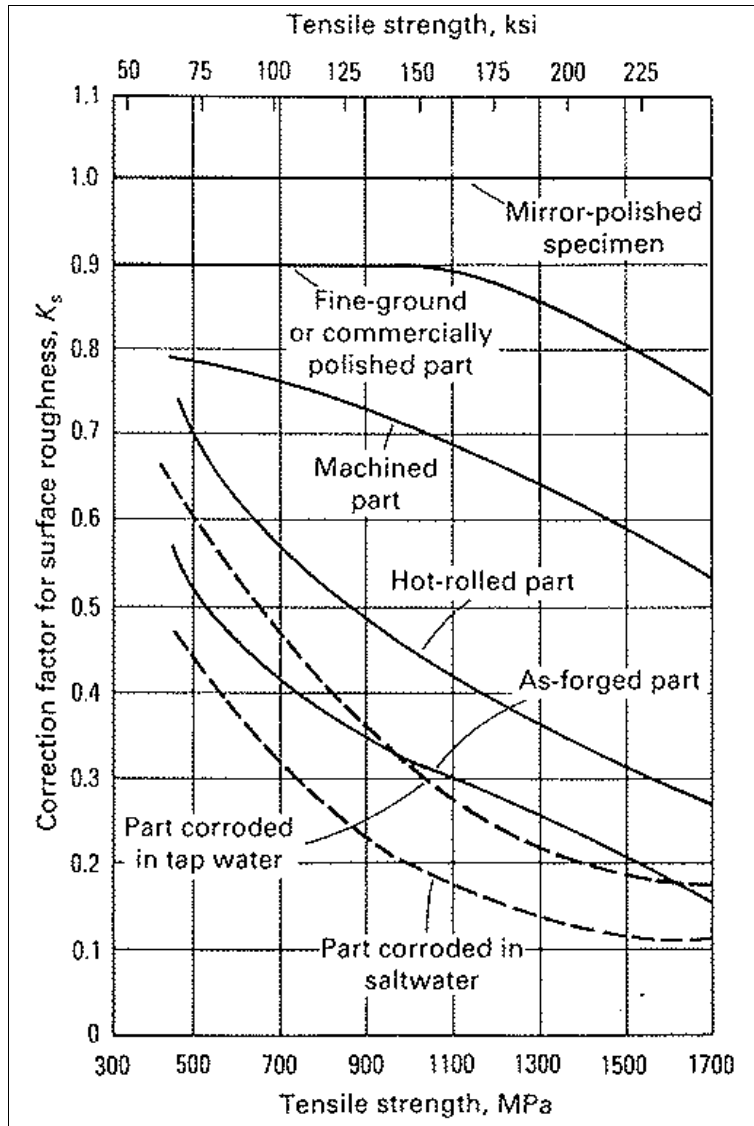


Figure C.8: Effect of Surface Finish on Fatigue Strength

Experimental strain life curves have been generated for the three materials used in the full scale dent fatigue test program. These curves are shown in Figure C.9.

Figure C.10 shows the same curves along with the maximum strain range for the full scale experimental specimens as obtained from the FEA models for each specimen.

Figure C.11 to C.13 shows the full scale test data and the strain life curves for modern grade X-52, Vintage X-52 and modern grade X-70 modified for the mean stress effect respectively.

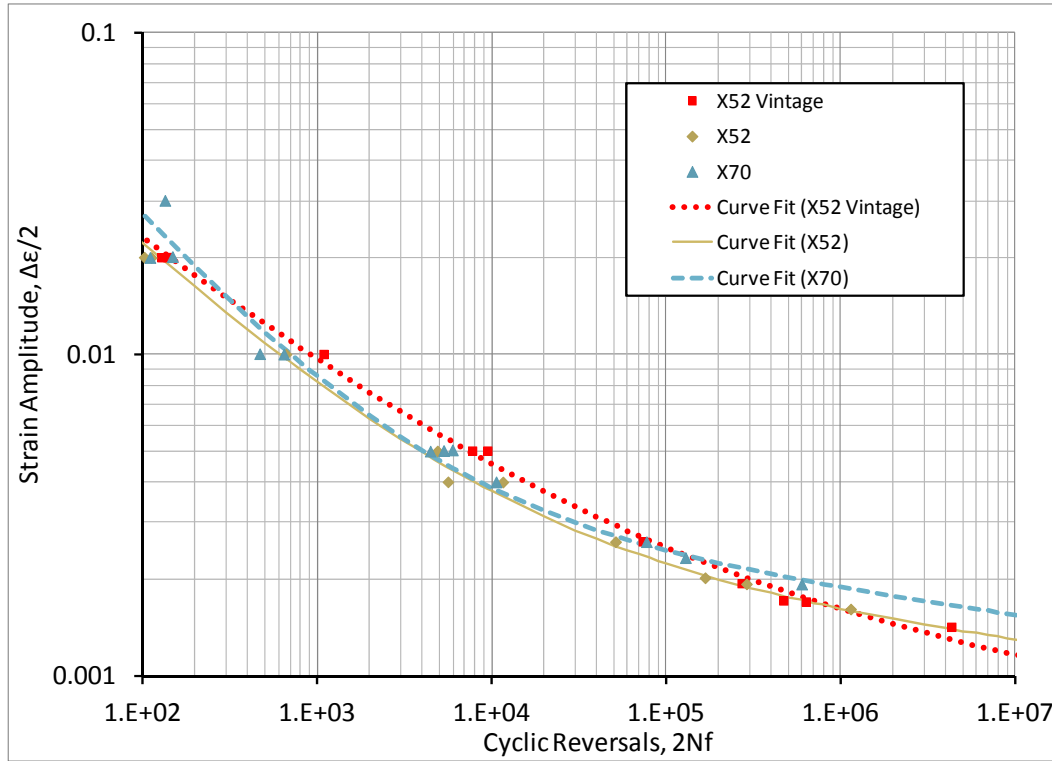


Figure C.9: Experimental Strain-Life Curves – X52, X52 Vintage and X70

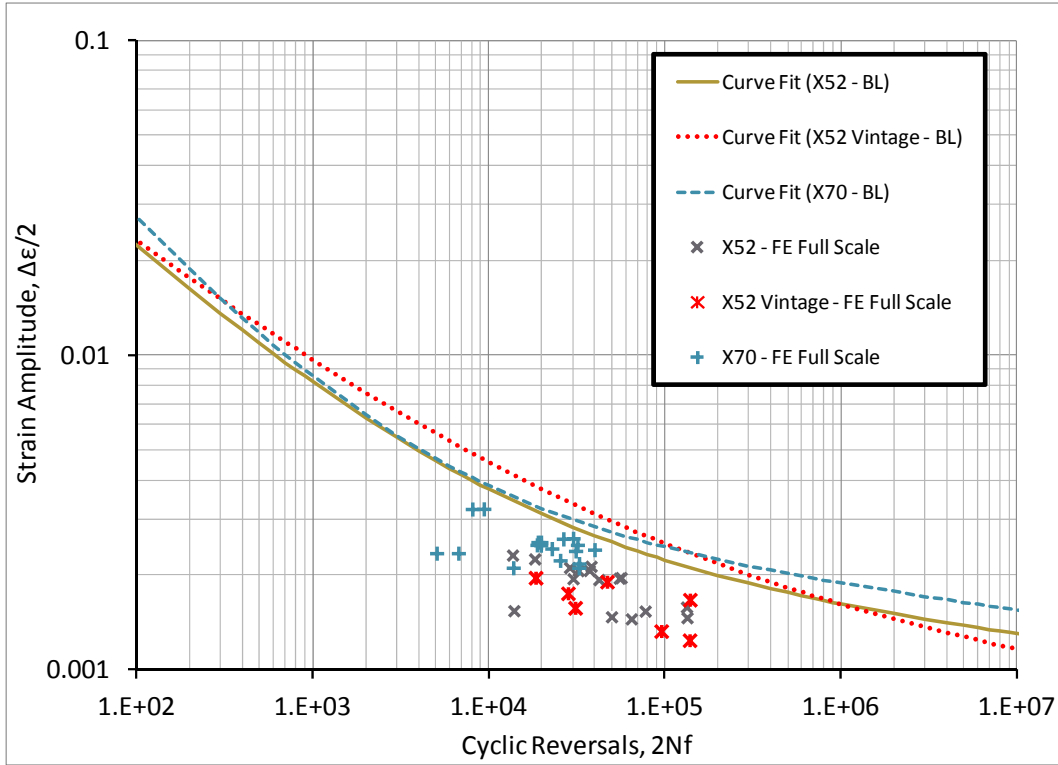


Figure C.10: Comparison of Experimental Strain Life Curves and Experimental Fatigue Lives

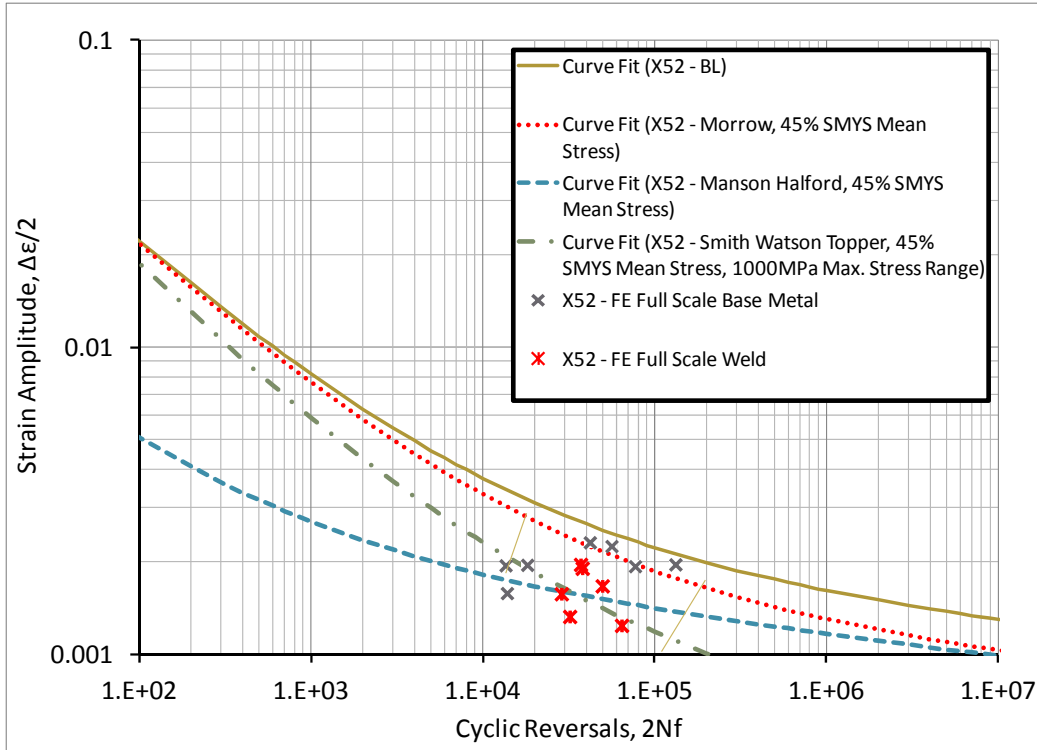


Figure C.11: Comparison of X52 Modified Experimental Strain Life Curves and Experimental Fatigue Lives

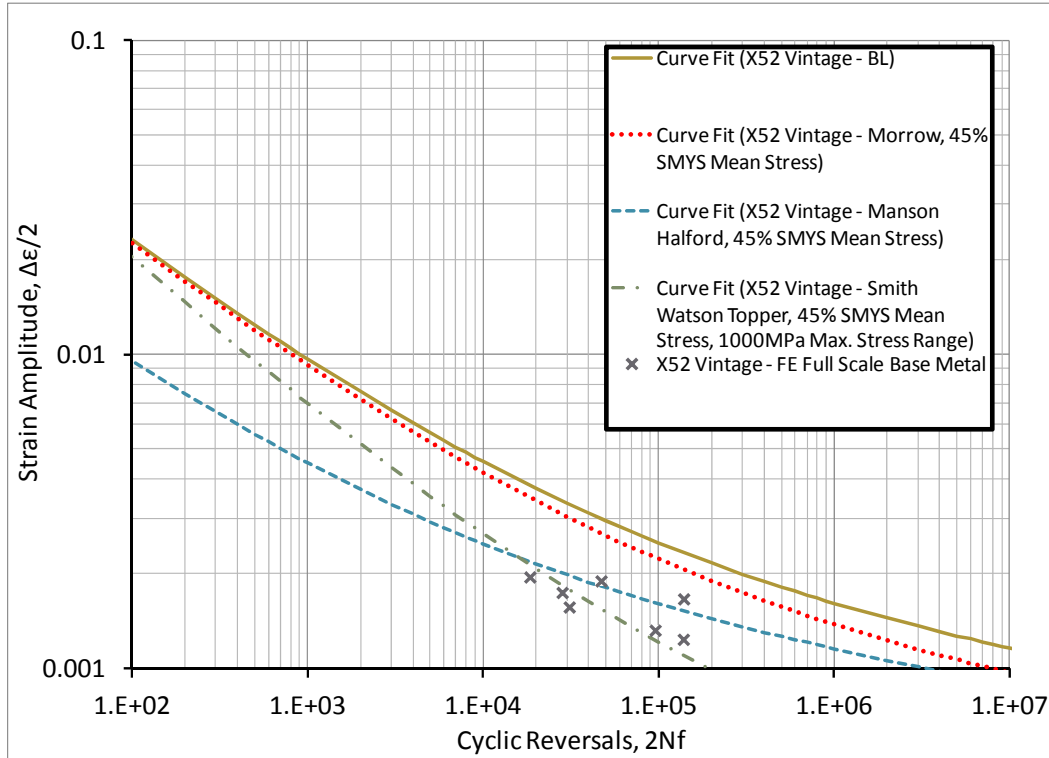


Figure C.12: Comparison of X52 Vintage Modified Experimental Strain Life Curves and Experimental Fatigue Lives

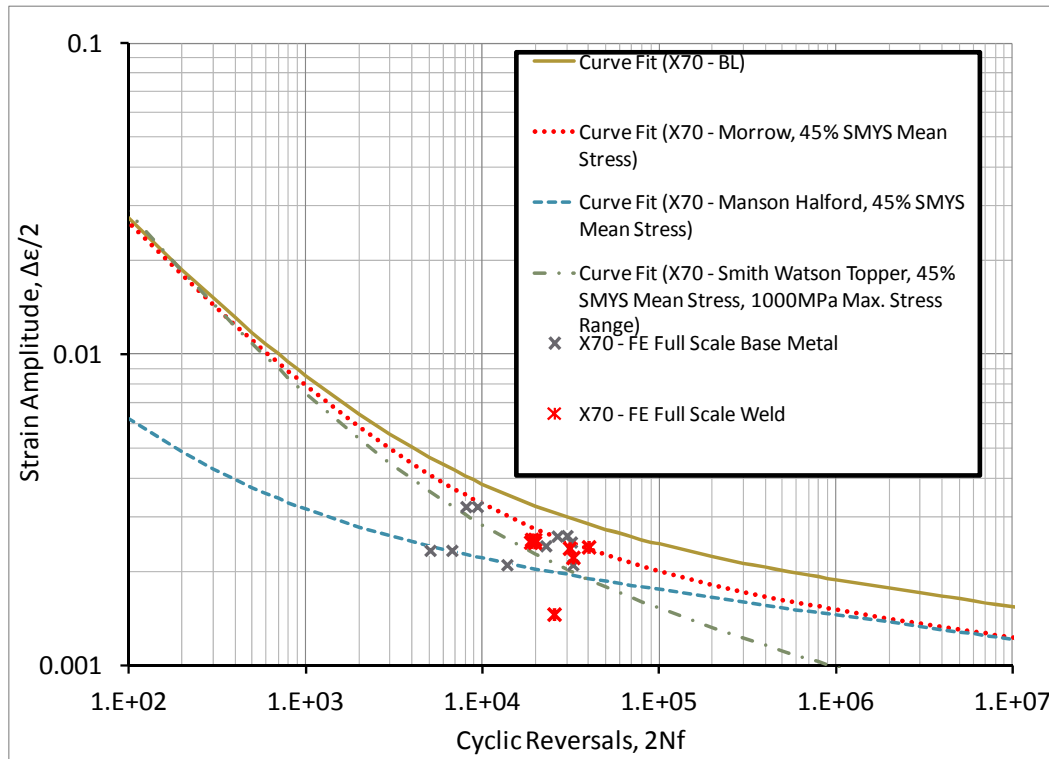


Figure C.13: Comparison of X70 Modified Experimental Strain Life Curves and Experimental Fatigue Lives

C.4 FRACTURE MECHANICS CRACK GROWTH ANALYSIS

The third fatigue life approach investigated as part of the project was the fracture mechanics based crack growth approach.

The fracture mechanics based approach to crack growth is characterized by the Paris crack growth rate equation, shown below, which relates the increase in crack length (da) per applied load cycle (dN) to the stress intensity factor range (ΔK) and two material parameter constants (C and m).

$$\frac{da}{dN} = C(\Delta K)^m \quad (C.6)$$

The general form of the stress intensity factor is shown below. It is a function of the crack length (a), the applied stress range ($\Delta\sigma$) and the geometry (encompassed by the function Y).

$$\Delta K = Y(\Delta\sigma)\sqrt{\pi a} \quad (C.7)$$

In the fracture mechanics based approach to fatigue life assessment, the fatigue life is estimated as the number of cycles (N) required to grow a crack like flaw from an initial size (a_i) to a critical size (a_{crit}) while undergoing cyclic stress ranges of $\Delta\sigma$. In terms of using a fracture mechanics based approach to estimate the fatigue life of pipeline dent features, a number of the parameters that govern crack growth must be established; primarily the crack growth rate data and the initial flaw size to use. Establishing and demonstrating the effect of these was the primary focus of the development work carried out to date as part of this project.

A summary of the steps used to develop a fracture mechanics based approach to estimating the fatigue life of pipeline dent features is presented below.

1. Select appropriate crack growth rate parameters (representative of typical pipeline steels).
2. For each of the experiment specimens, use fracture mechanics crack growth calculations to determine a calibrated initial flaw size that results in a fatigue life estimate similar to the experimental fatigue life.
3. Based on the results of step 2, develop a single initial flaw size that is suitably representative of the experimental data.
4. Calculate the fatigue lives of all the experimental specimens using the initial flaw size determined in step 3 and the material properties selected in step 1.

The crack growth rate parameters selected for use in the fracture mechanics based approach were the simplified parameters described in BS 7910 (Section 8.2.3.5). These parameters, summarized below, are considered a conservative estimate of the crack growth rates experienced by typical steels and were developed for preliminary screening and for assessments that can be compared directly with calculations based on fatigue design rules.

$$C = 5.21 \times 10^{-13} \text{ (for } da/dN \text{ in mm/cycle and } \Delta K \text{ in N/mm}^{3/2}\text{)}$$

$$m = 3$$

The detailed fracture mechanics based crack growth calculations were carried out based on the methodologies and equations provided in BS 7910. The BMT Fleet Technology software FlawCheck (which uses the methods and equations from BS 7910) was used to carry out the numerous crack growth calculations required in developing the approach.

In Step 2, the development of the calibrated initial flaw size for each of the experimental specimens used the detailed results of the finite element analyses described previously. For each specimen the calibrated initial flaw size was developed using the following approach:

1. Determine the stress range on the inner and outer surface of the pipe model, for each node in the dent region.
2. Carry out crack growth analysis for each node in the dent region based on the stress ranges determined in the previous step assuming the existence of a semi-elliptical initial crack with a crack depth of a_i and a crack length of $10a_i$. The crack orientation (i.e., axial or circumferential) is chosen based on the orientation of the crack in the experimental specimen. The fatigue life is taken as the number of cycles required to grow the crack from the initial flaw size to a depth equal to 95% of the pipe wall.
3. Vary the initial flaw size used in step b until the minimum calculated fatigue life for any node in the dent region is similar to the experimental fatigue life.

Note that the initial flaw size is characterized by the flaw depth (a_i) and a length ($2c_i$) to depth aspect ratio of 10.

A summary of the resulting calibrated initial flaw sizes is presented in Table C.5. The results include only those specimens for which accurate, validated experimental data was available. Also included in Table C.5 are the means and standard deviations for the flaw sizes appropriate for plain dents and dents interacting with weld features.

The initial flaw size statistics were used to develop four initial flaw sizes (mean, mean + 1sd, +2sd and +3sd), summarized in Table C.6, which were then used to estimate the fatigue life of all of the experimental specimens.

Table C.4: Summary of Calibrated Initial Flaw Sizes

Spec.	Pipe Mat	Indent. Dia (inches)	Indent. Depth (%OD)	Rest	Inter	Exp Life Ne (cycles)	Calibrated Initial Flaw Depth a_i (mm)
21	A	2	5	R	G. Weld	66871	0.010
22	A	4	10	R	G. Weld	66429	0.011
23	B	4	10	R	G. Weld	12722	0.056
24	B	4	10	R	G. Weld	16278	0.037
25	A	2	15	U	G. Weld	19063	0.025
27	A	2	15	U	G. Weld	18633	0.029
28	A	2	15	U	G. Weld	16107	0.041
29	A	4	15	U	G. Weld	14400	0.051
31	B	2	15	U	G. Weld	9890	0.062
32	B	2	15	U	G. Weld	9506	0.066
33	B	4	15	U	G. Weld	9386	0.081
34	B	4	15	U	G. Weld	9871	0.072
35	B	4	15	U	G. Weld	19959	0.015
36	B	4	15	U	G. Weld	15568	0.032
19	A	2	5	R	L.S. Weld	32282	0.043
20	A	2	5	R	L.S. Weld	24919	0.067
Mean (Welds)							0.044
S.D. (Welds)							0.022
1	A	2	5	R	Plain	6948	0.509
2	A	2	5	R	Plain	38685	0.015
3	B	4	10	R	Plain	6886	0.080
4	B	4	10	R	Plain	16234	0.080
5	B	4	10	R	Plain	2531	0.671
6	B	4	10	R	Plain	3359	0.671
7	A	2	15	U	Plain	21103	0.027
8	A	2	15	U	Plain	28211	0.017
9	A	2	15	U	Plain	6825	0.143
10	A	2	15	U	Plain	9116	0.088
11	A	4	15	U	Plain	15063	0.060
12	A	4	15	U	Plain	27575	0.013
13	B	2	15	U	Plain	13262	0.030
14	B	2	15	U	Plain	15065	0.021
15	B	2	15	U	Plain	4035	0.135
16	B	2	15	U	Plain	4684	0.099
17	B	4	15	U	Plain	11415	0.062
18	B	4	15	U	Plain	15949	0.026
41	C	2	5	R	Plain	69099	0.032
42	C	4	10	R	Plain	69393	0.020
46	C	12	5	R	Plain	125525	0.015
48	C	2	15	U	Plain	23482	0.089
52	C	4	15	U	Plain	9226	0.156
54	C	12	15	U	Plain	47702	0.044
56	C	4	20	U	Plain	15473	0.073
57	C	12	20	U	Plain	14091	0.117
Mean (Plain dents)							0.059
S.D. (Plain dents)							0.042

Table C.5: Summary of Initial Flaws Sizes Considered

Category		Initial Flaw Depth a_i (mm)	Initial Flaw Length $2c_i$ (mm)
Plain Dents	Mean	0.059	0.590
	Mean + 1sd	0.101	1.014
	Mean + 2sd	0.144	1.438
	Mean + 3sd	0.186	1.861
Dents / welds	Mean	0.044	0.436
	Mean + 1sd	0.066	0.660
	Mean + 2sd	0.088	0.884
	Mean + 3sd	0.111	1.107

A comparison of the fatigue lives predicted using the calibrated fracture mechanics based approach, for each of the four initial flaw sizes summarized above, is presented in Table C.7. The results show that at the mean initial flaw size, the average predicted to experimental fatigue life ratio is 0.82, with a maximum ratio of 2.66 and over predicted fatigue lives for seven experimental specimens. Increasing the initial flaw depth to the mean plus two standard deviations results in a decrease in the average predicted to experimental fatigue life ratio down to 0.54, with a maximum ratio down to 1.69 and only three fatigue life over predictions.

Table C.6: Comparison of Experimental and Predicted Fatigue Lives – Fracture Mechanics

Spec.	Pipe Mat	Indent. Dia (inches)	Indent. Depth (%OD)	Rest	Inter	Exp Life Ne (cycles)	Initial Flaw Size			
							Mean		Mean + 1sd	
							Pred Life Np (cycles)	Np/Ne	Pred Life Np (cycles)	Np/Ne
21	A	2	5	R	G. Weld	66871	22501	0.34	18439	0.28
23	B	4	10	R	G. Weld	12722	9546	0.75	7787	0.61
24	B	4	10	R	G. Weld	16278	10054	0.62	8202	0.50
25	A	2	15	U	G. Weld	19063	10230	0.54	8372	0.44
27	A	2	15	U	G. Weld	18633	10646	0.57	8720	0.47
28	A	2	15	U	G. Weld	16107	10415	0.65	8477	0.53
29	A	4	15	U	G. Weld	14400	10409	0.72	8498	0.59
31	B	2	15	U	G. Weld	9890	7828	0.79	6416	0.65
32	B	2	15	U	G. Weld	9506	7695	0.81	6280	0.66
33	B	4	15	U	G. Weld	9386	8432	0.90	6931	0.74
34	B	4	15	U	G. Weld	9871	8427	0.85	6926	0.70
35	B	4	15	U	G. Weld	19959	8948	0.45	7320	0.37
36	B	4	15	U	G. Weld	15568	9151	0.59	7521	0.48
19	A	2	5	R	L.S. Weld	32282	21027	0.65	17125	0.53
20	A	2	5	R	L.S. Weld	24919	19914	0.80	16217	0.65
1	A	2	5	R	Plain	6948	14353	2.07	10989	1.58
2	A	2	5	R	Plain	38685	14942	0.39	11413	0.30
3	B	4	10	R	Plain	6886	8897	1.29	6779	0.98
4	B	4	10	R	Plain	16234				
5	B	4	10	R	Plain	2531	6730	2.66	5140	2.03
6	B	4	10	R	Plain	3359				
7	A	2	15	U	Plain	21103	9797	0.46	7443	0.35
8	A	2	15	U	Plain	28211	9562	0.34	7264	0.26
9	A	2	15	U	Plain	6825	7003	1.03	5330	0.78
10	A	2	15	U	Plain	9116	7345	0.81	5585	0.61
11	A	4	15	U	Plain	15063	10137	0.67	7730	0.51
12	A	4	15	U	Plain	27575	10143	0.37	7738	0.28
13	B	2	15	U	Plain	13262	6542	0.49	5009	0.38
14	B	2	15	U	Plain	15065	6369	0.42	4847	0.32
15	B	2	15	U	Plain	4035	4022	1.00	3075	0.76
16	B	2	15	U	Plain	4684	4001	0.85	3057	0.65
17	B	4	15	U	Plain	11415	7767	0.68	5932	0.52
18	B	4	15	U	Plain	15949	7407	0.46	5675	0.36
41	C	2	5	R	Plain	69099	36748	0.53	28125	0.41
42	C	4	10	R	Plain	69393	27277	0.39	20944	0.30
46	C	12	5	R	Plain	125525	70935	0.57	56052	0.45
48	C	2	15	U	Plain	23482	20272	0.86	15840	0.67
52	C	4	15	U	Plain	9226	19099	2.07	14990	1.62
54	C	12	15	U	Plain	47702	28460	0.60	21635	0.45
56	C	4	20	U	Plain	15473	23461	1.52	18222	1.18
57	C	12	20	U	Plain	14091	19330	1.37	14904	1.06
							Average	0.82	0.64	
							Max	2.66	2.03	
							Min	0.34	0.26	
							# > 1.0	7	5	

Table C.6: Comparison of Experimental and Predicted Fatigue Lives – Fracture Mechanics – Continued

Spec.	Pipe Mat	Indent. Dia (inches)	Indent. Depth (%OD)	Rest	Inter	Exp Life Ne (cycles)	Initial Flaw Size			
							Mean + 2sd		Mean + 3sd	
							Pred Life Np (cycles)	Np/Ne	Pred Life Np (cycles)	Np/Ne
21	A	2	5	R	G. Weld	66871	15994	0.24	14244	0.21
23	B	4	10	R	G. Weld	12722	6730	0.53	5975	0.47
24	B	4	10	R	G. Weld	16278	7089	0.44	6295	0.39
25	A	2	15	U	G. Weld	19063	7253	0.38	6453	0.34
27	A	2	15	U	G. Weld	18633	7560	0.41	6730	0.36
28	A	2	15	U	G. Weld	16107	7311	0.45	6476	0.40
29	A	4	15	U	G. Weld	14400	7347	0.51	6523	0.45
31	B	2	15	U	G. Weld	9890	5566	0.56	4958	0.50
32	B	2	15	U	G. Weld	9506	5429	0.57	4821	0.51
33	B	4	15	U	G. Weld	9386	6027	0.64	5380	0.57
34	B	4	15	U	G. Weld	9871	6022	0.61	5374	0.54
35	B	4	15	U	G. Weld	19959	6340	0.32	5639	0.28
36	B	4	15	U	G. Weld	15568	6539	0.42	5836	0.37
19	A	2	5	R	L.S. Weld	32282	14775	0.46	13094	0.41
20	A	2	5	R	L.S. Weld	24919	13990	0.56	12397	0.50
1	A	2	5	R	Plain	6948	9183	1.32	8046	1.16
2	A	2	5	R	Plain	38685	9521	0.25	8329	0.22
3	B	4	10	R	Plain	6886	5647	0.82	4935	0.72
4	B	4	10	R	Plain	16234				
5	B	4	10	R	Plain	2531	4288	1.69	3753	1.48
6	B	4	10	R	Plain	3359				
7	A	2	15	U	Plain	21103	6179	0.29	5382	0.26
8	A	2	15	U	Plain	28211	6029	0.21	5252	0.19
9	A	2	15	U	Plain	6825	4432	0.65	3866	0.57
10	A	2	15	U	Plain	9116	4639	0.51	4044	0.44
11	A	4	15	U	Plain	15063	6436	0.43	5620	0.37
12	A	4	15	U	Plain	27575	6445	0.23	5630	0.20
13	B	2	15	U	Plain	13262	4185	0.32	3666	0.28
14	B	2	15	U	Plain	15065	4031	0.27	3517	0.23
15	B	2	15	U	Plain	4035	2566	0.64	2246	0.56
16	B	2	15	U	Plain	4684	2551	0.54	2231	0.48
17	B	4	15	U	Plain	11415	4947	0.43	4326	0.38
18	B	4	15	U	Plain	15949	4745	0.30	4158	0.26
41	C	2	5	R	Plain	69099	23494	0.34	20574	0.30
42	C	4	10	R	Plain	69393	17536	0.25	15382	0.22
46	C	12	5	R	Plain	125525	48017	0.38	42925	0.34
48	C	2	15	U	Plain	23482	13453	0.57	11944	0.51
52	C	4	15	U	Plain	9226	12774	1.38	11372	1.23
54	C	12	15	U	Plain	47702	17970	0.38	15659	0.33
56	C	4	20	U	Plain	15473	15392	0.99	13598	0.88
57	C	12	20	U	Plain	14091	12519	0.89	11010	0.78
							Average	0.54	0.48	
							Max	1.69	1.48	
							Min	0.21	0.19	
							# > 1.0	3	3	

ANNEX D
TASK 5- DEVELOPMENT AND CALIBRATION
OF GENERALIZED SEVERITY RANKING

TABLE OF CONTENTS

ACRONYMS AND ABBREVIATIONS iii

D.1 DEVELOPMENT AND CALIBRATION OF GENERALIZED SEVERITY RANKING CRITERIA 1

 D.1.1 Dent Geometric Parameter Definitions 1

 D.1.1.1 Transverse and Axial Shoulder Sharpness 1

 D.1.1.2 Dent Skew 2

 D.1.1.3 Flatness Ratio 2

LIST OF FIGURES

Figure D.1: Dent Geometry Measurement of a Single Peak Dents 3

Figure D.2: Dent Shoulder Slope to Life Relationship for Unrestrained Dent Models 4

Figure D.3: Dent Acuity to Life Relationship for Unrestrained Dent Models 4

Figure D.4: Dent Depth to Life Relationship for Unrestrained Spherical Indenters 5

D.1 DEVELOPMENT AND CALIBRATION OF GENERALIZED SEVERITY RANKING CRITERIA

The objective of this task is to develop a generalized dent severity ranking based on the dent geometry, line pipe geometry and the material grade. The dent severity criteria will take into account the dent shape and size, pipe geometry (d/t), material grade and the effect of welds in order to relatively rank the potential severity of various dents with respect to the cyclic fatigue performance of the dented pipeline.

The task involves developing an extensive numerical modeling matrix, encompassing a wide range of dent scenarios, analyzing each scenario using the detailed nonlinear finite element modeling methodology discussed previously and then estimating the fatigue life of the scenarios using the fatigue life assessment methodology developed in the previous task. The resulting data, i.e. dent shape, pipe geometry, material properties and fatigue life, will then be used to develop a regression equation that is capable of ranking the relative severity of the dents, in terms of the fatigue life, based on the dent and pipe geometries and material grade. The suggested dent scenario parameters and the number of variations that will be considered are summarized in the Table D.1.

Table D.1: Proposed Matrix for Numerical Modeling

Parameters	Minimum Number of Variations
Pipe diameter /Wall thickness	3
Material Grade	2
Condition	2
Dent depth	5
Indenter Size	6

D.1.1 Dent Geometric Parameter Definitions

– Depth Ratio	– Transverse Inner Shoulder Sharpness	– Pipe Stiffness, D/t
– Transverse Shoulder Sharpness	– Axial Inner Shoulder Sharpness A	– Dent Skew
– Axial Shoulder Sharpness		– Flatness Ratio

While the depth ratio = max depth/pipe diameter (in percent) and D/t ratio are self explanatory, the remaining geometric parameters are defined as:

D.1.1.1 Transverse and Axial Shoulder Sharpness

These parameters have been defined to provide a degree of the sharpness of the outer shoulder of the dent in both the transverse and axial orientations, i.e., the higher the sharpness value, the sharper the dent. The values are calculated according to the ratio:

$$\text{Transverse of Axial Shoulder Sharpness} = \frac{\text{Distance to Point of Inflection on Outer Shoulder (P.I. - A)}}{\text{Distance to the Peak}}$$

D.1.1.2 Dent Skew

The skew ratio applies to single peak dents and identifies the amount of asymmetry of a dent. For example a dent with a cross-section that resembles a lognormal statistical distribution would have greater skew than one that resembles a normal distribution. The skew parameter is calculated as follows:

$$\text{Dent Skew} = \frac{\text{Max}(\text{Dist to Peak} - \text{Dist to First PI}, \text{Dist to Second PI} - \text{Dist to Peak})}{\text{Dist to Second PI} - \text{Dist to First PI}}$$

D.1.1.3 Flatness Ratio

The flatness ratio is used to determine if a dent has a flat bottom. The flatness ratio is calculated in the longitudinal and transverse direction to define one and two dimensional flat bottom dents. A one dimensionally flat bottom dent is likely formed by an indenter resembling a long rod, while a dent with a two dimensionally flat bottom is likely formed by a flat plate indenter. The flatness ratio as defined in this document refers only to unrestrained dents and is calculated as follows:

The first step in the ranking methodology is the measurement of the dent geometry to determine the required geometric parameters. The dent geometry is represented by the geometric parameters outlined in Figure D.1. The geometry of the pipe (diameter and wall thickness), dent depth and distance between a reference point and several geometric features are determined. The figure illustrates the measurement of the dent geometry on a longitudinal section of the dent through its apex. The same geometry measurements need to be made on a transverse section through the apex of the dent using the radial deflection data.

After the pipe and dent geometry is characterized, the information is used to calculate a set of geometric parameters found to be useful in characterizing the relative ranking of the dent fatigue lives based upon the Dent Assessment Modeling. The geometric parameters are defined in detail in the following paragraphs and include:

$$\text{If } \left(\frac{\text{Trans Dist to Peak} - \text{Dist to PI}}{\text{Trans Dist to Center} - \text{Dist to PI}} \neq 1 \ \& \ \frac{\text{Long Dist to Peak} - \text{Dist to PI}}{\text{Long Dist to Center} - \text{Dist to PI}} \neq 1 \right)$$

$$\text{Flatness Ratio} = \frac{\text{Trans Dist to Peak} - \text{Dist to PI}}{\text{Trans Dist to Center} - \text{Dist to PI}}$$

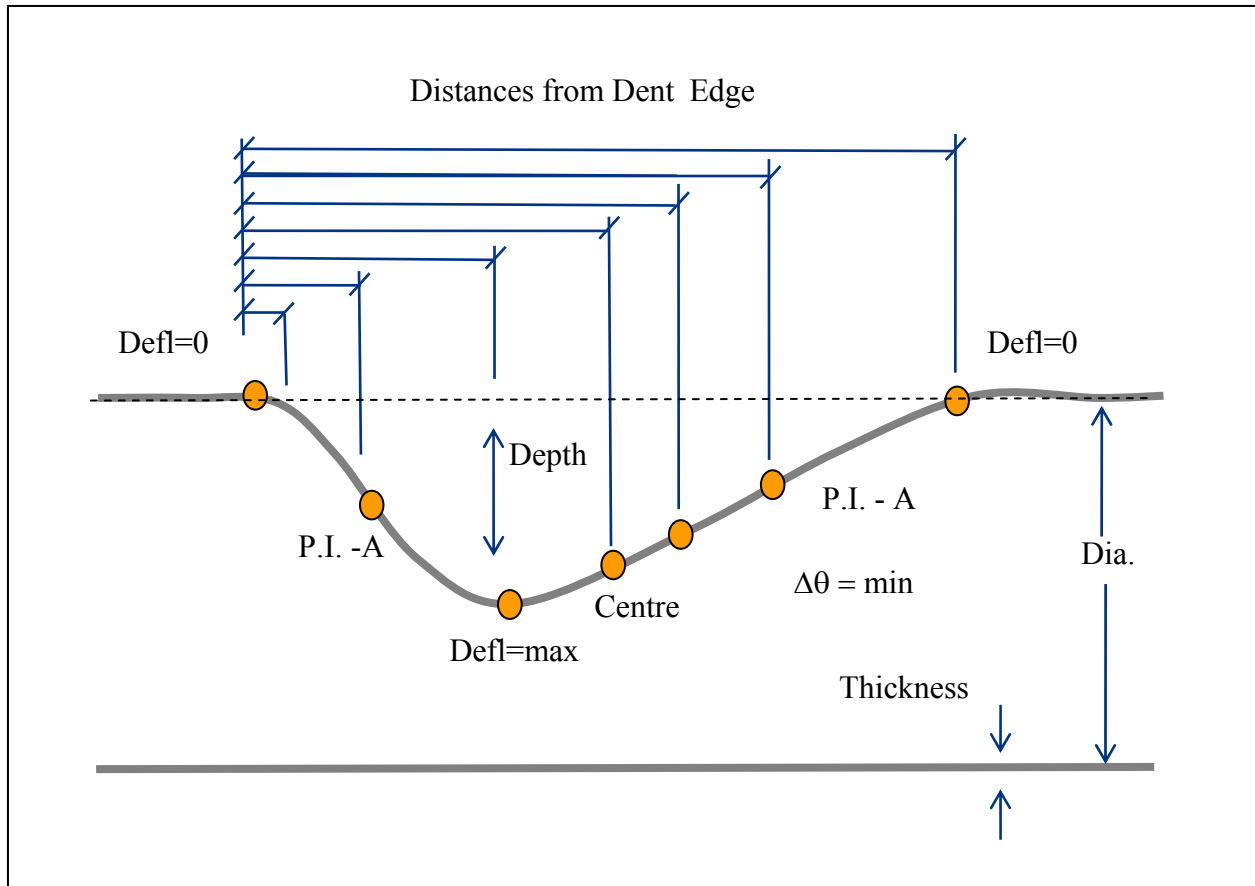


Figure D.1: Dent Geometry Measurement of a Single Peak Dents

Previous dent characterization work carried out by BMT and others will be reviewed prior to finalizing the detailed finite element modeling matrix. Figures D.2 through D.4 illustrate various trends between the geometric parameters summarized above and the estimate fatigue lives for a variety of finite element based dent scenarios. This data along with trends identified by other researches will be taken into account when defining the modeling matrix and when determining what geometric parameters are most significant in terms of affecting the fatigue life of dented pipelines.

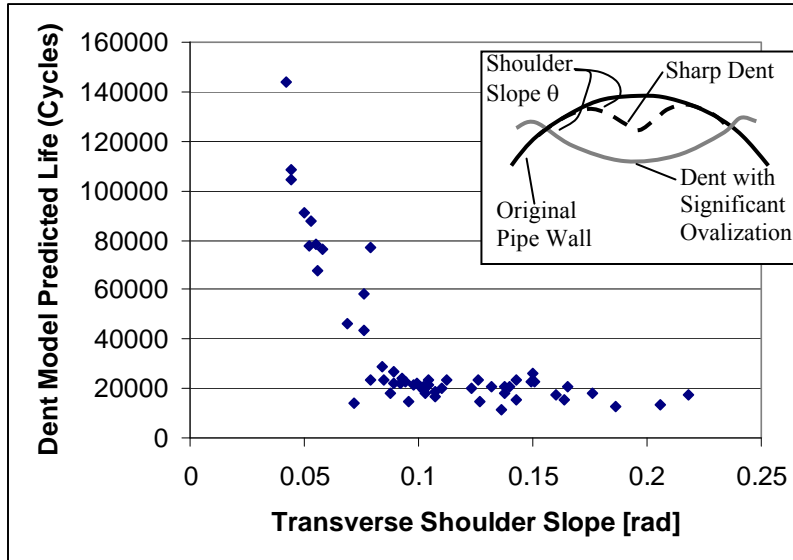


Figure D.2: Dent Shoulder Slope to Life Relationship for Unrestrained Dent Models

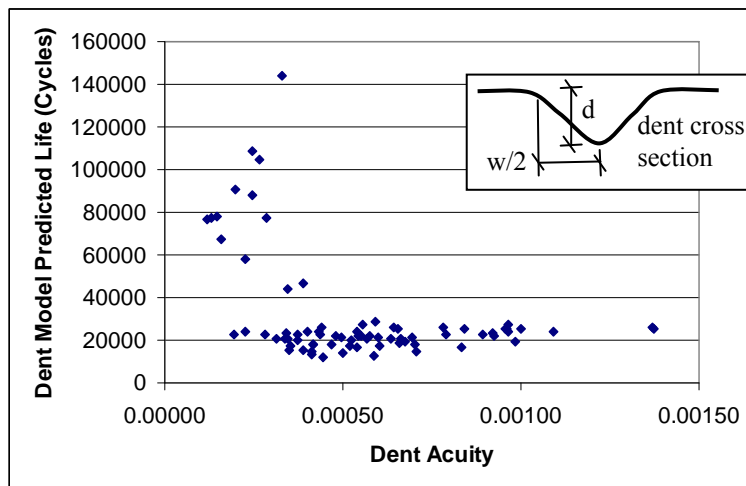


Figure D.3: Dent Acuity to Life Relationship for Unrestrained Dent Models

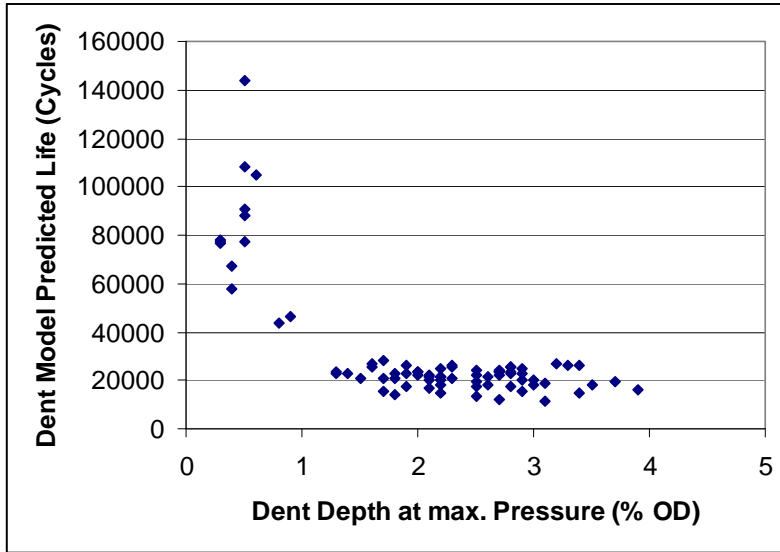


Figure D.4: Dent Depth to Life Relationship for Unrestrained Spherical Indenters

BMT Fleet Technology is an innovative leader in providing through-life engineering support from concept development through design, construction, operations, life extension/upgrade and disposal. The company employs its technological expertise and practical experience to provide services to clients in the Marine, Defence, Energy & Environment, Civil & Industrial Infrastructure, and Transport industry sectors. We are committed to retaining and applying practical knowledge of sector-specific factors in developing responsive solutions to customer's needs. The company's hallmark of engineering excellence involves the provision of leading edge structural and mechanical system damage assessment, materials and welding engineering, inspection and maintenance management, naval architecture and marine engineering, environmental and cold regions engineering services.

Head Office - Ottawa

311 Legget Drive
Kanata, ON, Canada, K2K 1Z8
Tel: 613-592-2830

St. John's

25 Kenmount Road
St. John's, NL, Canada, A1B 1W1
Tel: 709-753-5690

Vancouver

611 Alexander Street, Suite 412
Vancouver, BC, Canada, V6A 1E1
Tel: 604-253-0955

Victoria

Shoal Point, 101-19 Dallas Road
Victoria, BC, Canada, V8V 5A6
Tel: 250-598-5150

Email: fleet@fleetech.com

Web: www.fleetech.com

Or contact us through any of our sister BMT companies with over 60 offices worldwide to serve you.



Canadian offices certified to ISO 9001:2008. We are dedicated to ongoing quality and management systems.